Complex Fluids of Poly(oxyethylene) Monoalkyl Ether Nonionic Surfactants

Renhao Dong and Jingcheng Hao*

Key Laboratory of Colloid and Interface Chemistry, Shandong University, Ministry of Education, Jinan 250100, PR China

Received November 12, 2009

Contents

* To whom correspondence should be addressed. E-mail: jhao@sdu.edu.cn. Tel: +86-531-88366074(o).

1. Introduction

Nonionic surfactants are in widespread use in consumer products, industrial processes, and research laboratories. One

10.1021/cr9003743
Published on Web 06/18/2010

Renhao Dong received his Bachelor of Science degree in Chemistry from Shandong University, Jinan, P. R. China, in 2008. He is currently working with Professor Jingcheng Hao for his Ph.D. at Shandong University on the self-aggregation of surfactants in solution.

Jingcheng Hao received his Ph.D. from Lanzhou Institute of Chemical Physics, Chinese Academy of Sciences (CAS), Lanzhou, P. R. China, in 1995. Subsequently, Dr. Hao had a series of postdoctoral research positions at Lanzhou Institute, Nagoya University (Japan) as a Daiko Foundation Fellow, Bayreuth University (Germany) as an Alexander von Humboldt Foundation Fellow, and finally at SUNY-Stony Brook (USA) as a Research Specialist. In December 2002, he joined Shandong University, Jinan, P. R. China, where he is currently Professor and Director of the Key Laboratory of Colloid and Interface Chemistry, Ministry of Education. His research focuses on colloid and interfacial sciences, including surfactants in solution and self-assembly at all scales in bulk solutions and at surfaces. He has obtained National Outstanding Youth Funds (2006), Changjiang Scholars Award (2007), Lectureship Award of Japan Research Institute of Material Technology (2008), A Contribution Award to the Advancement of Asian Society of Colloid and Interface Sciences (2009), Chinese Chemical Society-BASF Innovation Prize (2009), and other scientific awards. Dr. Hao has published over 170 articles including original papers, reviews, books, and book chapters.

of the most important classes of nonionic surfactants is comprised of poly(oxyethylene) monoalkyl ethers, having the formula, $RO(C_2H_4O)_mH$, where R denotes a saturated alkyl chain, and the subscript m indicates the number of oxyethylene groups that comprise the headgroup of the surfactant. In this review, these surfactants are abbreviated, C_nEO_m, where the subscript n denotes the carbon number of the normal alkyl chain and the subscript m is used as above. Such surfactants are widely used in pharmaceutical formulations and cosmetics, as emulsifying agents in tanning, and as detergents.[1,2] The general synthesis of poly(oxyethylene) monoalkyl ethers is illustrated in Scheme 1. Typical catalysts are strong alkali or alkaline earth metals.

This class of surfactants is considered to be environmentally friendly and may be modified to have special properties

Scheme 1. Generalized Synthesis Scheme for Poly(oxyethylene) Monoalkyl Ethers[1]

$$CH_3\text{-}(CH_2)_{n-1}\text{-}OH + (CH_2\text{-}CH_2)_m \xrightarrow{\text{catalyst}} CH_3\text{-}(CH_2)_{n-1}\text{-}O\text{-}(CH_2\text{-}CH_2\text{-}O)_m\text{-}H$$

by varying the poly(oxyethylene) hydrophilic headgroup (abbreviated EO) or the hydrophobic alkyl chain. Often, contradictory properties are produced by increasing the EO headgroup versus increasing the alkyl chain length, for instance, C_nEO_m water-solubility increases with larger EO headgroups, but there is a commensurate decrease in surface activity with molecules containing the same alkyl chain. Therefore the hydrophile−lipophile balance (HLB) between the EO headgroup and the alkyl chain is an important parameter governing the physical properties of this type of surfactant.

The aim of this review is to provide an overview of the phase behavior, the microstructures, and the physicochemical properties presenting in bulk solutions of C_nEO_m surfactants, including binary and ternary mixed systems. It should be noted that this review does not encompass multicomponent systems with four or more components. In addition to bulk phenomena, adsorbed layer properties, and structures of nonionic surfactant micelles on solid substrates are also important phenomena that may be directly determined by atomic force microscopy (AFM).[3] These observations can demonstrate the correlations between bulk and surface structures, for example, surfactant adsorbed layer modalities on solid surfaces (such as silica) and the corresponding bulk solution show similar aggregate structures.[4] Hence, AFM provides strong support for the indirectly observed aggregates in bulk solution. Because of the great complexity of systems with four or more components and the diversity of adsorbed layer structures of nonionic surfactants on solid substrates, they are difficult to summarize as a single category. However, some excellent reviews address the nonionic surfactant adsorbed layer phenomena on solid surfaces;[5−7] thus they are not addressed in the present review.

When nonionic surfactants are dissolved in aqueous solution, characteristic orderly aggregates are observed; these structures are spherical, rod-like, disk-like, or worm-like micelles, bilamellar and multilamellar vesicles, liquid crystals, or other forms. Nonionic surfactant (C_nEO_m) aggregation is mainly induced by three driving forces: hydrophobic interactions, hydration (i.e., the hydration structures surrounding the EO headgroups), and hydrogen bonding; of the three, hydrophobic interactions provide the largest contribution. Corresponding to amphiphilic self-assembly, binary nonionic surfactant−water systems show rich phase behavior arising from these systems' dependence on temperature and concentration. Mesophases observed in these systems are normal micelles (L_1), reversed micelles (L_2), swelled sponges (L_3), and hexagonal (H_1), reversed hexagonal (H_2), normal "bicontinuous" cubic (V_1), reversed "bicontinuous" cubic (V_2), lamellar (L_α), and cubic spherical micelle (I_1) phases.[2,8,9]

These surfactant phases may be generally explained by applying the simple models of the geometric packing parameter (P) and the curvature free energy (i.e., the bending curvature energy). It is postulated that the hydration forces of the EO headgroups decrease as temperature increases,[10−12] resulting from a decrease in the number of water molecules H-bonded to the EO headgroups. According to this assumption, the dimensionless geometric packing parameter P will change according to the function, $P = v/(l_c a_s)$, in which a_s

is the interfacial area occupied by a surfactant headgroup, and l_c and v are the length and volume of the hydrophobic group, respectively.[13] The variously observed structures may be predicted as follows: if $0 < P < {}^1/_3$, spherical micelles will form; if ${}^1/_3 \leq P < {}^1/_2$, elongated micelles form; if ${}^1/_2 \leq P < 1$, disk-like micelles, lamellar structures, or vesicles are expected; if $P = 1$, mainly lamellar structures should form; and finally, if $P > 1$, microemulsions or reversed micelle structures generally appear. From a *quantitative* point of view, the packing parameter (P) cannot perfectly predict the formation of all structural types, but it *qualitatively* explains the formation of the aggregates. The spontaneous mean curvature of the polar/nonpolar interface (H_0) is also used to describe the phase behavior of surfactant systems; this parameter will decrease as the temperature increases. Olsson et al.[14,15] have reported the general effect of temperature on the spontaneous mean curvature of C_nEO_m/H_2O systems. When H_0 is positive, the system tends to form spherical micelles at low temperature. H_0 decreases progressively with increasing temperature and passes through zero at a temperature at which a lamellar phase is stable. Strey et al.[16] experimentally confirmed this effect of temperature using small-angle neutron scattering and freeze-fracture electron microscopy. These concepts are the most important and widely used in research regarding nonionic amphiphiles and are also primarily considered for the self-assembly behavior of C_nEO_m surfactants.

Since the physiochemical properties of mixed surfactant systems are usually superior to those of single surfactant ones, and because surfactants used for industrial processes generally contain impurities (chemical precursors or homologues, etc.), it is important to understand the effects of additives on C_nEO_m/water systems. This review describes ternary *n*-alkyl−EO surfactant systems in bulk solution, including C_nEO_m/salt/water, C_nEO_m/oil/water, C_nEO_m/alcohol/water, C_nEO_m/nonionic surfactant/water, C_nEO_m/polymer/water, and C_nEO_m/ionic surfactant/water. Reports on such ternary mixed systems have mainly focused on their properties, such as the phase behavior, structural models, thermodynamics, dynamic motion, and the mechanism of interaction between the surfactants. The driving forces leading to the various structures formed in these systems (hydration, hydrophobic effects, steric interactions, and salt-in or salt-out effects) are also described.

In addition, room-temperature ionic liquids (RT-ILs), which are idiosyncratic as amphiphile self-assembly media, have been widely studied.[17,18] This class of nonaqueous solvents has special properties, which lead to interesting phase behavior in binary surfactant systems. Warr et al.[19−21] have done an outstanding job investigating the C_nEO_m/ethylammonium nitrate (EAN, the earliest studied room-temperature ionic liquid) binary mixed systems. C_nEO_m surfactant systems in RT-ILs will also be discussed in detail.

2. Binary Mixed Systems

2.1. Binary Systems of C_nEO_m in Aqueous Solution

Systems of C_nEO_m in water have been investigated widely,[2] and this class of nonionic surfactants represents an important model of amphiphilic self-assembly because of three advantages. First, the molecular structures of C_nEO_m surfactants can be changed systematically, so their HLB may be controlled. Second, since the hydrophobic interaction is the most significant driving force for the formation of self-assembled structures in the C_nEO_m/water systems, their behavior may be more easily understood without taking electrostatic interactions into consideration. Finally, the surfactant phase behavior is visible and can be adjusted simply by changing the temperature or the composition.

In 1983, Tiddy et al.[9] reviewed the detailed phase behavior of a series of pure poly(oxyethylene) monoalkyl ether surfactants in water by optical microscopy over the temperature range of 0 to 100 °C and included various phase diagrams of the surfactant behavior. The phase transitions are rather complex in these systems and were explained as multiple mechanisms acting together. The transition mechanisms proposed included factors described as "order/disorder, shape transitions, entropy, secondary aggregation, hydration 'structure' of EO headgroups, and reversed curvature"; these factors were indicated as the most significant contributors to the particular phase boundaries. In a later report, these investigators studied the interaction of water and oxyethylene groups in lyotropic liquid crystalline phases of poly(oxyethylene) *n*-dodecyl ether surfactants using deuterium nuclear magnetic resonance (NMR)[22] and only needed to assume a simple model to explain their data.

Esumi et al.[23] summarized pre-1996 reports on microstructures (mainly micelles and liquid crystals) formed in binary C_nEO_m/water systems and focused on the relationship between self-aggregation and constituent composition or temperature. Hence, this review will consider the work in the field of the C_nEO_m/water binary systems from 1996 to the present. The current review discusses micelle shape and a thermodynamic model of micelle formation and growth, as well as the transformation from lamellar phase to cubic and hexagonal phases in liquid-crystal solutions.

From the work of Tiddy et al.,[9] a summary of some poly(oxyethylene) monoalkyl ether surfactants with observed phase transformations is given in Table 1, which provides additional values of surfactant critical micelle concentration (cmc) and HLB. The surfactants in this table are grouped according to their alkyl chain length (for surfactants longer than C_8). Generally, a C_nEO_m nonionic surfactant must have hydrocarbon chains longer than C_8 to show complex phase behavior in water[9,24] due to the solvophobicity effect. Note that the cmc values were all obtained at 25 °C and that the phase transformations listed may not be contiguous but occur at some particular temperature or concentration. Two-phase regions are not given since they are usually narrow in bulk solution.

2.1.1. Temperature-Dependent Solubility of C_nEO_m Surfactants

Cloud point is a principal feature of nonionic surfactants, that is, a C_nEO_m nonionic surfactant solution exhibits a lower consolute temperature. Below the cloud point, surfactants dissolve in water, and above it a phase separation may occur to form two isotropic liquid phases; one is a diluted solution, the other is the concentrated surfactant solution. As a result, the cloud point provides an indication of maximum solubilization of a nonionic surfactant.[2] Thus, the cloud point indeed reflects the temperature dependence of the nonionic surfactant.

The explanation of the decrease in solubility of a C_nEO_m surfactant in water with increasing temperature is generally accepted to be a decrease in the hydration of the EO headgroups and a rapid increase in the effective attraction

Table 1. Summary of Poly(oxyethylene) Monoalkyl Ether Surfactants in Aqueous Media[a]

surfactant	cmc[b] at 25 °C (10^{-5} mol·L^{-1})	cloud point (°C)	HLB	observed phases[d]	refs
$C_{10}EO_3$	60		9.1[c]	L_1,L_3,L_α,L_2	9, 25, 26
$C_{10}EO_4$	68	21	10.5[c]	L_1,L_2,L_3,L_α,H_1	2, 9, 25, 27
$C_{10}EO_5$	80	44	11.6[c]	L_1,L_α,V_1,H_1	2, 9, 25, 28
$C_{10}EO_6$	90	59	12.5[c]	L_1,L_α,V_1,H_1	2, 9, 28, 29
$C_{10}EO_7$	95		13.2[c]	L_1,H_1	30, 31
$C_{10}EO_8$	100	85	13.8[c]	L_1,H_1	25, 28, 32
$C_{12}EO_2$	3.3	32−35	6.4[c]	L_1,L_α,L_3,V_2,L_2,	25, 33, 34
$C_{12}EO_3$	5.2		7.5	L_1,L_3,L_α,L_2	2, 9, 25, 35, 36
$C_{12}EO_4$	4.3 (6.4)	6	9.0	L_1,L_3,L_α,L_2	2, 9, 25, 29, 32
$C_{12}EO_5$	6.4	30	10.0	$L_1,L_3,L_\alpha,H_1,V_1,L_2$	2, 9, 30, 35, 37
$C_{12}EO_6$	6.8	48	11.7[c]	L_1,L_α, H_1,V_1,L_2	2, 9, 37, 38
$C_{12}EO_7$	5.0	70	12.5[c]	L_1,L_α,H_1,V_1,L_2	2, 9, 30, 37, 39
$C_{12}EO_8$	7.1	77	13.1[c]	$L_1,L_\alpha,H_1,V_1,I_1,L_2$	2, 9, 37, 38
$C_{12}EO_9$	10	88	13.6[c]	L_1,H_1,I_1,L_2	25, 32, 37
$C_{12}EO_{10}$		96	14.1[c]	L_1,H_1,L_2	32, 37
$C_{12}EO_{12}$	14.0	98	14.8[c]	L_1,H_1,I_1	9, 38
$C_{12}EO_{23}$	17.5		16.9	L_1,I_1,L_2	37, 38, 40
$C_{14}EO_3$		<20	7.6[c]	L_1,L_3,L_α,V_2,L_2	2, 9
$C_{14}EO_6$	0.8	42	11.0[c]	L_1,L_α,H_1,V_1	2, 9, 29
$C_{14}EO_7$	0.95	58	11.8[c]		30, 41
$C_{14}EO_8$	0.99	70	12.4[c]	L_1,L_α,H_1,V_1,I_1	25, 32, 42
$C_{16}EO_3$		<20	7.0[c]	L_1, $L_3,L_\alpha,V_2,L_2,L_\beta$	9
$C_{16}EO_4$		<20	8.4[c]	L_1,L_3,L_α,V_2,L_2	2, 9
$C_{16}EO_6$	0.40	37	10.4[c]	$L_1,L_\alpha,L_\alpha{}^H,H_1,V_1,L_\beta{}^e,L_2$	9, 43−45
$C_{16}EO_7$	0.30	52	11.2[c]	L_1,L_α,H_1,V_1	41, 43, 46
$C_{16}EO_8$	0.12	63	11.9[c]	$L_1,L_\alpha,H_1,V_1,I_1,L_2$	2, 9, 25
$C_{16}EO_{12}$	0.23	92	13.7[c]	L_1,L_α,H_1,V_1,I_1	2, 9, 38
$C_{16}EO_{20}$	0.77		15.7[c]		47

[a] Expanded from ref 9. [b] The values of cmc's are approximate due to different experimental measurements. [c] HLB was calculated as HLB = wt % EO/5.[48] [d] Phase abbreviations are as described in the text. [e] L_β represents a gel phase.

between EO headgroups on adjacent micelles. Three different models have been employed to provide proof for this explanation.[49,50] In the earliest model, Kjellander and Florin described the enthalpy and the entropy changes of poly(oxyethylene) surfactants at their cloud point and proposed that water forms an ordered structure around the EO headgroup at low temperatures. With increasing temperature, the ordered water structure is destroyed owing to the unfavorable entropy contribution.[51] A second model has been proposed based on the idea of Hirschfelder et al. in 1937.[52] These authors suggested that a solubility gap forms between two types of molecules and has small regions that are attractive (e.g., via hydrogen-bonding) and large regions that are repulsive. With increasing temperature, molecules move from the small attractive regions to larger repulsive regions, leading to a phase separation. Therefore, the explanation of the cloud point temperature dependence is that hydrogen bonding between EO headgroups and water are destroyed at elevated temperature.[53] Similar conclusions were also obtained in the studies of phase behavior of $C_{10}EO_m$ ($m = 5-7$) in aqueous solution.[27,28,31] The third model is ascribed to the conformational changes of the EO headgroups with temperature. Upon heating, the EO segments change from a polar conformation (gauche−trans isomers) to less polar structures, and as a result, the dipole−dipole interactions between EO headgroups and water decrease, which become unfavorable for dissolution.[49,50,54] While there are three models to explain cloud point, an exact mechanism has not been established. Evans et al.[55] proposed that a combination of dehydration processes and micelle growth may account for the separation phenomena. In contrast, when C_nEO_m surfactants are dissolved in the nonaqueous solvent formamide, with strong hydrogen bonding similar to water, clouding behaviors are also observed, which is in agreement with hydrogen-bonding and EO conformational change models.[49,56,57]

Separately, the hydration of C_nEO_m has been found to be approximately 2−6 moles of water per EO headgroup by measuring the self-diffusion coefficient of water.[50,58] The hydration becomes stronger with increasing length of EO headgroup; in other words, a larger EO headgroup will lead to a higher cloud point, though the relation is not linear, as seen in Table 1. This conclusion was also obtained in the cloud point research of $C_{12}EO_m$ ($m = 2-8$) in water; it was found that the lower consolute temperature shifted toward a lower temperature as the number of EO groups decreased.[59]

Accordingly, the question of the models describing the aggregation behavior of C_nEO_m surfactants near the cloud point has attracted the most attention in this area. Specifically, how do micelles change, such as in their shape and size, with temperature? This is further discussed in section 2.1.4.

2.1.2. Phase Diagrams of C_nEO_m/Water Systems

Phase diagrams of $C_{10}EO_6$, $C_{12}EO_2$, $C_{12}EO_{12}$, and $C_{16}EO_6$ in aqueous solutions are illustrated in Figures 1−4. Inoue et al.[27,28,31] investigated a homologous series of decyl poly(oxyethylene) ether surfactants ($C_{10}EO_m$, $m = 4-8$) in aqueous solutions over a rather wide temperature range using differential scanning calorimetry (DSC), Fourier transform infrared spectroscopy (FT-IR), and polarized optical microscopy (POM). As indicated in their phase diagrams, a normal hexagonal H_1 phase occurred in the $C_{10}EO_7$/water and $C_{10}EO_8$/water systems; lamellar L_α, bicontinuous cubic V_1, and H_1 phases appeared in the $C_{10}EO_5$/water and $C_{10}EO_6$/water systems; and micelles L_1, reversed micelles L_2, swelling sponge L_3, L_α, and H_1 phases existed in the $C_{10}EO_4$/water system above −10 °C. The sequence of phases indicates that for $C_{10}EO_m$ surfactants, the stability of L_α phase decreases with the increase of EO number, that is, the increase of interfacial area per molecule (a_s) is unfavorable

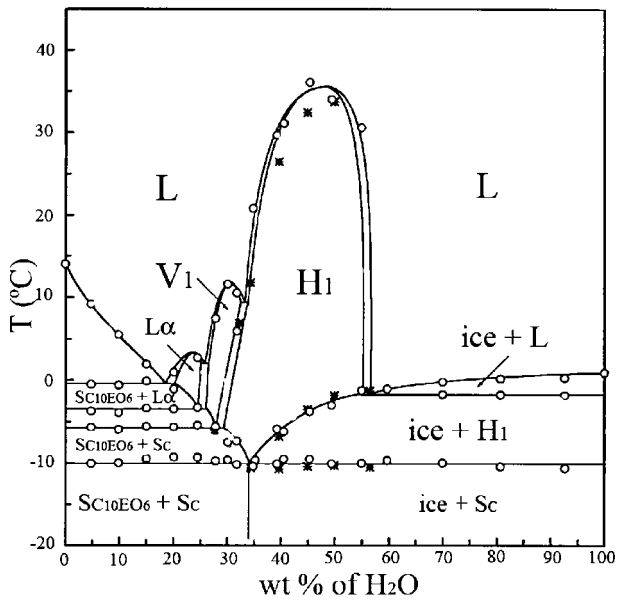

Figure 1. Temperature−composition phase diagram of $C_{10}EO_6$/H_2O mixtures. Phase boundaries were determined by DSC (○) and POM (∗). $S_{C_{10}EO_6}$ represents pure, solid $C_{10}EO_6$, and S_C represents the hydrated compound formed in a solid phase. For other symbols in the figure, see text. Reproduced with permission from ref 28. Copyright 1998 Elsevier Inc.

to the formation of a lamellar phase. A phase diagram of the $C_{10}EO_6$/water system is reproduced in Figure 1.[28] As Chernik[8] discussed for the phase diagram of nonionic surfactant−water systems, three-phase transitions of the eutectic types, that is, $S_{C_{10}EO_6} + L_\alpha \rightleftharpoons L$, $S_{C_{10}EO_6} + V_1 \rightleftharpoons L_\alpha$, $S_{C_{10}EO_6} + H_1 \rightleftharpoons V_1$, and H_1 + ice $\rightleftharpoons$ L exist in $C_{10}EO_6$/water system (Figure 1). These phase transitions obey the phase rule. However, two-phase regions can be found in phase diagram, including $S_C + S_{C_{10}EO_m}$ and S_C + ice regions. If the compound S_C exists, then the coexistence of four phases at −10 °C contradicts the phase rule, where a maximum of three phases may coexist in a binary system at constant temperature and pressure. The aqueous phase behavior of surfactants has been clearly explained by R. G. Laughlin,[60] and the simplest explanation is that the phase diagram in Figure 1 contradicts the phase rule and there is probably a small temperature difference between the melting point of S_C (if it exists) and the eutectic temperature of H_1−ice−$S_{C_{10}EO_6}$ or a supercooling artifact at the eutectic composition. Similar arguments could also be applied to the evaluation of the series of phase diagrams of the $C_{10}EO_m$/water system ($m = 4-8$).[27,28,31]

The $C_{12}EO_{12}$/water binary system was investigated by Tiddy et al.[61] using optical microscopy and X-ray diffraction. These authors were the first to describe three different micelle (oil-in-water type) cubic phases in a single surfactant system (Figure 2). The cubic phase, an isotropic intermediate phase without birefringence, has two fundamental types: first, the bicontinuous network structure, having four lattices (*Im3m, Ia3d, Pn3m*, and *R3c*) and usually denoted as V_1 (normal) or V_2 (reversed); second, discontinuous micellar (spherical or spheroidic) cubic mesophases, having three lattices (*Pm3n*, *Im3m*, and *Fm3m*), usually denoted as I_1.[62]

In the phase diagram of the $C_{12}EO_{12}$/water system (Figure 2), the hexagonal H_1 phase transformed into a discontinuous micelle cubic phase I_1 with the space group of *Pm3n*, as hydration increases. On further hydration, this system formed a second micellar cubic phase of space group *Im3m*. In

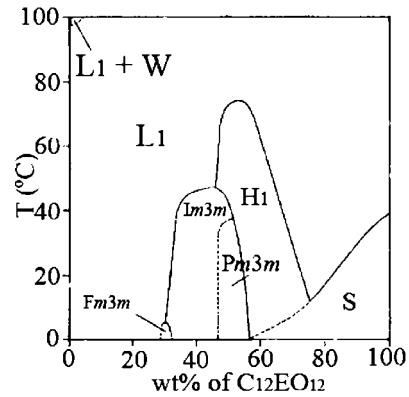

Figure 2. Binary phase diagram of the $C_{12}EO_{12}$/water system. Dashed lines indicate phase boundaries whose positions are not precisely known. Narrow two-phase regions are not indicated. Reproduced with permission from ref 61. Copyright 1997 American Chemical Society.

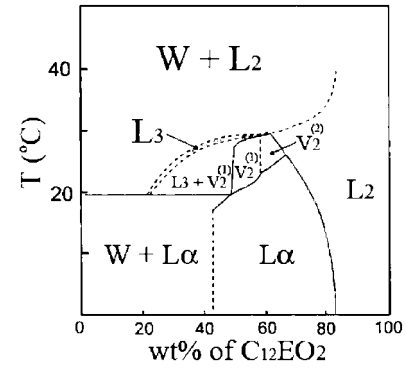

Figure 3. Binary phase diagram of the $C_{12}EO_2/D_2O$ system. The *Ia3d* structure was assigned as a bicontinuous $V_2^{(1)}$, while the *Pn3m* structure was related to $V_2^{(2)}$. Reproduced with permission from ref 33. Copyright 1997 American Chemical Society.

addition, a third micellar cubic phase of space group *Fm3m* forms at low temperature and high hydration, adjacent to the L_1 micellar solution. Though the cubic space groups were identified by indexing their powder diffraction patterns, there was no other direct evidence to determine whether these phases were bicontinuous or micellar. The authors also studied the process of the H_1−*Im3m*, *Im3m*−*Pn3n* and H_1−*Pn3n* transitions, proposing a phase transition mechanism with three major considerations: (i) the structure of the micelles in dilute solution, (ii) the maximum fraction of each different mesophase, and (iii) the ordered phase with the largest possibility of micellar curvature.[9,61]

Funari et al.[33] investigated binary mixtures of $C_{12}EO_2$/water with optical microscopy and time-resolved X-ray diffraction. At concentrations in the range from 48 to 70 wt % of $C_{12}EO_2$, a sequence from lamellar L_α to bicontinuous cubic *Ia3d* to bicontinuous cubic *Pn3m* to L_2 was found upon heating. This also demonstrates that temperature can drive phase transitions. Figure 3 gives the binary phase diagram of the $C_{12}EO_2$/D_2O system.[33,63] Two cubic phases with the same symmetry (*Ia3d*) appeared at high concentrations in the system and showed different thermal behaviors owing to a kinetic effect in this nonequilibrium condition. The transition between *Ia3d* and *Pn3m* cubic phases had the characteristics of a Bonnet transformation, that is, the rod units reorganized without a change of their mean curvature. Upon comparison of Figure 2 with Figure 3, the V_2 and L_α phases can be observed in $C_{12}EO_2$ system, while the H_1 and I_1 phases appear in the $C_{12}EO_{12}$ system. The extensive difference may be principally

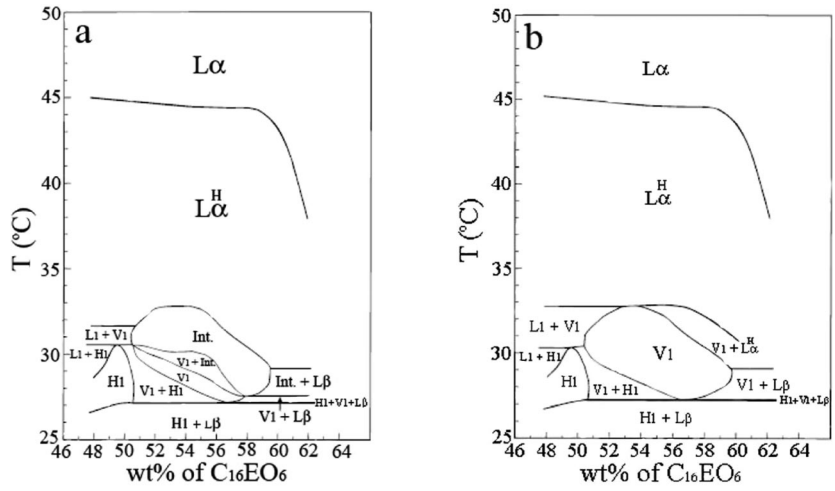

Figure 4. Comparison of phase diagrams of the $C_{16}EO_6/D_2O$ system in the region of 48−62 wt % $C_{16}EO_6$. The samples were cooled from 50 °C (a) and heated from 25 °C (b). The phase regions were established by ^2H NMR measurements, and the phases were identified by optical microscopy and small-angle X-ray scattering measurements. Reproduced with permission from ref 45. Copyright 1997 American Chemical Society.

related to the effective surface area per surfactant molecule, mainly depending on the EO headgroup; increases in the EO group length lead to the phase formation. Alternatively, the curvatures of the surfactant molecule layers in the self-organizing process are altered from negative to positive as the EO group length increases,[64] thus leading to the phase variation.

The structure and morphology of the intermediate phase region in the nonionic $C_{16}EO_6$ surfactant/water system was studied by Holmes et al.,[44,45] who reported two similar phase diagrams, conforming to a cooling process (Figure 4a) and a heating process (Figure 4b), in which the samples were equilibrated at corresponding temperature in the cooling or heating process. Both of the diagrams cover the concentration range of 48−62 wt % in the $C_{16}EO_6$/water system.

For the $C_{16}EO_6$/water system, upon cooling from the lamellar phase (L_α), the phase sequence includes disrupted lamellar (L_α^H, i.e., continuous bilayers containing irregular ribbon-shaped water channels), mesh intermediate (Int.), *Ia3d* cubic (V_1), and hexagonal (H_1) or hexagonal plus gel biphasic ($H_1 + L_\beta$) regions. On heating from the hexagonal or two-phase region, the region of intermediate and cubic phases formed on cooling was replaced by an *Ia3d* cubic phase. The mesh intermediate phase formed during cooling was demonstrated to have a rhombohedral mesh structure of space group $R\bar{3}m$. Each phase in this system was described in detail, especially the hexagonal H_1, random mesh L_α^H, and intermediate/cubic phases. The intermediate phases of $C_{16}EO_6$/water mixtures have been recently reviewed.[65] The phase behavior seen in this system is a result of two mechanisms. The hydration of the ethylene oxide head groups decreases as temperature increases, which results in a decrease in the surface area per molecule at the surfactant/water interface and a reduction in the interfacial curvature. The cooling process phases arise from an interaggregate headgroup overlap from the interaction of ethylene oxide head groups in the aqueous region. The main interaggregate repulsion forces result from steric repulsion between solvated EO groups.

2.1.3. Effects of Molecular Structure on Micelles

Globular micelles appear above the critical micelle concentration in C_nEO_m/H_2O solutions.[66] This micellization has significant internal factors (the number of EO groups and the length of the alkyl chain), as well as external factors (the temperature and the concentration) that influence the micelle shape, size, aggregation number, and further transformations. Here, the molecular structure affecting the micellar properties is discussed.

Three sets of micellar solutions, C_nEO_4 ($n = 6$ and 8), C_nEO_8 ($n = 10$, 12, and 16), and $C_{10}EO_m$ ($m = 4$, 6, and 8), were investigated through static light scattering (SLS) and dynamic light scattering (DLS).[67,68] The C_nEO_4 systems were described by a model of spherical or nearly spherical micelles interacting via an attractive van der Waals potential, a stabilizing repulsive brush potential, and a hard, core-excluded volume interaction. In contrast, the C_nEO_8 systems were described with a model of cylindrical micelles interacting via an effective excluded volume between the C_nEO_8 molecules[67] following a modified Flory−Huggins theory.[69] The authors also made the interesting observation that $C_{10}EO_m$ molecules with longer hydrophilic EO headgroups form smaller micelles.[68] Moreover, surface tension measurements indicate that the cmc values of C_nEO_m in water directly decrease with increasing alkyl chain length,[70] which plays a more effective role than the EO headgroups, as seen in Table 1. In conclusion, not only the relative sizes of the hydrophobic and hydrophilic moieties but also the absolute chain lengths influence the micellar properties.

2.1.4. Variation of Micelles with Temperature

In dilute C_nEO_m surfactant solutions, micelles grow and change shape with increasing temperature, but well below the cloud point, as a result of interactions between the micelles and water, and especially as the cloud point is approached.[23,68,71] A number of technologies have been mutually used to accurately monitor micelle growth with temperature. The techniques include self-diffusion NMR,[71−74] small-angle neutron scattering (SANS),[75−78] light scattering,[41,79−81] and cryogenic transmission electron microscopy (cryo-TEM).[82,83] In addition, the cmc of C_nEO_m solutions will decrease markedly with increasing temperature below the cloud point,[23] because increasing the temperature weakens the hydration of the EO headgroups, which favors micellization. This is the predominant driving force for the decrease in cmc, even though repulsive interactions between water

and the alkyl chains simultaneously become weaker at high temperature, which is unfavorable for micelle formation.

However, there has been a controversy of whether the aggregate patterns are giant micelles (rod or wormlike micelles), the aggregation of attractive small spherical micelles, or some other large aggregates near the cloud point. This contention between the aggregate models has been resolved by the identification of branched micelles.[83−88]

Some authors propose that the thermotropic sphere-to-rod transition of micelles appearing in C_nEO_m dilute solutions approaching the cloud point is in accord with the experimental data of self-diffusion NMR,[72−74] SANS,[75,78,89] and light scattering.[79,72,59,90−93] Among the measurement methods, only the validity of the explanations derived from light scattering showing the increasing apparent aggregate size with temperature has been questioned. Corti and Degiorgio measured the mass diffusion coefficients of $C_{12}EO_6$ aqueous solution in the temperature range of 30−50 °C and suggested that the critical concentration fluctuations but not the micellar growth accounted for the increasing intensity of light scattering.[81] However, using NMR, Nilsson et al.[73] found that the self-diffusion obviously decreased in the $C_{12}EO_5$/water system as the cloud point was approached, which indicated a growth of micelles. The micelles seem to be flexible and lacking a definite shape close to the cloud point. Similar experiments were performed in $C_{12}EO_8$/water solutions, but the results showed that the increasing temperature had a less pronounced effect on the $C_{12}EO_8$ micelle size. Brown et al.[74] also propose that the interpretation of the critical concentration fluctuations for critical phenomena at the cloud point has been overemphasized; their self-diffusion NMR results found that the micelle size increases markedly with increasing the temperature from 20 °C to the cloud point in the $C_{12}EO_6$/water system. The above disagreement focuses on the micellar size but does not address the micellar shape. Kato et al. employed light scattering and NMR to measure the mutual diffusion coefficients and self-diffusion coefficients and suggested that small globular micelles grew to form wormlike micelles in $C_{12}EO_5$,[91,92] $C_{12}EO_6$,[72] and $C_{16}EO_7$[93] aqueous solutions when the temperature was increased toward the cloud point.

Direct observation of wormlike micelles was described by Lin et al.[82] using cryo-TEM in the $C_{16}EO_6$/water system. This study was conducted with and without the presence of an electrolyte, NaSCN or NaCl, and the data were compared with SANS measurement data.[75] The micelles in this system were often curved, bent, and looped and sometimes even formed rings and polygonal structures. In all the solutions, the micelles were circular cylinders with diameters of about 60 Å, while the lengths of the micelles varied from several hundred angstroms to more than a micrometer. At certain concentrations, the micelle length obtained by cryo-TEM observations or SANS measurements in the $C_{16}EO_6$/water system without electrolyte decreased with increasing temperature until reaching the cloud point. However, the micelle length was less sensitive to the concentration above the cmc. There were two different trends observed in this system: first, the addition of the electrolyte, such as NaSCN, induced the micelle length to increase to a maximum, but it then decreased at higher temperature; and second, in systems with added NaCl, the micelle length decreased with increasing temperature. These trends with different types of salts are discussed in section 3.1. The ultimate formation of wormlike micelles with a cross-sectional diameter of 2.4 nm was also obtained in the $C_{14}EO_6$ system at 40 °C, and they varied from 50 nm to several hundreds of nanometers in length with the surfactant concentration approaching the phase boundaries.[79] A similar effect of the temperature on the apparent micelle size or shape was obtained in $C_{12}EO_4$,[94] $C_{12}EO_{23}$,[95,96] $C_{17}EO_{84}$,[97] $C_{14}EO_7$,[41,98] and $C_{16}EO_7$[99,100] aqueous solutions.

In contrast, a model of the aggregation of attractive small spherical micelles has also been proposed for the critical region.[76,101,102] This model in fact does not preclude the increase of the micellar aggregation number in a narrow concentration range as a function of temperature.[77] Nevertheless, the micellar growth model is not related to the effects of attractive interaction between micelles on the scattering intensity.[88] Zulauf and co-workers[101,102] investigated the aqueous micellar solutions of short chain poly(oxyethylene) nonionic surfactants C_8EO_4 and C_8EO_5 as a function of temperature by SANS. They found the unusual phenomenon that increasing temperature did not induce the micelles to grow to form larger aggregates, even as the scattering intensities and the viscosity of the solutions increased. It was assumed that a short-ranged attractive pair potential between spherical micelles increased with temperature, which induced the interaction of adjacent micelles to form loose micellar clusters. These authors also found there was little variation in micelle size with temperature up to surfactant concentrations of 35% with the longer-chain $C_{12}EO_6$, $C_{12}EO_8$, and $C_{16}EO_8$.[76] Apparently attractive interactions between micelles became stronger approaching the consolute phase boundaries. Corti et al.[90] suggested that the cloud point transition for the short-chain C_6EO_3 and C_8EO_4 seems to be described by the model of aggregation of small globular micelles, but in contrast there may be micellar growth with temperature for the long-chain $C_{12}EO_8$ and $C_{14}EO_7$ surfactants. There is still some controversy regarding the micellar growth model and the attractive micelle model. Cebula and Ottewill have proposed that the two mechanisms are not mutually exclusive and a cylindrical model would be fit for the SANS experimental data.[77] Glatter et al.[103] found that a sphere-to-rod transition occurs with increasing temperature in the C_8EO_5 and $C_{12}EO_6$ systems, while C_8EO_4 and $C_{12}EO_5$ can form rodlike micelles even at low temperature, and the attractive interaction is applied to explain these micelle behavior approaching the cloud point. Thus, these authors propose that the two models depended on the nature of the surfactants.

At present, the controversy described above may have been resolved by direct evidence of branched micelles near the cloud point. Talmon et al.[83] studied micellar growth in an aqueous solution of $C_{12}EO_5$ by cryo-TEM observations and light scattering measurements. The coexistence of short, disconnected cylindrical and spherical micelles could be observed at low temperature and under dilute conditions. With increasing temperature and concentration, uniaxial micelles grew into threadlike or wormlike objects. The results of static and dynamic light scattering confirmed the phenomena above, where both the mean micelle contour length and the average micelle hydrodynamic diameter increased with temperature. The light scattering measurements also indicated that the micelle length reached a maximum value as the temperature approached the critical point, due to scattering from the mesh rather than the micelles. The subsequent connected network structure was clearly observed by cryo-TEM. A detailed progression of the micellar size and shape with temperature was observed as follows: at 8 °C, spherical and short threadlike micelles (<50 nm); at 18

°C, spherical and cylindrical micelles (50−100 nm); at 29 °C, networks of longer micelles (>100 nm).

A proposal of an equilibrium with networks near the critical point has been employed to interpret the critical phenomena of nonionic surfactant microemulsions[85] and cationic surfactant systems.[86] Zilman et al.[87] has extended the theory by combining the formation of networks with the spontaneous curvature of surfactant layers; namely, the spontaneous curvature is high and favorable for the spherical or unbranched micelles at low temperature, but it decreases with increasing temperature, favoring the formation of branched micelles and phase separation. Since an adsorbed layer of surfactant on silica can show similar aggregate structures to those in bulk solution, Warr et al.[88] have used AFM to observe the micelle changes of C_nEO_m aqueous solutions with increasing temperature on silica and graphite. A sphere-to-rod-to-mesh structure transition was observed approaching the cloud points of the solutions from a lower temperature, which indirectly reflects the variation of micelles in C_nEO_m bulk solution as a function of temperature, thus providing strong support for the branching model.

2.1.5. Self-Organization into Vesicles in C_nEO_m Systems

While it is well-known that micelles, bilayers, and vesicles form in the bulk phase when a nonionic surfactant is dissolved in aqueous solution, further evolution of the system with changing temperature or concentration leads to aggregate structures that transform into two-dimensional structures, lamellar or hexagonal liquid-crystals, and then into complex three-dimensional periodic patterns, cubic liquid-crystals, or a micellar cubic phase. Micelles have been mentioned above as the primary structures observed; other aggregates and their transitions will be described in the following paragraphs.

Traditionally, vesicles can be constructed by dispersing lipids in aqueous solution. In 1989, Kaler et al.[104] reported the spontaneous formation of stable vesicles in dilute aqueous solutions of cationic and anionic (catanionic) single-chain surfactant mixtures, which had excess salt as a result of their counterions. In recent years, salt-free vesicle phases have been produced successfully in mixed catanionic surfactant systems via electrostatic interactions[105] or in mixed anionic and zwitterionic surfactant systems[106] by metal−ligand complexation. However, vesicle formation in the C_nEO_m/water binary system has been rarely reported.[94,107−110] Olsson et al.,[108] studied normal and reverse vesicle systems with $C_{12}EO_4$, considering both their stability and the average vesicle size. The vesicle size was obtained by measuring the amount of solvent inside the vesicles, while their stability was studied by monitoring how the vesicle size varied with time. The solvent self-diffusion coefficient was measured by Fourier transform pulsed gradient spin−echo ^{1}H NMR (PGSE NMR). In the normal vesicle phase formed by the $C_{12}EO_4$/water binary system, the solvent, water, was found to exchange rapidly between the inside and outside of the vesicles on the experimental time scale (∼0.1 s). In the reverse vesicle phase obtained in the $C_{12}EO_4$/DKE (sucrose monoalkanoate, containing 10 wt % C_{14}, 40 wt % C_{16}, and 50 wt % C_{18})/decane/water system, either a fast or a slow exchange was observed, depending on the oil and the bilayer composition. In a separate article about the $C_{12}EO_4$/water system,[94] vesicles were formed from wormlike micelles upon a temperature change that allowed the system to jump across a liquid−liquid region. Heating the dilute solution caused the micelle phase ("L_1" and "L_1'" are used in ref 94) to rapidly fuse into larger aggregates forming the concentrated liquid phase (L_1'') with a structure of branched cylindrical micelles, a so-called "living network". Beyond the coexistence region ($L_1 + L_1''$), a two-phase region was observed with a lamellar phase (L_α) and excess water vesicles. The process could be described by a flexible surface model considering spontaneous curvature (H_0).[16] The vesicles were large and polydisperse with an average radius on the order of 200 nm, which was affected by the rate of temperature increase, since a slower temperature gradient would result in larger vesicles. The mechanism was attributed to the aggregation of the micelles into network particles, which was analyzed in terms of classical colloidal aggregation.

2.1.6. Lyotropic Liquid Crystals and Mesophases in C_nEO_m/Water Systems

Lyotropic liquid crystals and mesophases are fascinating ordered self-assemblies that can appear in nonionic surfactant−water systems as lamellar (L_α), hexagonal (H_1), and cubic mesophases; their topological changes are also of interest to researchers. Transitions from a micelle phase to a mesophase or transitions between the various mesophases arise from temperature and concentration changes and may also arise from the effect of various additives. The research groups headed by Tiddy and Holmes have published a series of outstanding papers in the area of self-assembly of C_nEO_m surfactants into lyotropic liquid crystals in aqueous solution.[22,44,45,111−113] In their earlier work, the interactions of water and EO groups in a series of $C_{12}EO_m$ ($m = 3−6, 8$) surfactants in hexagonal and lamellar liquid-crystal phases were investigated by measuring the ^{2}H NMR quadrupole splitting (Δ) of heavy water.[22] Increasing the temperature can cause a general decrease of Δ, while an increase in the surfactant concentration causes an initial sharp increase of Δ, followed by a leveling off or a shallow maximum, indicating a phase transition of L_1 to L_α to H_1. The observed changes were attributed to the size of EO headgroups, because while the H-bonding interaction decreased with increasing temperature, it concomitantly increased with the number of EO groups. On the basis of this phenomenon, typical liquid-crystal phases of the binary $C_{12}EO_6$/water and $C_{16}EO_6$/water systems were described.

The phase behavior in aqueous solution of $C_{12}EO_6$ has also been investigated by Rancon and Charvolin.[114,115] They compared the relation between the Bragg diffraction obtained by X-ray and neutron scattering experiments and the structural transformations of the surfactant liquid-crystal phases.[114] These authors observed epitaxial relationships between the lamellar, hexagonal, and cubic phases of the $C_{12}EO_6$ aqueous system; specifically, the {211} planes of the cubic phase are related to the {001} planes of the lamellar phase and the {100} reticular planes of the hexagonal phase; thus the {211} planes of the cubic phase played a central role in the structural transformations observed in the system. In the case of the cubic phase transforming into the hexagonal phase, the cylinders of $C_{12}EO_6$ surfactant in the hexagonal phase grew parallel to the {111} direction of the cubic phase. A mechanism explaining the transitions among the three liquid-crystal phases in $C_{12}EO_6$ systems was proposed based on X-ray scattering data in a later work.[115] It appears that the lamellar or hexagonal phase was transformed into the cubic phase not directly by contact and fusion of the lamellae or hexagonal structures, but rather by contact and fusion of

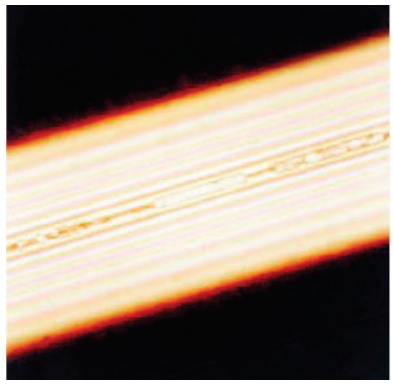

Figure 5. Optical polarizing micrograph with $D_2O/C_{12}EO_6$ (mole ratio) = 9.6 at 300 K previously oriented in a 14.1 T magnetic field. Reproduced with permission from ref 116. Copyright 1999 American Chemical Society.

the cylinders created in the lamellae or in the hexagonal phase as fluctuations, which then led to the orientation of the cubic phase. Conversely, hexagonal and lamellar phases grew from the {111} axes of the cubic phase with a decrease in the correlations along the {111} direction, which became the cylinders of the hexagonal or lamellar phases.

Moreover, Briganti et al.[116] observed an interesting iso-oriented lyotropic lamellar phase in the $C_{12}EO_6$/water system. As shown by ^1H and ^2H NMR spectra, cooling induced the isotropic phase to become an almost completely iso-oriented lamellar phase under a high-strength magnetic field (14.1 T). Optically polarized microscopy confirmed the above observation, showing the occurrence of fine grained mosaics, as shown in Figure 5. Two parameters were relevant to rationalize ordering of the optical axis and the related anisotropy in the uniaxial mesophase. Namely, the observed orientation was due to a combination of the magnetic field and a geometric container wall (capillary) effect. In addition, Henriksson et al.[117] found that a magnetic field could affect the orientation of the cubic phase structure formed in the $C_{12}EO_6$/water system.

The phase diagram of the $C_{16}EO_6$/water systems has been presented in Figure 4.[44,45] The large liquid-crystal domain appears upon either cooling or heating. By optical polarizing microscopy, the oily sheen stripe and the parabolic focal conic texture of the lamellar phase and the fine mosaic texture of the intermediate phase could be observed separately. Figure 6 shows the phase structures observed spectroscopically. Figure 6a shows the changes in the one-dimensional SAXS patterns as the temperature decreases in a 52 wt % $C_{16}EO_6$ system. This was used to identify the transformation L_α (50 °C) → L_α^H (35 °C) → Int. (with the space group $R\bar{3}m$ at 31 °C) → V_1 (with the space group $Ia3d$ at 29 °C) → $H_1 + L_\beta$ (25 °C). Figure 6b illustrates the phase transitions monitored by ^2H NMR upon cooling a 54 wt % $C_{16}EO_6$ sample from 50 °C.

Pertinent to the regions of lamellar and hexagonal phases are the observations in aqueous solutions of two nonionic surfactants, hexa(ethylene glycol) *cis*-13-docosenyl ether ($C_{22}EO_6$)[113] and nona(ethylene glycol) mono(11-oxa-14,18,22,26-tetramethylheptacosyl) ether ($C_{30}EO_9$).[111,112,118] A low-temperature fluid intermediate phase was found between the L_α and H_1 phases in the $C_{22}EO_6$ system, while an extensive intermediate phase (a mesh with space group $R\bar{3}m$, consisting of six connected rhombohedra) bridged a higher temperature lameller phase and a lower temperature hexagonal phase in the $C_{30}EO_9$ system. Neither $C_{22}EO_6$ nor $C_{30}EO_9$ is a normal monoalkyl nonionic surfactant. The former has a double bond in the alkyl chain, which reduces the packing efficiency in the crystalline state, and the latter should be regarded as a short diblock copolymer. However, both have long alkyl chains and EO groups, which indicate that flexibility and intermolecular interactions are the determining factors in the formation of the intermediate phases. Three different mathematical models for the $R\bar{3}m$ structure in the $C_{30}EO_9$ system were interpreted by Holmes et al.[111] to include a minimal curvature surface, a rod−box model, and a simple rod model. In addition, in the $C_{22}EO_6$ system, models of ribbons, disks, and holes were proposed to explain the L_α^H phase.[113]

Topological structures and the mechanisms of transformation in liquid-crystal phases of the different amphiphile/water systems studied have been extensively described. Funari et al.[119] present a schematic diagram of the topological changes for the $C_{16}EO_6$ system that may serve as an excellent example (Scheme 2) of the phases and changes in surfactant systems.

2.1.7. Monitoring Phase Transformations of C_nEO_m/Water Systems

In our description of the liquid crystalline phases in C_nEO_m/water systems, we have illustrated how the transformations between the different liquid-crystal phases primarily involve temperature and concentration. In these studies, deuterium NMR spectroscopy and rheology measurement are very useful in monitoring the self-transitions and shear-induced transitions of various phases[120] by monitoring quadrupole interactions between the spin of the deuterium

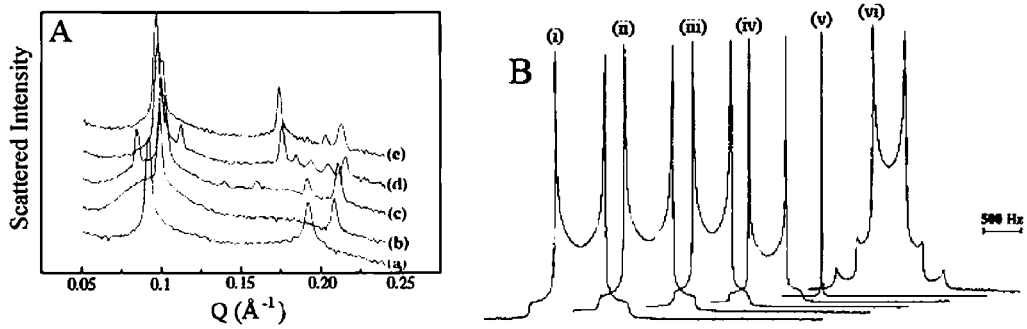

Figure 6. (A) Small-angle X-ray scattering from a 52 wt % $C_{16}EO_6$/water sample as the temperature was decreased: (a) 50 °C (L_α), (b) 35 °C (L_α^H), (c) 31 °C (Int.), (d) 29 °C (V_1), and (e) 25 °C ($H_1 + L_\beta$). (B) ^2H NMR spectra for a 54 wt % $C_{16}EO_6$ sample obtained upon cooling: (i) 50 °C (L_α), (ii) 45 °C ($L_\alpha - L_\alpha^H$), (iii) 35 °C (L_α^H), (iv) 32 °C (Int.), (v) 29 °C (V_1), and (vi) 25 °C ($H_1 + L_\beta$). Reproduced with permission from ref 45. Copyright 1997 American Chemical Society.

Scheme 2. Models of Different Phases formed by the $C_{16}EO_6$/Water System[a]

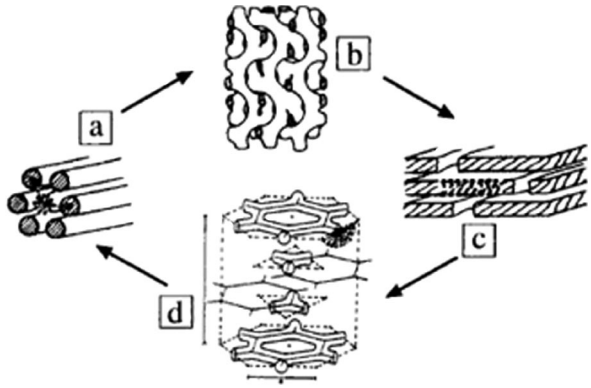

[a] Heating the hexagonal phase (a) from room temperature led to a lamellar phase via an *Ia3d* cubic structure (b). Cooling from the lamellar phase (c) initially led to an epitaxial intermediate $R\bar{3}m$ (d) before the hexagonal phase was reached. Reproduced with permission from ref 119. Copyright 1999 National Academy of Sciences of the USA.

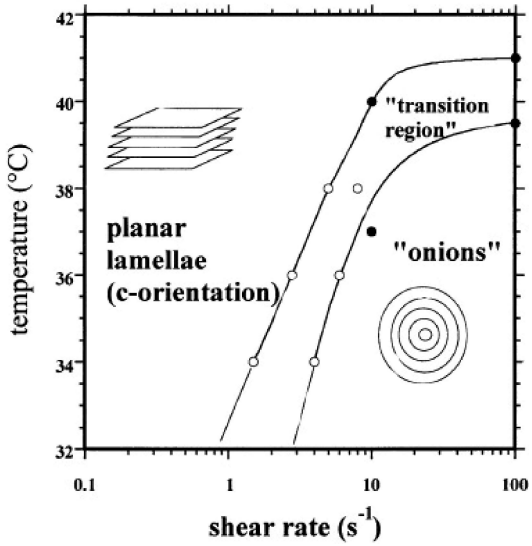

Figure 7. The partial dynamic phase diagram for a system of 40 wt % $C_{10}EO_3$ in D_2O. Open symbols represent boundaries determined from viscosity data of the present system. Filled symbols are taken from ref 109 and represent boundaries determined from rheo-SANS experiments. Reproduced with permission from ref 126. Copyright 2003 Elsevier Inc.

nuclei and the protonated surfactant structural units[121−123] and by monitoring the flow behavior and viscoelasticity of complex fluids.[124,125]

Olsson et al.[126] studied the influence of shear on the planar lamellar phase (L_α) of the $C_{10}EO_3/D_2O$ system along an isoplethal path (40 wt % $C_{10}EO_3$) in a temperature range of 25−42 °C. They determined a dynamic phase diagram using steady-rate rheometry, where shearing of the lamellar phase transformed it into multilamellar vesicles (MLVs), as shown in Figure 7. They also used rheo-SANS data of the same system from ref 109, in which the lamellae-to-onion transition as a function of temperature at fixed shear rates was studied. They found that the location of the "onions" in the dynamic phase diagram only depended on the temperature and the applied shear rate. For higher shear rates, a lamellar-to-onion transition occurs at an approximately constant temperature, while for lower shear rates the transition temperature decreases rapidly with decreasing shear rate. For a temperature around 40 °C, the influence of shear on the lamellar phase changes dramatically; above that temperature the lamellar phase remains the unchanged with the shear rate, while below 40 °C, the lamellae are transformed into onions at shear rates below 10 s^{-1}.

Using the phase diagram in Figure 7 as a guide, Olsson et al. studied the influence of the shearing rate on the lamellae structure formed in the system of 40 wt % $C_{10}EO_3$ with water by deuterium rheo-NMR spectroscopy, an effective technique in studying real-time transitions of micellar systems as a function of time in start-up experiments at several temperatures and shear rates. Figure 8 is reproduced from the results of Olsson et al.[107] The shear rate was set at 10 s^{-1} and two sets of ^2H NMR spectra as a function of time, indicating the transformation from lamellae to MLVs at 25 °C and vice versa at 42 °C, are shown in Figure 8, panels A and B, respectively. For the lower temperature, additional results from rheological and ^2H NMR measurements are shown in Figure 8C and D for comparison. They proposed two different mechanisms to depict the process of reciprocal transformation.

The transformation from planar layers to onions was found to be continuous and strain-controlled. The transition in this direction not only shows strain scaling for different shear rates at constant temperature but also exhibits approximately the same dependence on strain for different temperatures. In contrast, a discontinuous nucleation-and-growth process with a coexistence region was observed when transforming MLVs into an oriented lamellar phase. They concluded that the nature of the transitions did not depend on whether the shear rate or the temperature was changed but only on the direction of the transition. Furthermore, Olsson et al.[121] proposed the formation of random mesh phases in $C_{16}EO_6$/water and $C_{12}EO_5$/water systems based on evidence from their ^2H NMR studies. Figure 9 shows the ^2H NMR spectra of the 57.41 wt % $C_{12}EO_5/D_2O$ system in the lamellar, random mesh, and hexagonal phases as it is cooled. Recently, these authors used cryo-TEM to observe the lamellae formed directly in 40 wt % $C_{10}EO_3$ with water at 25 °C, as well as an interesting random mesh phase formed at lower temperature (<10 °C).[127] The images of the lamellar phase showed that the edges of individual bilayers and the random mesh structure had perforations distributed randomly in the bilayers.

Another interesting experiment about factors influencing the phase transitions was carried out by Bossev et al.[128] who investigated the effect of pressure on micelle phase (L_1) in a solution of 1 wt % $C_{12}EO_5$ in D_2O at 20 °C and pressures up to 3000 bar. Their SANS results revealed that pressure induced a phase transformation from a network of threadlike micelles (L_1) into hexagonally ordered bundles of cylindrical micelles (H_1). Increasing pressure caused the formation of unfavorable three-arm junctions due to the compression of the micelle hydrophobic core, leading to an unstable network. The fluidity of the core decreased under pressure, which reduces the repulsive undulation forces that offset van der Waals attractions between micelles, allowing hexagonally ordered bundles of cylindrical micelles to form.

Binary systems of C_nEO_m in aqueous solution display rich phase behavior, which can be characterized by different methods, such as cmc measurements, optical microscopy, electron microscopy, light scattering, and deuterium NMR. However, while rheology has been credited as a powerful method not only to show the macroproperties of surfactant

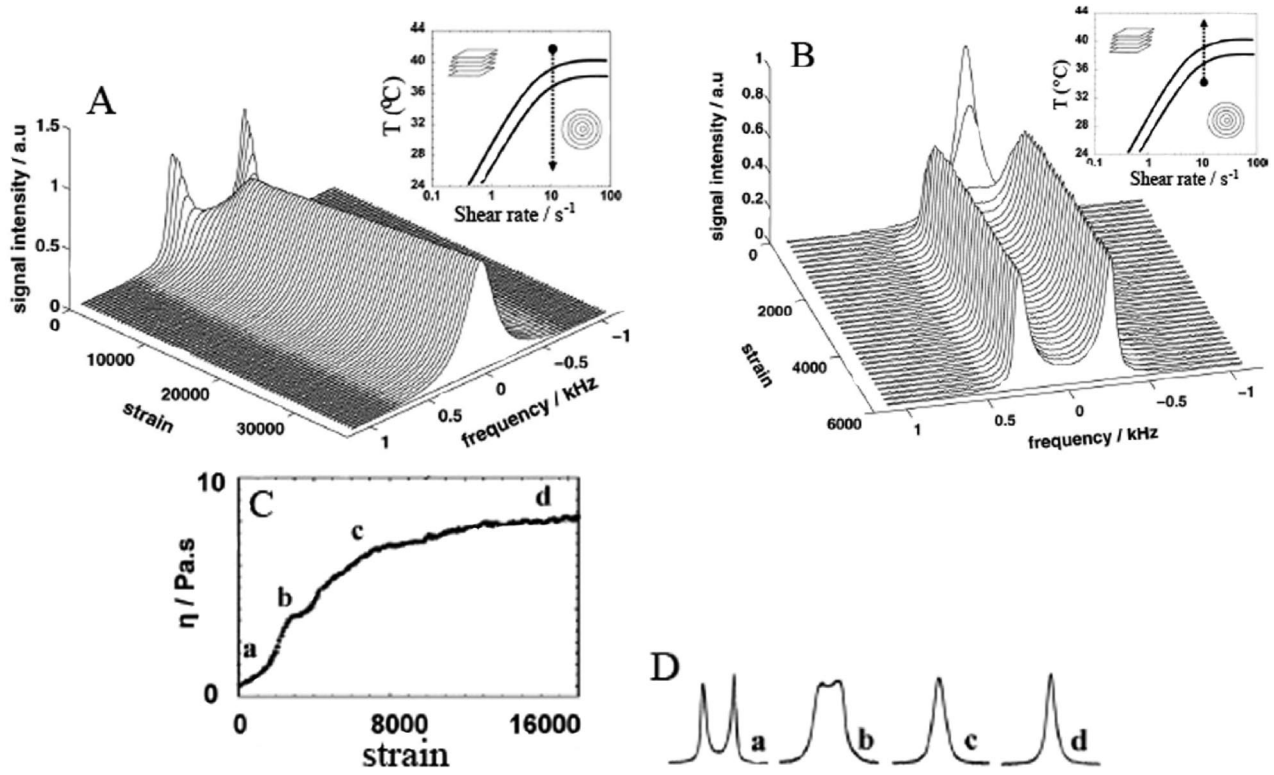

Figure 8. (A) Strain evolution of spectra during the transformation from planar layers to MLVs at 25 °C and a constant shear rate of 10 s^{-1}. Spectra were recorded every 12 s (only every second spectrum is shown) up to $t = 3600$ s (36 000 strain units). (B) Strain evolution of spectra during the transformation from MLVs to planar lamellae at 42 °C at the shear rate of 10 s^{-1}. Spectra were recorded every 20 s up to $t = 600$ s (6000 strain units). (C) Viscosity versus time curve during the MLV formation at 10 s^{-1}. (D) ^2H NMR fingerprints of the initial, intermediate, and final structures. Reproduced with permission from ref 107. Copyright 2008 American Chemical Society.

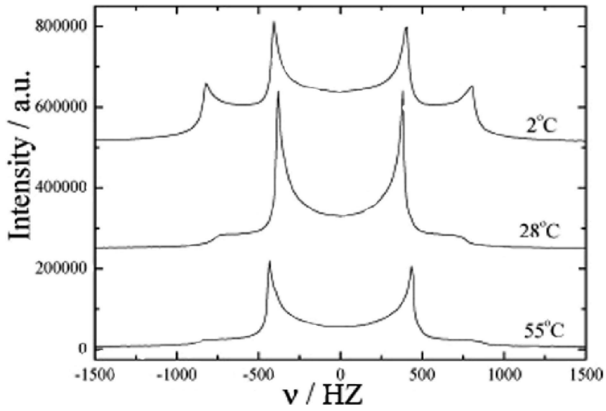

Figure 9. Quadrupolar nuclear magnetic resonance spectra recorded in the lamellar (55 °C), random mesh (28 °C), and hexagonal (2 °C) phases of a 57.41 wt % $C_{12}EO_5$ sample in ^2H_2O. Reproduced with permission from ref 121. Copyright 2006 American Chemical Society.

Scheme 3. (a) Ethylammonium Nitrate (EAN); (b) R = $-CH_3CH_2$, $X^- = [(CF_3SO_2)_2N]^-$, 1-Ethyl-3-methylimidazolium Bis(trifluoromethylsulfonyl)imide ([emim]Tf_2N); R = $-CH_3(CH_2)_3$, $X^- = Cl^-$, 1-Butyl-3-methylimidazolium Chloride ([bmim]Cl); R = $-CH_3(CH_2)_3$, $X^- = PF_6^-$, 1-Butyl-3-methylimidazolium Hexafluorophosphate ([bmim]PF_6); R = $-CH_3(CH_2)_3$, $X^- = BF_4^-$, 1-Butyl-3-methylimidazolium Tetrafluoroborate ([bmim]BF_4)

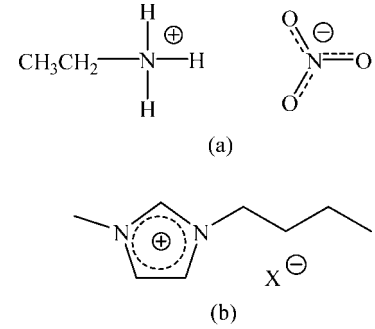

systems but also to confirm the microstructures of complex fluids,[129−132] the detailed rheological behavior of different phase states has been rarely reported.[133]

2.2. Self-Assembly of C_nEO_m Surfactants into Lyotropic Liquid Crystals in Room-Temperature Ionic Liquids

Room-temperature ionic liquids (RT-ILs) are a special class of organic salts that are liquid around room temperature. They are regarded as "green solvents" when used as media in organic synthesis, chemical separations, and catalysis, due to their low vapor pressure, high thermal stability, nonflammability, high conductivity, and tunable physical properties by selection of cation, anion, and substitutents. Amphiphilic molecular self-assembly in RT-ILs is a new and growing research field, which will undoubtedly open RT-ILs to additional applications. Hao et al.[17] and Drummond et al.[18] have reviewed the self-assembled structures and chemical reactions in room-temperature ionic liquids. Reports show that amphiphilic molecules are able to form micelles,[134−136] vesicles,[137,138] microemulsions[139,140] and lyotropic liquid crystals[141−143] in RT-ILs, analogous to those in water. The chemical structures of the RT-ILs considered here are shown in Scheme 3.

2.2.1. Self-Assembly of C_nEO_m in Imidazolium Ionic Liquids

Studies on self-assembled structures obtained from C_nEO_m nonionic surfactants in imidazolium ionic liquids have only recently been reported. Armstrong et al.[136] published the first observation of self-assembly of C_nEO_m into micelles in imidazolium ionic liquids in 2003. Dissolution of the nonionic surfactants Brij35 ($C_{12}EO_{23}$) and Brij700 ($C_{18}EO_{100}$) in [bmim]PF_6 or [bmim]BF_4 decreases the surface tension of RT-ILs in a manner analogous to aqueous solutions. In these mixtures, micelles begin to form in the bulk solution at C_nEO_m concentrations above the cmc, which is estimated easily by surface tension measurements. However, the cmcs obtained in C_nEO_m/IL solutions are far higher than those in C_nEO_m/water systems. Inverse gas chromatography (IGC)[144] was used to show that solvophobic interactions between RT-ILs and the hydrocarbon portion of the C_nEO_m surfactant cause the aggregation behavior.

Though the determination of a cmc is somewhat ambiguous as the primary evidence for aggregation, it is helpful to identify that aggregates are able to form in the bulk solution. For instance, cmc values of about 115 and 20 mmol·L^{-1} for Brij35 and Brij700 in [bmim]PF_6, respectively, have been identified repeatedly by different techniques such as a solvochromic probe[145] and near-infrared (NIR) spectroscopy.[146] In addition, Patrascu et al.[147] compared micelles formed with C_nEO_m ($n = 12-16$; $m = 4-8$) in water and [bmim]BF_4. Smaller surfactant aggregation numbers in [bmim]BF_4 compared with water are observed, an observation always linked to higher cmcs in [bmim]BF_4. Surprisingly, the area per molecule is also smaller in [bmim]BF_4 than in water, even though there is no strong lateral repulsion between headgroups in room-temperature ionic liquids.

Recently, the cloud point phenomenon has been investigated systematically for solutions of C_nEO_m ($n = 10-14$, $m = 5-7$) in [bmim]BF_4.[148] The cloud point increased with larger EO headgroups: specifically, stronger solvophilicity of C_nEO_m led to a higher cloud point temperature. In contrast, the cloud point decreased with an increase in the hydrocarbon chain length. This demonstrates that the solvophilicity/solvophobicity property of C_nEO_m surfactants in RT-ILs arises from a balance of EO group and alkyl chain. In particular, the effect of hydrocarbon chain length on the cloud point was much stronger for the RT-IL systems than for aqueous systems. The tendency of the cloud point changes with surfactant concentration was similar in water or RT-ILs, however, the minimum cloud point in RT-ILs was lower than that in water. Another common feature of these systems was that the micelles grew as the temperature increased below the cloud point of a mixture.

At present, there have been no mesophases observed for C_nEO_m in imidazolium ionic liquids at any temperature and concentration, unlike water. However, formation of a liquid crystal phase was reported when the binary system of C_nEO_m with imidazolium ILs contained excess water. Friberg et al.[149] studied the ternary system of $C_{12}EO_4$, [bmim]PF_6, and water by visual observation and small-angle X-ray diffraction (SAXD) measurements. The system showed a lamellar liquid crystal phase solubilizing [bmim]PF_6 to a maximum of 15%. The [bmim]PF_6 was localized to just within the polar part of the layered structure of a lamellar phase, without changing the dimensions of the amphiphile layer or the interlayer spacing. A similar technique was applied later by Wang et al.[150] who identified the existence of both lamellar and hexagonal liquid crystal phases in Brij97/[bmim]PF_6/water and Brij97/[bmim]BF_4/water ternary systems using small-angle X-ray scattering (SAXS), polarized optical microscopy (POM), and rheological techniques. Figure 10 shows the phase diagrams for the two systems. Note that Brij97 is a $C_{18}EO_{10}$ nonionic surfactant with a double bond at the C_9-C_{10} position.

There are three driving forces for the phase behavior in C_nE_m/imidazolium ionic liquid systems: the interaction between the hydrocarbon chain and ILs, strong hydrogen bonding between EO groups and the BF_4^- or PF_6^- anions, and possible interactions between the cationic unit (-N^+) of the ILs and the lone pairs on the oxygen atoms of the EO groups. SAXS data showed that [bmim]PF_6 predominantly penetrated between the EO groups of Brij97 molecules, which causes an increase in the effective equilibrium area per surfactant molecule at the hydrophile−lipophile interface. In contrast, [bmim]BF_4 was localized in the water layer of the hexagonal phases and resulted in an increase in the thickness of the water layer between cylinders. The rheological behavior was also examined with a cone−plate sensor. The frequency dependence of the storage modulus G' and loss modulus G'' for classical hexagonal liquid crystalline phases was demonstrated, as shown in Figure 11. At low frequencies, $G'' > G'$, and the hexagonal sample showed viscous behavior, while at higher frequencies, $G' > G''$, and the sample exhibited viscoelastic behavior.

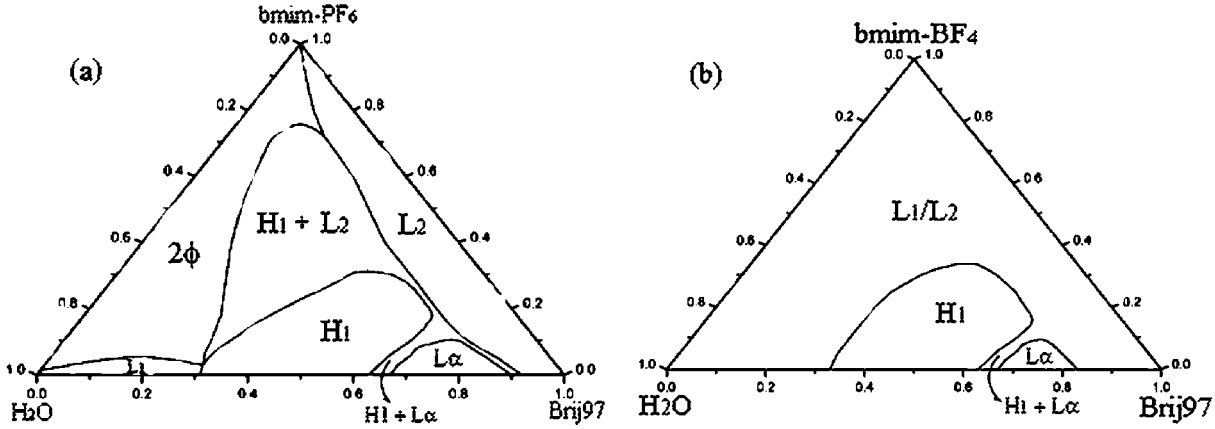

Figure 10. Phase diagrams for (a) Brij97/[bmim]PF_6/water and (b) Brij97/[bmim]BF_4/water at 25 °C: L_1, isotropic solution (water-rich); L_2, isotropic solution (Brij97-rich); L_α, lamellar liquid crystal phase; H_1, hexagonal liquid crystal phase. Reproduced with permission from ref 150. Copyright 2005 American Chemical Society.

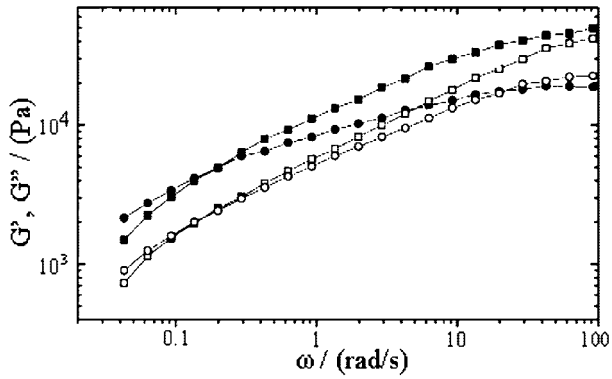

Figure 11. Storage (square) and loss (circle) modulus as a function of angular frequency for 50/20/30 wt % of the Brij97/[bmim]BF_4/water system (filled) and Brij97/[bmim]PF_6/water system (hollow). Reproduced with permission from ref 150. Copyright 2005 American Chemical Society.

2.2.2. Self-Assembly of C_nEO_m in Ethylammonium Nitrate

Compared with most other ILs of current interest, the chemical properties of ethylammonium nitrate (EAN) are the closest to water. EAN at room temperature is proposed to form a three-dimensional hydrogen-bond network, an essential feature in supporting self-assembly.[151] The existence of micelles formed by surfactants in EAN,[134,135] as well as lamellar liquid crystals[141−143] formed by lipids, was reported over 20 years ago. Since then there have only been rare reports considering the behavior of C_nEO_m surfactants in EAN. Warr et al. have recently published a series of pioneering studies on the self-assembly of nonionic C_nEO_m into lyotropic liquid crystals,[19] microemulsions,[20] and micelles[21] in EAN. Two typical phase diagrams of the binary $C_{16}EO_6$/EAN and $C_{18}EO_6$/EAN systems are shown in Figure 12.

These authors found a similar mesophase sequence of lyotropic liquid crystals in each binary system. The relative size of alkyl chains versus the EO headgroups plays an important role in the phase formation, following expectations for aqueous solution. Generally, a C_nEO_m must have hydrocarbon chains longer than C_{12} to form liquid crystal phases in EAN,[19] but only longer than C_8 in water,[9,24] due to the solvophobicity difference of the hydrocarbon portion. $C_{14}EO_m$ in EAN showed some evidence of lyotropic liquid crystal phase formation. A hexagonal phase in $C_{14}EO_8$ and a lamellar phase in $C_{14}EO_4$ were observed at low temperature. Considering surfactants with longer alkyl chain lengths, both $C_{16}EO_m$ and $C_{18}EO_m$ in EAN exhibited the full range of common phases analogous to those in water, including L_1, I_1, H_1, V_1, and L_α phases. Another determining factor for the existence of liquid crystal phases is related to hydrogen bonding between EO headgroups and solvent, in this case, EAN. For $C_{18}EO_m$, only lamellar phases were formed with the surfactants with the smallest solvophilic ethoxy chains and hence the lowest spontaneous curvature (highest surfactant-packing parameter), for example, $C_{18}EO_2$ and $C_{18}EO_4$. Increasing the ethoxy groups to $C_{18}EO_6$ produced H_1 and V_1 phases, but these melted at temperatures lower than L_α, suggesting that low curvature was still preferred. However, upon increasing the ethoxy group to $C_{18}EO_8$, the lamellar phase melted at a lower temperature than the hexagonal phase. In summary, binary C_nEO_m/EAN systems have many features in common with C_nEO_m/aqueous systems, including phase behavior, cmc, and cloud point phenomena.

Recently, Warr et al.[21] used SANS measurements to study conventional micelle formation in C_nEO_m/EAN binary systems as a function of alkyl and EO headgroup, concentration, and temperature. The structure of the micelles in EAN was similar to those in water; increasing the alkyl chain length caused an enhancement of the surfactant solvophobicity, leading to a decrease in the cmc. As the EO headgroup increased at constant alkyl chain length, the micelles transformed from rods to spheres. This phenomenon was clearly seen in $C_{14}EO_m$ and $C_{16}EO_m$ surfactant systems as the number of EO units changed from four to six. The micelles in EAN also grew into rods at higher temperature as their cloud point was approached.

In the studies of C_nEO_m in EAN or imidazolium ionic liquids, it is clear that the self-assembly of the amphiphilic molecules is related to the solvophobic effect, which is smaller in EAN than in water. Unlike ionic surfactants, there are no exotic salts or counterions in the C_nEO_m/IL systems, but the presence of H-bonding between EO headgroups and ILs leads to the higher solubility of the surfactant. The phase behavior is rich and is affected by many factors as described above. In addition, there is much that remains to be explored, including the mechanisms of phase formation, the process of phase transitions, and the interesting effect of the addition of water in some ILs. The addition of water changes the polarity of the mixture and is accompanied by changes in the microstructures of C_nEO_m/ILs.

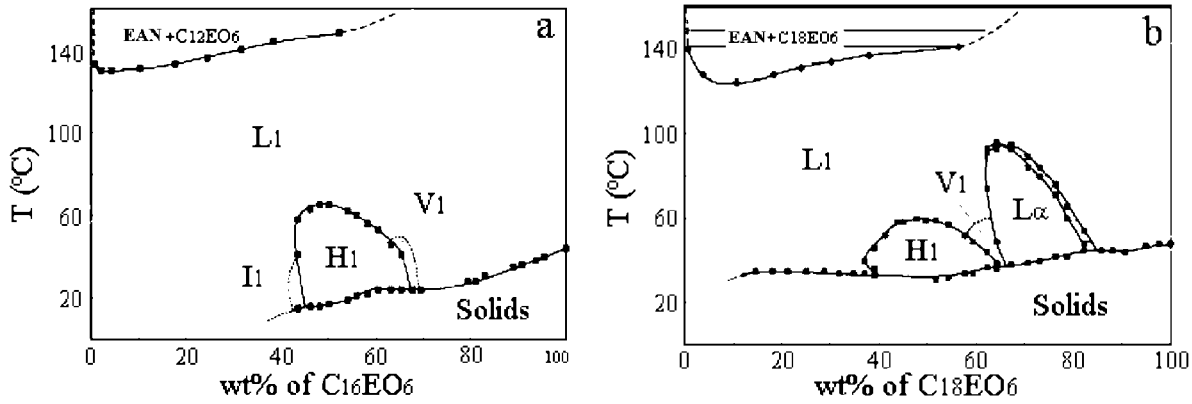

Figure 12. Phase diagrams of the binary $C_{16}EO_6$/EAN (a) and $C_{18}EO_6$/EAN (b) systems, showing a large single-phase isotropic (L_1) region, along with discrete cubic (I_1, in $C_{16}EO_6$/EAN system), hexagonal (H_1), bicontinuous cubic (V_1), and lamellar phases (L_α). Dashed lines indicate approximate phase boundaries determined for the smaller lyotropic phases, and horizontal hatching denotes tie lines for two-phase coexistence. Reproduced with permission from ref 19. Copyright 2005 American Chemical Society.

2.3. Self-Assembly of C_nEO_m in Other Nonaqueous Solvents

In recent years, the study of nonionic surfactants in nonaqueous solvents has expanded rapidly. This has been due to the interest in the study of the basic properties of amphiphile aggregates, for example, the hydrophobic effect on the formation of micelles. It is useful to compare surfactant properties in these media to those in pure water. There is also particular application to processes that are prevented from the use of water in certain chemical reactions and some industrial applications. However, compared with the reports in aqueous solution, those in nonaqueous solution are still relatively rare. Some properties of nonaqueous solvents, such as their high dielectric constant and higher viscosity, as well as their poor miscibility with nonionic surfactants, present some difficulties in detecting the aggregates in nonaqueous solvents using conventional technologies.[152,153] Hence, a limited amount of work about the solution behavior of C_nEO_m surfactants in nonaqueous solvents has been reported in the past 20 years. This review will introduce and discuss the aggregation of C_nEO_m nonionic surfactants in three solvent types: supercritical carbon dioxide ($ScCO_2$), ethylene glycol (EG), and formamide.

2.3.1. C_nEO_m in Supercritical Carbon Dioxide

Supercritical carbon dioxide is an attractive solvent alternative to volatile organic compounds (VOCs) since it is environmentally benign, essentially nontoxic, recyclable, readily available, and easily removable. As a solvent, the properties of $scCO_2$, such as density, viscosity, and dielectric constant, are tunable through small changes in temperature or pressure; $scCO_2$ has moderate critical conditions and is easily accessible (31 °C and 73.8 bar).[154,155] Furthermore, $scCO_2$ is nonflammable, inexpensive, plentiful, and importantly one of the few solvents not regulated as a VOC by U.S. Environmental Protection Agency (EPA). Hence, $scCO_2$ is well suited to "green" applications, especially in the food and pharmaceutical industries.[156,157] However, $scCO_2$ is generally a very poor solvent for polar and high molecular weigh solutes, which limits its wide application. One effective strategy to overcome this limitation has been to solubilize insoluble solutes within reverse micelles or microemulsions formed with surfactants in a CO_2-continuous phase.[158,159] Unfortunately, most of the commercially available conventional hydrocarbon surfactants are insoluble in CO_2[160] while fluorinated surfactants,[161] custom-designed amphiphiles, and polymers[155−158,162] can be effectively dissolved in $scCO_2$. In contrast, C_nEO_m nonionic surfactants are found to be highly soluble in $scCO_2$.[163−165] Liu et al.[163] found that $C_{12}EO_4$ can dissolve in $scCO_2$ (313.15 K, 19.65 MPa, $C_{C_{12}EO_4} = 2.92$ wt %) and the solubility was dependent on pressure and temperature. The solubility of $C_{12}EO_4$ increases with increasing pressure (or density) of CO_2 at constant temperature and increases with temperature at a constant density of CO_2. The next question was whether C_nEO_m nonionic surfactants can assemble into any aggregates in $scCO_2$. Smith et al.[164] found that $C_{12}EO_3$ and $C_{12}EO_8$ could form small aggregates in $scCO_2$ by FT-IR. At 40 °C, the small aggregates of $C_{12}EO_3$ contain 4.0 surfactant molecules per aggregate at 417 bar, while those of $C_{12}EO_8$ have 2.5 molecules per aggregate at 450 bar. This may represent the formation of premicelles in $scCO_2$. However, Eastoe et al.[165] did not detect the presence of any aggregates in the $C_{12}EO_5$/CO_2 system by high-pressure SANS up to 12 vol % surfactant. Despite the experimental or technological hurdles, the assembly of C_nEO_m nonionic surfactants is deservedly studied. Of course, it is also found that the addition of water,[166] alcohol,[163,167] or alkane[165] can significantly enhance the solubility of C_nEO_m in $scCO_2$ and may induce the formation of micelles.

2.3.2. C_nEO_m in Ethylene Glycol

Ethylene glycol (EG) is thought to be a good alternative nonaqueous media for investigating the aggregation of surfactants because EG has similar properties to water; that is, it has high cohesive energies, high dielectric constant, and hydrogen-bonding ability.[168] Of particular interest is hydrogen bonding, since it is generally recognized as a requirement for micellization;[169] indeed, micelles[170] and liquid crystals[171] have been reported to form with cationic surfactants in EG. Recently, the aggregation of C_nEO_m in pure glycol solvents has attracted attention, and Eastoe et al.[152,172−174] have completed comprehensive studies. A series of C_nEO_8 nonionic surfactants ($n = 12, 14, 16$) were dissolved in pure EG and propylene glycol (PG), and the cmc and aggregate structures were determined by surface tension and SANS measurements, respectively.[152] The cmc value in EG is ~0.2 M for $C_{12}EO_8$, which is much higher than that in pure water and also allows the formation of micelles in EG. The SANS data indicate that the micelles formed by $C_{12}EO_8$ tend to change from spheroidal into prolate ellipsoids as water is gradually exchanged for pure EG.[173] When C_nEO_m nonionic surfactants are dissolved in pure EG, they exhibit similar behavior to that in water. On the other hand, PG exhibits distinctly different properties for $C_{12}EO_8$. When $C_{12}EO_8$ is dissolved in pure PG, no significant adsorption or aggregation behavior nor any detectable cmc can be found, and the SANS signals are very weak.[152,173,174] Hence, appropriately mixing EG and PG with C_nEO_m and tuning solvent and surfactant identities may be an effective way to control the formation of aggregates in nonaqueous systems.[174] Finally, the addition of water in EG or PG with C_nEO_m also provides a strategy to induce changes in adsorption and aggregation behavior; this approach is widely studied and will be described in section 3.2.7.

2.3.3. C_nEO_m in Formamide

Formamide possesses analogous properties to water and EG and was used earlier than EG to substitute for or compare with water in investigating the solubilization, adsorption, and aggregation behavior of surfactants. Most studies have focused on the micellization of surfactants in formamide, especially the ionic surfactants. Results indicate that micellization takes place above the Krafft point of an ionic surfactant, for example, hexadecyltrimethylammonium bromide (CTAB) and sodium dodecyl sulfate (SDS) aggregate in formamide at temperatures above 43 and 55 °C, respectively.[175] The cmc values for these surfactants, 0.09 M for CTAB and 0.22 M for SDS, were obtained at 60 °C by surface tension measurements. Micelle formation in formamide is mainly driven by strong hydrogen-bond interactions with the surfactant and the high dielectric constant of the solvent. This observation was confirmed by comparing surfactant solutions in formamide, *N*,*N*′-dimethylformamide, and *N*,*N*′-dimethylacetamide; the latter solvents possess

medium dielectric constants and weak hydrogen-bonding characteristics.[176]

NMR[177] and SAXS[178] measurements have demonstrated the existence of spherical micelles in the CTAB/formamide binary system. However, there has been only a limited amount of work on solutions of nonionic surfactants in formamide. A nonionic PEO−PPO block polymer was found to display a cloud point phenomenon (phase separation) in formamide.[49] Surprisingly, another block polymer, $(PEO)_{37}-(PPO)_{58}-(PEO)_{37}$, was found to exhibit rich phase behavior in formamide by SAXS.[179] In this case, increasing polymer concentration led to the observation of micellar, micellar cubic, hexagonal, bicontinuous cubic, and lamellar phases over the range of 20 to 80 °C. The author proposes that the occurrence of these phases is related to the high solubility of both PEO and PPO in formamide and the ratio of PEO and PPO in the block polymer. At present, studies of phase behavior of C_nEO_m nonionic surfactant in pure formamide have only been performed by a few research groups, such as Warnheim et al.[56,153,180] and Couper et al.[181] Analogous to the corresponding aqueous systems, $C_{12}EO_m$ (m = 3, 4, and 6) systems also exhibit lower consolute temperatures in pure formamide[56,180,181] and are also strongly temperature dependent. For the $C_{12}EO_3$/formamide system, a lower consolute curve occurs with a minimum temperature near 16 °C for the critical concentration, about 10 wt % surfactant.[56] Micelles, but no liquid crystal phases, form in the $C_{12}EO_m$ (m = 3, 4, and 6)/formamide systems, which have been detected by surface tension and NMR self-diffusion measurements. These measurements also show that the cmc values of these surfactants in formamide are several orders of magnitude higher than those in water; for example, $C_{12}EO_4$ has cmc = 0.064 mM in H_2O but 25 mM in formamide.[147,153] The micelles were shown to be smaller in formamide than in water since there was no sign of aggregate growth when the temperature was varied to approach the cloud point.[153] The $C_{16}EO_m$ (m = 4, 6, and 8) series follows a similar but less complex phase behavior in formamide, but in contrast to that in aqueous systems, the formation of liquid crystal phases is found in formamide systems. Specifically, $C_{16}EO_4$ exhibits a lamellar phase near 60 wt % surfactant, $C_{16}EO_6$ a hexagonal phase over the range of 40−60 wt % surfactant, and $C_{16}EO_8$ a micellar cubic phase and a hexagonal phase between 40 and 80 wt %. The observation of only liquid crystal phases also indicates that formamide complements aqueous studies and is a good substitute for water.

The studies above provide a picture of the basic considerations of C_nEO_m nonionic surfactant phase behavior in nonaqueous environments and indicate that such studies provide important insight into the corresponding aggregation in water, for example, cloud point and micellization. Cloud point phenomena are usually ascribed to the interactions between surfactant and solvent, namely, the dehydration of EO headgroups,[49] and micellization may also be related to the hydrogen-bonding characteristics of the solvent.[176] Finally, we note that reports regarding C_nEO_m in other nonaqueous solvents or cosolvents, such as glycerol,[182] hydrazine,[183] and DMSO, are relatively rare and represent a potential growth area for future nonionic surfactant research.

3. Ternary Mixed Systems

Ternary mixed systems of C_nEO_m/water with additives, such as oil, salts, ionic surfactants, homologous poly(oxyethylene) nonionic surfactants, or polymers, exhibit more complex phase behaviors. The combination of these additives and C_nEO_m surfactants usually results in synergistic effects, leading to variations of the phase behavior, aggregation microstructures, and physicochemical properties, compared with simple binary C_nEO_m/water mixtures. This section covers recent reports on the properties of ternary mixed systems, their microstructures, and their phase behavior in bulk solution.

3.1. Ternary Systems of C_nEO_m/Water/Inorganic Salts

In section 2.1.4, it was noted that two different trends are observed in the micelle length in $C_{16}EO_6$/water systems in the presence of the inorganic salts, NaSCN and NaCl. Namely, in the presence of the former salt the micelle length increased and then decreased with temperature, while in the presence of the latter, the micelle length only decreased.[75,82] The reasons for these effects are not exactly understood but are related to the salt effect, because NaSCN is a salting-in type while NaCl is a salting-out type. In this section, theories of the inorganic salt effect on surfactant systems and salt effects on the cmc, cloud point, surface tension, and the phase behavior in C_nEO_m aqueous solutions are presented from the recent literature.

3.1.1. Theories of the Inorganic Salt Effect

Salt effects are ubiquitous in colloid and interface science. On the whole, different salts induce either salting-out or salting-in effects, which are now generally used to denote, respectively, an increase or a decrease in the activity coefficient of the nonelectrolyte with increasing concentration of electrolyte.[184] The mechanisms at work in brine solutions have been studied more widely than those in other liquid solutions, and a series of theories have been proposed to explain the differences. According to Long and McDevit,[184,185] there are four main theories to explain salt effects in solution. The first is hydration theory, namely, the salting-out effect may arise from the removal of water molecules from their solute role due to the hydration of salt ions. In another line of thought in hydration theory, the preferred orientation of water molecules in the hydration shell around ions promotes nonelectrolyte solubility. Second, salt effects may be accounted for by electrostatic interactions, namely, salt ions influence the ion atmosphere of the solute and the dielectric constant of the solvent, and then the incremental increase or decrease of electrostatic forces causes the salt effects. The third possibility for the salt effect focuses on van der Waals forces, primarily dispersion forces, as being responsible for the specific salt effects of large ions. This has been especially studied by Ninham et al.[186] Finally the effect of internal pressure of the solution may account for salt effects. Specifically the degree of salting-out or salting-in of a nonpolar solute is determined by the extent to which the solvent medium is compressed or loosened when ions are present; extra pressure increases the activity of the nonpolar molecules in the mixture and causes the salting-out effect. This summary of four theories is oversimplified, but sufficient to highlight their development. The theoretical details and their relative merits should be assessed using the original papers. In practical terms, electrolyte addition to surfactant systems causes changes in electrostatic interactions and the internal pressure of the solution.

The addition of inorganic electrolyte to aqueous solutions of *ionic* surfactants will decrease the surface tension and the critical micelle concentration because of the increase in electrostatic interactions; that is, counterions will compress the ionic atmosphere of the headgroup, reducing the repulsive forces between the head groups, thus promoting surfactant absorption on the solution surface to continue forming micelles in the bulk solution.[187−190] However, salt effects on *nonionic* surfactant aqueous solutions are different, due to the absence of charge interactions among the nonionic surfactants. Salts primarily influence the hydrophobic chains of nonionic surfactants by salting-out and salting-in effects.[191−194] In addition, electrolyte addition may disrupt hydrogen bond formation between the oxygen atoms of EO headgroups and water, causing a decrease in hydration of EO headgroups;[193,195] however, this effect is much less than that on the hydrophobic chains.

The Hofmeister series of ions can be qualitatively and quantitatively used to distinguish salt effects, as has been reported commonly in the literature.[196−201] Established for more than a century, Hofmeister showed that the log[solubility] of proteins in brine solutions depends linearly on salt concentration.[196,202] The theory includes three parts, where initially the effects of ions on a liquid mixture can be considered as "solvent sorting by ions".[203,204] Most inorganic salts decrease the water solubility of organic solutes (salting-out), while some salts (NaI, $NaClO_4$, and NaSCN) increase it (salting-in). The salting-out effectiveness of the common inorganic anions follows approximately the series $SO_4^{2-} > HPO_4^{2-} > CO_3^{2-} > F^- > Cl^- > Br^- > NO_3^- > I^- > ClO_4^- > SCN^-$; the common cation series is $K^+ > Na^+ > Li^+ > Ca^{2+}$.[197,198] Second, the effect arising from the nature of cations is usually smaller than that from anions. Finally, the Hofmeister series is general and does not depend on the nature of the organic solutes, whether alcohols, proteins, nonionic surfactants, or other solute.

Why is the Hofmeister series observed, even though some of the ions have the same valence? Four explanations for this phenomenon have been proposed. The first perspective proposes that salts affect the "solvent quality" of water.[201,203,205−207] The Hofmeister series can be thought to be the sequence of agents that are increasingly able to disrupt water structure and weaken hydrophobic interactions. For the Hofmeister sequence of anions, ions to the left of NO_3^- reduce the solubility of organic solutes by enhancing their crystallization. They are generally called salting-out ions, lyotropic ions, or "water-structure makers". The ions to the right side of NO_3^- have the opposite effect and are referred to as salting-in ions, hydrotropic ions, or "water-structure breakers". Thus, the characteristics of the ions can be summarized. The salting-out ions are usually small and have relatively small polarizability, have high electric fields at short distances, and lose their water of hydration with great difficulty; the salting-in ions have the opposite characteristics.

A second approach to explain the Hofmeister series posits that the salting-out and salting-in phenomena have an interfacial origin.[204] Salting-out ions desorb at the water−organic solute interface while salting-in ions absorb, which produces an increase in the solute free energy and, thereby, modifies the phase equilibrium. A model relating to the increase of the monolayer spontaneous curvature due to salt depletion at the nonionic surfactant monolayer was proposed by Kabalnov et al.,[204] who showed that the salting-out effect was driven by a depletion of ions at the surfactant interface monolayer.

According to a third idea, dispersion forces between ions and surfaces play an important role in specific ions' effects.[186,208−210] The dispersion potential of an ion depends not only on the charge but also on the excess polarizability and the electronic structure of the ion. Different ions in solution have different polarizabilities, which differ from the polarizability of the surrounding water. The excess polarizability gives rise to ion-specific dispersion forces toward or away from interfaces. The Hofmeister effect depends markedly on the anion rather than the cation, due to the greater polarizability and greater variation in the polarizability of anions.

The final proposal for the Hofmeister series is related to an individual ion's ability to penetrate into the alkyl chain environment of the monolayer, thus disrupting hydrocarbon packing and causing an attenuation of surface potential.[211] For the Hofmeister series, those ions to the left of NO_3^- show relatively little tendency to insert into the monolayer, while those on the right side exhibit facile penetration. So, ions that most efficiently partition into the monolayer will cause the greatest attenuation of the potential, while those that are excluded show the least effect.

3.1.2. Salt Effects on the Formation of C_nEO_m Micelles

Micelle formation, expressed usually by reference to the critical micelle concentration, is one of the most important properties of aqueous surfactant solutions. Salting-out ions decrease the cmcs of nonionic C_nEO_m surfactants and increase the attractive interactions between micelles. This salting-out leads to an increase of the micelle aggregation number and subsequently to the formation of larger micelles; conversely, salting-in ions have an opposite effect. The various salts' effects on the cmcs are approximately in accord with the Hofmeister series; however, few experimental papers have come to this conclusion directly.[39,194,212,213] A general statement of the trend was deduced by considering the observed salt effects on nonionic surfactants, such as alkylphenoxy polyethyleneoxide (C_nPhE_m)[193,194] and PEO/PPO/PEO block copolymers.[214−218] For example, Schott et al.[212,213] summarized experimental data from studies of cloud point, surface tension, and critical micelle concentration of nonionic surfactants in aqueous solution comparing the salting-in effect of di- and trivalent cations with the salting-out effect of sulfate ions. They proposed that the surfactant poly(oxyethylene) chains act as polydentate ligands for the cations in the solution.

Schick et al.[39] studied salt effects on the micelle structure of nonylphenol (C_9PhEO_{50}) and octadecanol poly(oxyethylene) ($C_{18}EO_{100}$) surfactants. Addition of electrolyte increased the aggregation number of the C_9PhEO_{50} micelles. The increase is proportional to the salt concentration but is inversely proportional to the lyotropic number of ions. The effect of variation in the lyotropic number resulting from added anions is more pronounced than that of cations, in line with the Hofmeister theory. However, upon NaCl addition, the aggregation number of $C_{18}EO_{100}$ decreases markedly with salt concentration. The aggregation behavior of another nonionic surfactant, C_8EO_5, in the absence and the presence of sodium halides was studied by time-resolved fluorescence quenching.[219] In this study, the surfactant aggregation number increases with temperature below the

cloud point, while the addition of salt amplifies the increase. The cause of the difference between $C_{18}EO_{100}$ and C_8EO_5 systems in the presence of sodium halides is still ambiguous. In addition, a quasi-elastic light scattering experiment showed that the apparent hydrodynamic radius of the C_8EO_5 micelles increased upon addition of NaCl.[220] In the C_nEO_7 (n = 12, 14, 16)/water micelle systems, Imae obtained similar results, in which both the aggregation numbers and the apparent hydrodynamic radii increased upon addition of NaCl.[221,222]

The effects of inorganic salts on $C_{12}EO_7$ micelles were investigated by measuring charge-transfer interaction between $C_{12}EO_7$ micelles and 7,7,8,8-tetracyanoquinodimethane in aqueous solution. Charge-transfer interactions showed whether addition of salts caused tightening or loosening of the micelles.[223] The compactness of $C_{12}EO_7$ micelles increased with the addition of LiCl, NaCl, KCl, KBr, and K_2SO_4, but decreased with the addition of KNO_3 and KSCN.

Several mechanisms can describe salt effects on micelles and are also adequate to explain C_nEO_m systems. For instance, McDevit−Long theory[184,185] evaluates the salt effects based on the activity coefficients of the surfactant hydrocarbon tails (their nonpolar portions). Alternatively, Mukerjee[191,192] uses a mass-action model for micelle formation, assuming a chemical equilibrium of the association of monomers and monodisperse micelles. This model of the salt effect on micelles can be described by

$$\ln \mathrm{cmc} = A - K_S c_S \quad (1)$$

where A is a constant relating to the nonelectrolyte, c_S is the salt concentration, and K_S is the salt addition coefficient with respect to the polar and nonpolar parts of the surfactant molecule in solution and in the micelle. With a mass-action model of micellization, the salt effect can be explained as being primarily related to the hydrophobic hydrocarbon moiety; that is, the salts decrease the solubility of the alkyl moiety in brine solution rather than affecting the EO headgroup.

Gordon[224] used a two-phase model for micellization to interpret salt effects, where micelle formation is considered as surfactant separation from the solution to form another phase, namely, a phase-separation phenomena. Then, the contribution of the poly(oxyethylene) headgroup plays a primary role. However, from experimental data, a more responsible interpretation, which has been widely accepted, is that of Mukerjee,[191,225] but neglecting the EO group.[193]

Blankschtein et al.[194] have proposed a third mechanism for the salt effect by investigating the cmc, surface tension, salt constant, and free energy of micellization in $C_{10}EO_6$, $C_{12}EO_6$, and $C_{12}EO_8$ aqueous solutions containing LiCl, NaCl, KCl, KBr, and KI. Their work also supports the idea that the salt effect depends on the alkyl moiety, but they ascribed various molecular contributions to the micellization process considering free-energy changes rather than activity coefficients based on blending a molecular theory of micellization[226] with a thermodynamic free-energy description of the collective macroscopic phase behavior of the micelle solution.[227]

3.1.3. Salt Effects on the Cloud Point and Phase Behavior of C_nEO_m in Aqueous Solution

Similar to the effect on cmc, salting-out ions decrease the cloud point in C_nEO_m/water systems, while the addition of salting-in ions increases the cloud point. Weckström et al.[228,229] investigated the lower consolute boundaries of the nonionic C_8EO_5 surfactant in aqueous solution in the presence of the monovalent salts NaF, NaCl, NaBr, NaI, KC1, CsCl, and LiCl. Figure 13 shows the cloud-point temperature of aqueous C_8EO_5 as a function of salt molarity.[228]

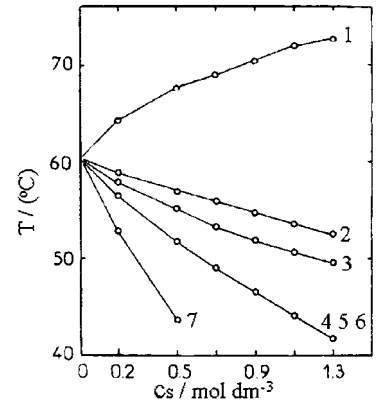

Figure 13. Cloud-point temperatures of aqueous C_8EO_5 solutions (2 vol %) versus salt molarity for the following salts: (1) NaI, (2) NaBr, (3) LiCl, (4) NaCl, (5) KCl, (6) CsCl, and (7) NaF. Reproduced with permission from ref 228. Copyright 1985 Royal Society of Chemistry.

At the cloud-point temperature, a solution suddenly separates into two transparent liquid phases in which one phase contains practically all of the surfactant. Hence, a simple phase diagram of temperature versus surfactant critical concentration can be obtained, in which the lower part of the closed curve of the miscibility gap is called the lower consolute boundary. A micelle solution region exists below the curve and a two-phase region exists above this boundary. The studies indicated that NaI shifted the lower consolute boundary to higher temperature but other salts shifted the lower consolute boundary to lower temperature. These authors applied the Flory−Huggins lattice theory (see ref 228 and references therein) to relate the shifts of the lower consolute boundary to changes in micelle−solvent interactions. Cloud point depression induced by lyotropic ions followed the expected sequence $F^- > Cl^- > Br^-$, while the hydrotropic ion I^- induced an increase of the cloud point. Anions effectively change the cloud-point temperature, but the effect of cations can be neglected. Overall, salting-out anions markedly weaken water−surfactant interactions; that is, the hydration between the EO group and water is disrupted. Anion size increases in line with the above sequence, leading to a decrease of the surface charge, which lowers the intermolecular attraction; in contrast, I^- is a water-structure breaker, resulting in increased hydration. Similar results have been observed in $C_{12}EO_m$ (m = 6, 9, and 10) aqueous solutions in the presence of various monovalent salts.[230]

Many experimental studies have examined the effects of salt on the phase behavior of C_nEO_m/water systems.[231−234] Rodríguez et al.[231] investigated the effect of the lyotropic salt NaCl and the hydrotropic salt NaSCN on the discontinuous cubic phases (I) formed in the highly hydrophilic $C_{12}EO_{25}$ system by optical phase observation and SAXS measurements. In the presence of the salts, there is a rather narrow two-phase region between the cubic phase (I) and the isotropic solution. The addition of salt causes a small decrease in the thermal stability of the cubic phase; that is, the phase boundary shifts toward lower temperature. However, each of the two salts has a slightly different effect.

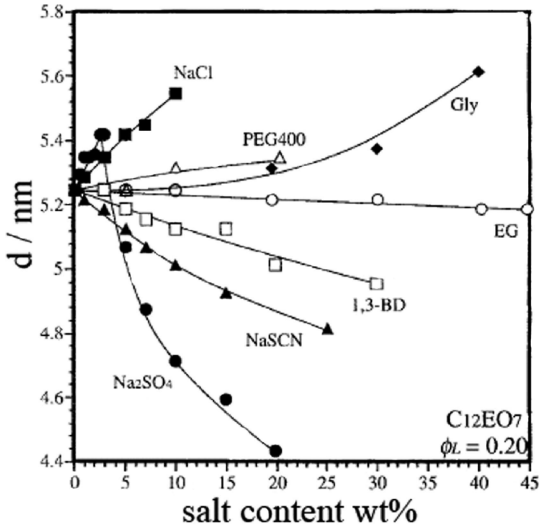

Figure 14. Effect of added salts on the change in interlayer spacing of liquid crystal in the $C_{12}EO_7$ system: (■) NaCl, (●) Na_2SO_4, and (▲) NaSCN. Reproduced with permission from ref 232. Copyright 1998 American Chemical Society.

The effective surface area per surfactant molecule, a_s, decreases slightly when NaCl is added, while in the case of NaSCN, a_s increases. The results are also ascribed to expected changes in the hydration of the EO headgroup, since the effective cross-sectional area mainly depends on the EO headgroup; thus, NaCl weakens the hydration interaction, resulting in the shrinkage of a_s, while NaSCN plays the opposite role.

An earlier study on the influence of NaCl, Na_2SO_4, and NaSCN on the liquid crystal structure of the $C_{12}EO_7$/water system was performed by Iwanaga et al.[232] Upon addition of NaCl and Na_2SO_4, both the melting temperature of the hexagonal crystal phase and the cloud point decreased with higher salt concentration due to dehydration. NaSCN addition causes the melting temperature to increase initially but then decrease at high salt concentration, until the liquid crystal region finally disappears. The cloud point increases with NaSCN due to increased hydration. The salt effects of NaSCN and NaCl on the effective cross-sectional area (a_s) are in accordance with the general trends mentioned above. In addition, SO_4^{2-}, causes a greater reduction of a_s than does addition of Cl^-, following the Hofmeister order. The authors make an interesting observation related to the changes of interlayer distance of the liquid crystals, as shown in Figure 14. Specifically, NaCl addition induces an increase in the interlayer distance, while NaSCN addition has the opposite effect. However, in the Na_2SO_4 system, the interlayer spacing value (d) first increases to a maximum and then rapidly decreases. The reason for this observation is not clear but may be related to the larger polyatomic ion structure of sulfate.

Inoue et al.[233,234] further systematically investigated the salt effect on the phase behavior of the $C_{12}EO_7$/water system by SAXS, DSC, and FT-IR measurements and obtained more detailed phase diagrams of the ternary systems to illustrate salt effects directly. Salting-out salts (LiCl, NaCl, and CsCl) induced an expansion of the lamellar (L_α) phase region at higher temperatures and a shrinkage of normal hexagonal (H_1) and bicontinuous cubic (V_1) phase regions at lower temperatures compared with the salt-free system.[233] The salting-out effect of the Cl^- anion overcomes the cation effect and influences the hydration, determining the observed

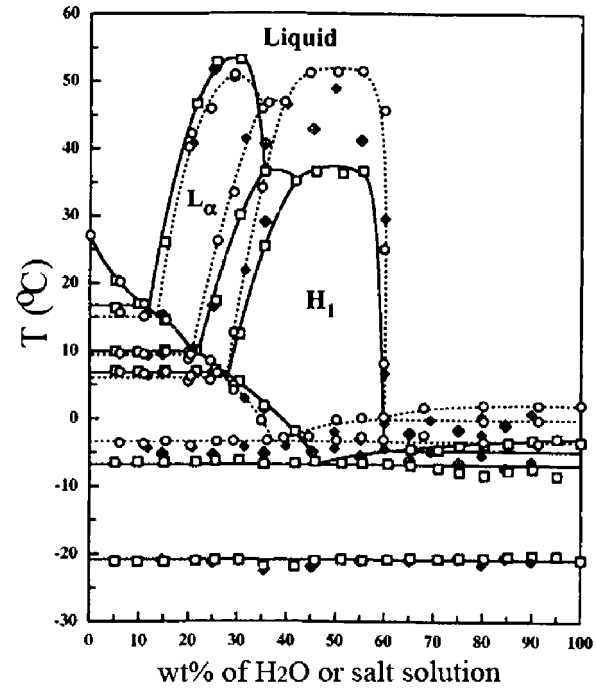

Figure 15. Phase diagrams of the mesophase region for the aqueous mixtures of $C_{12}EO_7$ in the presence or absence of added salts. The salt concentration is 1.0 mmol·L^{-1}: none (○), LiCl (□ and dotted line), NaCl (▲ and dashed line), and CsCl (◆). Reproduced with permission from ref 233. Copyright 2003 American Chemical Society.

changes. However, in terms of the synergistic action of the cations and anions, the salt effect is different due to the countercation. The expansion of the lamellar phase region area follows the sequence LiCl > NaCl > CsCl ≈ no salt. On the other hand, the shrinkage of the H_1 and V_1 phase regions toward lower temperature obeys the order of no salt < LiCl < CsCl < NaCl (Figure 15). Salting-in electrolytes (NaI and $NaClO_4$) induce shrinkage of the lamellar phase region and an expansion of the H_1 and V_1 phase regions, while NaCl had the opposite effect.[234] In addition, the area of the lamellar phase region decreases in the sequence NaCl > no salt > NaI > $NaClO_4$, following the Hofmeister series of anions. The authors ascribed the electrolyte effect on the phase behavior to changes of hydration between the EO group and water, leading to a decrease or increase of a_s, thus changing the dimensionless packing parameter P (refer to section 4.2 for the relationship between P and phase structure).

In recent years, a novel lyotropic liquid crystal phase of ternary mixed systems, containing nonionic C_nEO_m surfactants (such as $C_{12}EO_{10}$), water, and transition-metal aqua complex salts has been constructed by Dag et al.[235−238] The metal complex salts are different from the traditional salts (NaCl and $NaSO_4$), having formulas of $[M(H_2O)_x]Y_2$, where M is a first- or second-row transition-metal ion (Ni^{2+}, Co^{2+}, Zn^{2+}, Cr^{3+}, etc.) and Y is Cl^-, NO^{3-}, or ClO^{4-}. The liquid crystal phase structure, the interactions between surfactant and metal aqua complexes, the effect of the ions on the liquid crystal, and the nanoparticle preparation using the liquid crystal structure as a template have been investigated systematically. This work enriches not only the study of the phase behavior in these systems but also the application of the Hofmeister salt series in more complex systems. Furthermore, the effect of hexachloroplatinic acid (H_2PtCl_6) on the lyotropic liquid crystal formed in $C_{16}EO_8$ or $C_{12}EO_8$

aqueous solution systems has been studied by Attard et al.[239] Here, the addition of acid (H_2PtCl_6) significantly enhances the stability of the micelle cubic (I_1) and normal hexagonal (H_1) phases. Additionally, few papers consider the effect of adding acid or alkali on the physicochemical properties of the C_nEO_m aqueous solution systems, which may open up a new field.

3.2. Ternary Systems of C_nEO_m/Water/Oil

Oils, usually including hydrocarbons and medium- and long-chain alcohols, are another common additive that may influence the characteristics of the binary C_nEO_m/water system. When oil is added to homogeneous mixtures of nonionic C_nEO_m surfactants and water, novel microstructures such as microemulsions, reverse micelles, reverse vesicles, and sponge phases are observed, in addition to the traditional phases, micelles, lamellae, normal vesicles, and liquid crystals. In particular, oil microemulsion systems have been investigated for a broad range of theoretical considerations and technological applications. It is difficult to completely describe all of the phase diagrams of all the phases described, so characteristic phases will be introduced. Admittedly, hydrocarbons and alcohols play different roles with respect to their nonpolar and polar structures. In addition, studies of the C_nEO_m/water system with water-soluble alcohols, such as glycerol, propylene glycol, and 1-propanol, will be discussed, even though these are not oils.

This section will focus on the phase behavior and microstructures of the C_nEO_m/water/oil systems with additives as well as the interesting phase transitions that arise because of additive effects. The addition of oils or alcohols to the surfactant/water systems results in significant changes in interfacial properties, for example, the interfacial adsorption film, the surface or interface tension, and the partition of the surfactant among oil, alcohol, or water phases may all influence the structures that may exist in solution. In addition, we will briefly describe research on the ultralow interfacial surface of microemulsions, which has greatly advanced ternary crude oil recovery and yields.

3.2.1. Microemulsions in Ternary C_nEO_m/Water/Hydrocarbon Systems

Phase diagrams and microstructure determination are fundamental research tools in the investigation of the microemulsions formed by C_nEO_m/water/oil ternary systems. Microemulsions are thermodynamically stable, isotropic, transparent or translucent dispersions of two immiscible liquids such as water and oil, containing 10−100 nm droplets of oil or water in appropriate phases, which are stabilized by a surfactant or a mixture of surfactants and cosurfactant. For some time after the initial work of Schulman et al,[240,241] microemulsions were considered to invariably contain four components: surfactant, cosurfactant, oil, and water. However, since the work of Shinoda with nonionic surfactants,[242] it has been demonstrated that microemulsions can form with only three constituents: surfactant, oil, and water.

At present, many articles have reported the spontaneous formation of microemulsions in ternary systems of C_nEO_m/water/oil.[16,243−246] Research on microemulsions formed by C_nEO_m, water, and oil is representative, because this system has only three constituents that are easily controlled. The C_nEO_m surfactant can be systematically changed by lengthening or shortening the alkyl chain or the EO group, and the phase behavior is highly dependent on temperature. Like ordinary emulsions, there are three structures for microemulsions: oil droplets in water (O/W), water droplets in oil (W/O), and bicontinuous mesh-like structures. According to the pioneering work of Winsor,[247,248] ternary-component microemulsion phases can be expressed by a quasi-ternary phase diagram: an O/W microemulsion coexisting in equilibrium with an excess oil phase (Winsor I or lower phase microemulsion, usually denoted by $\underline{2}$ in the phase diagram); a W/O microemulsion coexisting in equilibrium with an excess water phase (Winsor II or upper phase microemulsion, denoted by $\overline{2}$); finally, three-phase bodies with a middle-phase microemulsion coexisting simultaneously in equilibrium with the excess oil and water phases (Winsor III or middle phase microemulsion, denoted by 3). For bicontinuous structures, Friberg[249] and Scriven[250] simultaneously proposed two structural models. The former defined a disordered lamellar structure while the latter described an ordered cubic liquid-crystal structure. However, neither of these two models has been confirmed directly. Later, the T−P model of bicontinuous structure was proposed by Talmon and Prager.[251] They proposed that inner phases with a polyhedral structure are scattered within the external phase and occupy a certain volume fraction. Initially, the inner phases are not linked, but after reaching an appropriate volume fraction, they become connected mesh-like structures. This model has been accepted widely in view of the configurational entropy and the camber pressure measured in nonionic surfactant systems. For the structures in Winsor I and Winsor II regions, though the microemulsion is considered to consist of small, thermodynamically stable droplets, experiments have demonstrated the existence of the micelles. Olsson et al.[252,253] used NMR to measure the self-diffusion coefficients of water, oil, and surfactant in the microemulsion phase of $C_{12}EO_5$/water/decane systems at a fixed surfactant-to-oil ratio. The self-diffusion coefficient data indicated a limited growth from sphere to prolate (oil-swollen) micelles as a precursor to the bicontinuous structure. Vasilescu et al.[254] studied the structure and the aggregation behavior in reverse micelle solutions of $C_{12}EO_4$/water systems with the addition of cyclohexane, *n*-decane, and *n*-dodecane. The aggregation number, size, and shape of the micelles were determined by time-resolved fluorescence quenching (TRFQ) and DLS measurements. The results showed that the reverse micelles in the cyclohexane system could be regarded as spheres that grew with added water content. The reverse micelles in the decane and dodecane systems appeared to grow in a nonspherical fashion and became much larger with the addition of water.

Microstructure formation and phase behavior in emulsions are mainly controlled by curvature free energy, usually expressed by the spontaneous mean curvature, H_0, as previously noted. When a surfactant layer is convex to the water, the curvature is usually regarded as positive. It has been found that H_0 changes gradually and nearly linearly with temperature from positive (Winsor I) to negative (Winsor II), passing through zero for bicontinuous microemulsions where these contain exactly equal volume fractions of water and oil.[16,255]

For C_nEO_m surfactant systems, the microemulsion I → III → II transition may occur upon increasing the temperature and is usually accompanied by the appearance of anisotropic lamellar (L_α) or hexagonal (H_1) mesophases or by cubic (V_1) phases in the complete phase transition process. From a macroscopic point of view, microemulsions show better

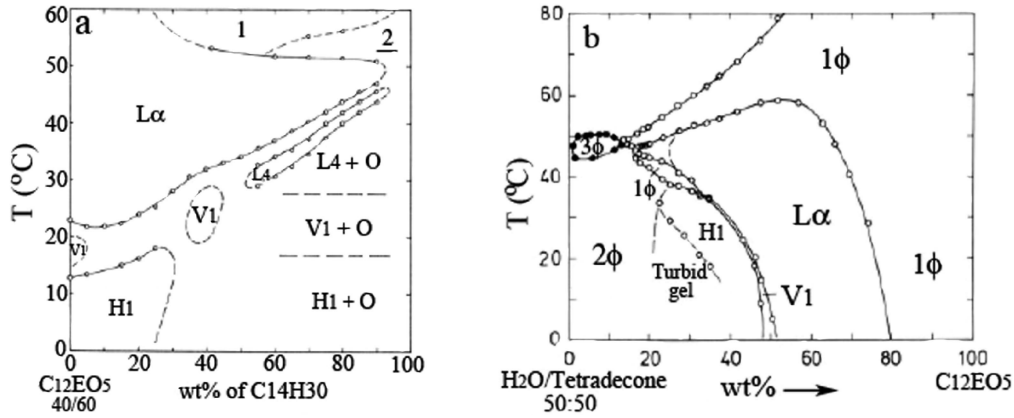

Figure 16. (a) Partial phase diagram of $C_{12}EO_5/C_{14}H_{30}/H_2O$ system at a constant surfactant-to-water weight ratio: $W_s/W_w = 1.5$. (b) Phase diagram at a constant oil-to-water weight ratio: W_o/W_w, in which 1Φ, 2Φ, and 3Φ represent the isotropic phase, two-phase regions, and three-phase body, respectively. Reproduced with permission from refs 256 and 257. Copyright 1993 and 1986 American Chemical Society.

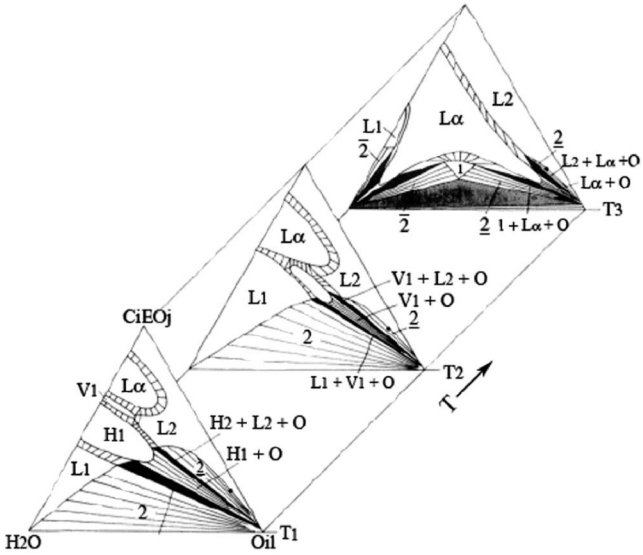

Figure 17. Schematic diagrams illustrating the evolution of the phase equilibrium with increasing temperature: $T_1 = 5$ °C, $T_2 = 25$ °C, and $T_3 = 48$ °C. Reproduced with permission from ref 256. Copyright 1993 American Chemical Society.

fluidity than mesophases, but do not show birefringence phenomena under a polarizing microscope. Figure 16a shows a temperature and oil concentration dependent, binary phase diagram of the $C_{12}EO_5/C_{14}H_{30}/H_2O$ system at a constant surfactant-to-water weight ratio: $W_s/W_w = 1.5$.[256] At lower temperature, a normal hexagonal region (H_1) occurs at low oil concentration. Above the H_1 region are two cubic regions (V_1), a multiply connected, two-phase region, and a sponge phase at higher oil content (L_4, which is distinguished from the more commonly observed water-rich analogue, usually denoted as L_3). Upon further increase of the temperature, a large area of lamellar phase (L_α) occurs. Above the L_α region, there is a stable Winsor I microemulsion with a reversed monolayer structure ($\underline{2}$). Figure 16b is a temperature and surfactant concentration dependent phase diagram of the same system where $W_o/W_w = 1$. This diagram shows the boundary of the two-phase regions (2Φ) and the three-phase body (3Φ), as well as the lyotropic mesophases at high $C_{12}EO_5$ concentration.[257]

Finally, Figure 17 illustrates an evolution of the phase equilibrium in the full ternary system where the temperature is raised from 5 to 25 to 48 °C[256] and indicates the influence of the temperature on the phase transitions. As temperature increases, the H_1 phase gradually disappears while the L_α phase expands over a large region; in addition, the $\underline{2}$ phase decreases, followed by the appearance of 3 and $\bar{2}$ phases. At 48 °C, the three-phase triangle is approximately symmetric and at the apex of the triangle a middle microemulsion is in equilibrium with an equal mass of water and oil. The height of the point where the system is balanced can be seen as a measure of the surfactant efficiency. The microemulsion apex may appear only at a low constant surfactant concentration when the amphiphile is very efficient.

3.2.2. "Fish" Diagrams To Illustrate the Phase Properties of Microemulsions in C_nEO_m Systems

In the development of microemulsion theory, a pioneering, pseudobinary "fish" diagram was proposed by Kunieda et al.[258−260] to describe the components of the partial regions and the phase behavior in microemulsions.

The "fish" diagram was also used to describe the phase behavior of a ternary system containing C_nEO_m surfactants with an alkane as a nonpolar part and EAN as a polar solvent.[20] The authors present phase diagrams of the ternary systems as a function of temperature and composition by taking "slices" through the phase prism at a 1:1 alkane to IL ratio while varying the surfactant concentration; this method leads to the phase boundaries having a characteristic "fish" outline. Figure 18 shows the phase diagram of $C_{12}EO_3$/EAN/dodecane and $C_{12}EO_4$/EAN/dodecane ternary microemulsion systems.

In Figure 18, the position at "X" indicates that the microemulsion is balanced, with zero mean curvature of the surfactant film, and a bicontinuous microemulsion forms. Point "X" thus defines a "surfactant efficiency", which is the minimum surfactant concentration required to solubilize the two immiscible solvents. Fuller explanations for "fish" phase diagrams have been presented by a number of authors.[20,261−263] Here, a brief explanation is adopted from Warr et al.[20] The middle phase of the three-phase state is a microemulsion, resulting from miscibility gaps in the three binary systems: EAN−surfactant, EAN−oil, and oil−surfactant. At low temperature, in the case of C_nEO_m dissolved in EAN, oil-swollen micelles form with an upper phase of excess oil. At higher temperatures, oil is a superior solvent for the surfactant, and EAN-swollen reverse micelles form in an oil continuous phase, in equilibrium with a lower

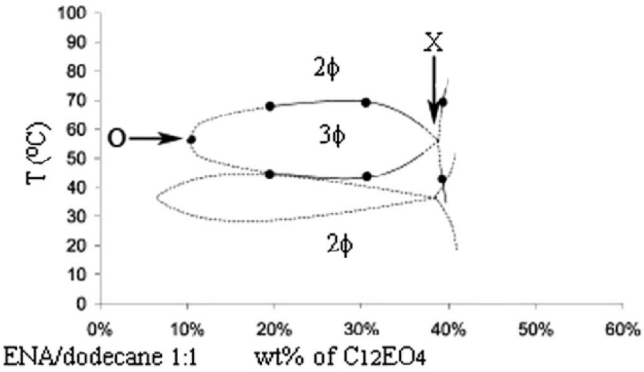

Figure 18. Vertical section through the phase prisms for $C_{12}EO_4$/EAN/dodecane with equal masses of EAN and dodecane. The dashed outline shows the results for $C_{12}EO_3$/EAN/dodecane as comparison. Reproduced with permission from ref 20. Copyright 2007 American Chemical Society.

phase of excess EAN. At intermediate temperatures, the surfactant has high solubility in both EAN and oil, which produces a surfactant-rich middle phase in equilibrium with both excess oil and EAN. For the last parameter, as concentration increases, the surfactant-rich phase increases in volume, and eventually produces a single phase. As noted above, EAN microemulsions have many features in common with aqueous systems and are affected by similar surfactant changes including changes in the length of the surfactant EO headgroup, tail chain, and alkane. With the increase of the amphiphilicity, the dimensions of the "fish" body initially increase and then decrease. A lamellar phase is often present at lower temperatures for surfactants with longer alkyl tails. The primary difference in EAN is that higher surfactant concentrations and longer surfactant tail groups are required to offset the decreased solvophobicity of the surfactant molecules in EAN compared with water.

For microemulsions formed in C_nEO_m/water/oil systems, a number of researchers have reported the particulars of surfactant systems using "fish" diagrams.[261−268] The "fish" diagram of a ternary system is drawn using the temperature (T) as the vertical axis and the mass fraction of surfactant in the total mixture (W_s) as horizontal axis, that is, the weight ratio of oil-to-water (W_o/W_w) is fixed while changing T and W_s. The point of the appearance of the three-phase microemulsion region, "O", is regarded as the "fish head" and the point of the disappearance of the phase microemulsion region, "X", is the start of the "fish tail", as seen in Figure 18. The "fish body" or the three-phase body within bicontinuous microemulsions is surrounded by two-phase regions and is approximately symmetric when $W_o/W_w = 1{:}1$. The "fish tail" region is usually a single-phase microemulsion but may also contain some mesophases, such as the L_α, H_1, and V_1 phases. At the X position, the middle-phase microemulsion forms with bicontinuous structures. Simultaneously, the value at X is a measure of the effectiveness of the amphiphile, representing the minimum mass fraction of the amphiphile needed to obtain a homogeneous solution of equal masses of oil and water.

In the temperature-component diagram, the three-phase region in equilibrium with excess water and oil usually occurs at the intermediate temperature, and is referred to as the hydrophile−lipophile balance (HLB) temperature or phase inversion temperature (PIT); it is where the middle-phase of the microemulsion occurs.[269] At a lower temperature (T_l represents the lower critical temperature of the three-phase

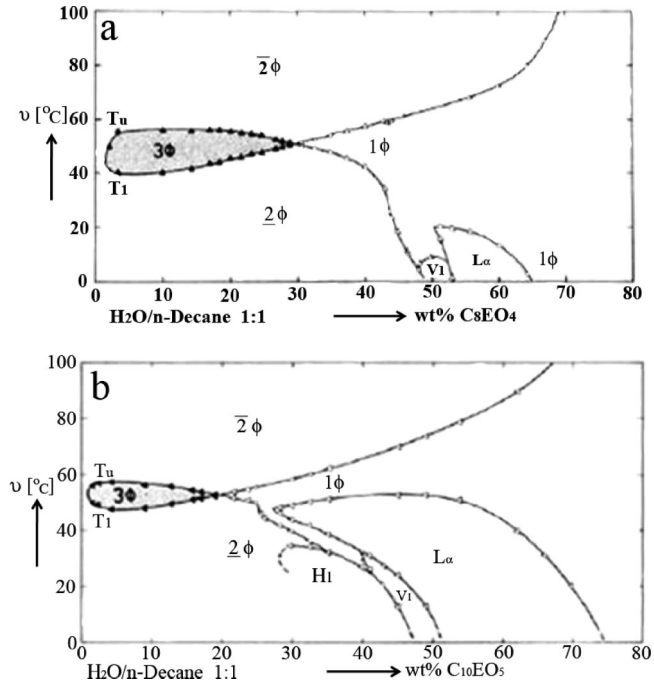

Figure 19. Phase diagrams of C_8EO_4/*n*-decane/water system (a) and $C_{10}EO_5$/*n*-decane/water system (b) with increasing the amphiphilicity of the amphiphile at a fixed weight ratio of *n*-decane and water: $W_o/W_w = 1{:}1$. Reproduced with permission from ref 265. Copyright 1986 American Chemical Society.

body), an O/W microemulsion (also regarded as an aqueous micelle phase) with excess oil phase is stable. At a higher temperature (T_u, the upper critical temperature), a W/O microemulsion (a reverse micelle phase with excess water) forms. Kahlweit et al.[265] published a series of "fish" diagrams of C_nEO_m surfactants with *n*-decane and water; two diagrams are reproduced here in Figure 19. By increasing the amphiphilicity in the surfactant from C_8EO_4 (Figure 19a) to $C_{10}EO_5$ (Figure 19b), the phase behavior becomes more complex with the appearance of an H_1 phase. The dimension of the "fish body" for $C_{10}EO_5$ remarkably decreases, indicating the enhancement of the amphiphile efficiency. Further, the width of the temperature interval ($T_u - T_l$) of the three-phase body narrows with the larger surfactant, that is, the mean temperature of the interval ($T = (T_u + T_l)/2$) increases. This diagram indicates exactly the influence of the C_nEO_m surfactants on the phase behavior and the microstructures of the C_nEO_m/oil/water ternary systems. More reliable evidence is presented elsewhere[265,270] where similar results are observed in the investigation of the "fish" phase transition in C_nEO_4 ($n = 6$, 8, 10, and 12)/*n*-octane/water systems and in the studies of the three-phase temperature intervals for C_nEO_m (where $n = 4$, 6, 8, 10, and 12 and $m = 2-7$)/*n*-alkane/water systems.

3.2.3. Influence of Alkyl Size on Microemulsions in C_nEO_m Systems

Oils can markedly influence the phase behavior of C_nEO_m/oil/water systems.[261−263,266,269−271] The effects of the homogeneous oils are associated with alkane chain length. Homogeneous phenylalkanes ($C_6H_5-(CH_2)_k-H$, $k = 3-9$) were added to C_4EO_2 aqueous solutions with the weight ratio of oil and water at 1:1.[261] From the "fish" phase changes, the three-phase body region decreased significantly and moved toward lower temperature with increasing alkane chain length. At $k = 6$ the three-phase body disappeared and

was replaced completely by a two-phase body. Similar results were obtained in another experiment that presented the "fish" phase diagrams of the C_8EO_4/*n*-C_kH_{2k+1} ($k = 6$, 10, and 14)/water systems.[266] The mean temperatures of the three-phase body ($\bar{T}$) in the C_8E_m/*n*-C_kH_{2k+1} ($k = 6-16$)/water systems were investigated,[263] and $\bar{T}$ was found to increase with increasing k value. It is clear that a three-phase microemulsion is stable over a larger region if the homogeneous oil chain is longer. Strey et al.[271] studied the phase behavior in microemulsions formed by C_nEO_m/*n*-alkyl methacrylate (*n*-C_kMA) /water systems and found that the value of $\bar{T}$ increased with increasing k; at the same time, the X value in the phase diagram initially decreased until $k = 4$ and then increased. Besides the dependence on the alkyl chain length of methacrylate, the phase behavior greatly depends on the surfactant alkyl chain length and headgroup size. At a consistent EO chain length, both $\bar{T}$ and X values decrease upon increasing the alkyl chain length. In contrast, with a constant alkyl chain length, $\bar{T}$ increases with increasing headgroup size while the X value also increases, indicating a decrease of the amphiphile efficiency. The general characteristic parameters of the microemulsions of the $C_{10}EO_6$/*n*-C_kMA ($k = 1$, 2, 4, 6, 8, and 12)/water systems and C_nEO_m/hexyl methacrylate/water at constant oil/water volume ratio 1:1 were also presented.[271] Finally, it should be noted that different types of oils produce different phase states due to their own physicochemical characteristics, for example, their oil solubility and their penetration ability. Kahlweit et al.[270] used *n*-dodecane, *n*-octane, cyclohexane, and toluene as oil phases in C_nEO_m ($n = 3-8$ and $m = 1-8$)/oil/water solutions. They found that the positions of the three-phase intervals on the temperature scale were determined by the properties of the oils and surfactants as well as on their proportions in solution.

3.2.4. Interfacial Properties of Microemulsions in C_nEO_m Systems

Though this review is mainly focused on the nature of bulk surfactant solutions, we note that it is important to investigate the interfacial properties of C_nEO_m/oil/water microemulsion systems, including their minimum and ultralow interface tension.[16,272−276] It was expected that the addition of medium-long chain alkanes to C_nEO_m aqueous solutions would cause an obvious decrease in the surface tension at the air−water interface compared with that in simple C_nEO_m/water binary systems.[30] However, the interfacial tension of the oil−aqueous phases in C_nEO_m/medium-long chain hydrocarbons/water systems decreases to the range of about $10^{-3}-10^{-4}$ mN·m^{-1}. Furthermore, in plots of interfacial tension versus temperature, it is found that a minimum tension value appears at the phase inversion temperature (PIT), depending on the chemical nature of the oil and the surfactant. Strey et al.[275] have measured interfacial tensions between oil- and water-rich phases for a series of ternary systems of water, *n*-alkanes, and C_nEO_m at temperatures necessary for Winsor I → III → II phase transitions. These authors found that the minimum value of the interfacial tension decreased by an order of magnitude upon reducing the carbon number of the alkane by six, reducing the number of EO groups by three, or increasing the number of carbon atoms in the surfactant tail by two. This interfacial phenomenon is related to the formation of the monolayer film within the microemulsion, since the amphiphile molecule is strongly polarized and adsorbs at the oil−water interface. The stability and the flexibility of the adsorption film are controlled by curvature energy and tuned by the structure of the surfactants as well as their interactions with the solvents. The curvature energy is usually expressed by spontaneous curvature (H_0), the bending elasticity modulus (κ), and the Gaussian curvature modulus ($\bar{\kappa}$).[276] Owing to these striking interfacial phenomena, these microemulsions are applied in ternary oil recovery.

3.2.5. Mesophases in Ternary C_nEO_m/Water/Hydrocarbon Systems

Besides the isotropic microemulsion structure, some other mesophases have been observed in ternary C_nEO_m/water/hydrocarbon systems, as illustrated in the phase diagrams in Figures 16, 17, and 19. The microstructures of the mesophases are usually anisotropic and show birefringence under a polarizing light, while the cubic phases are isotropic without birefringence.

The formation of vesicles, and reverse vesicles in particular, has been extensively investigated by Kunieda et al.[108,277−281] In their earliest work,[277] they used a video-enhanced microscope (VEM) to directly observe reverse vesicles in a mixed solution of water and dodecane containing 2.5 wt % $C_{12}EO_4$. Both the inside and outside of the reverse vesicles are oil; however, no liquid crystal structures were observed in the $C_{12}EO_4$/dodecane binary system. When a small amount of water was added to the binary mixture, an isotropic solution was formed, and the reverse phase was in equilibrium with excess oil. These authors also published a report on the systematic phase behavior of the $C_{12}EO_4$/dodecane/water system.[278] In this mixture, a middle-phase microemulsion occurred at the HLB temperature (about 25 °C). The lamellar liquid crystal phase, containing a large amount of water, was observed by SAXS and POM measurements and coexisted with an excess water phase in the water-rich region; normal vesicles formed in this region as well, as seen by VEM. In addition, lamellar liquid crystals, swelled with a large amount of oil, were in equilibrium with an excess oil phase in the oil-rich region in which the reverse vesicles formed. The shapes of the vesicles depended on the oil/water ratios.

Analogous to the aqueous system, reverse vesicles were observed to form spontaneously in the $C_{16}EO_6$/decane/sucrose monoalkanoate system in the absence of water.[279] In this ternary system, a lamellar phase appeared in the sucrose monoalkanoate-rich region while a reverse micelle phase formed in the $C_{16}EO_6$ region. By increasing the amount of sucrose monoalkanoate, a transition from reverse micelles to reverse vesicles occurred. Finally, the vesicles were stable in the two-phase region where a lamellar phase coexisted with excess oil. In this case, the vesicle formation resulted from similar conditions to the water systems, that is, the high solubility of $C_{16}EO_6$ in nonpolar liquids and the high insolubility of sucrose monoalkanoate in hydrocarbon favored the formation of the lamellar phase because of the strongly hydrophilic headgroups and the high solubility of the long chain alcohol.

The self-assembly behavior of an amphiphile in bulk solution is affected by the alteration in the curvature of the surfactant layers or by the changes of the effective equilibrium area per surfactant molecules. Different interactions between added oil and surfactant molecules will lead to different phase behavior. Kunieda et al.[280] studied the effect of added decane, *m*-xylene, or squalene on the phase behavior

Scheme 4. Schematic Representation of "Penetration" (Top) and "Swelling" (Bottom) Effects of Oil[a]

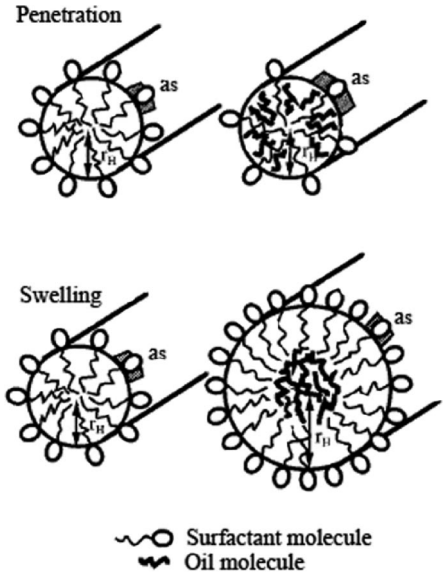

[a] Reproduced with permission from ref 280. Copyright 1998 American Chemical Society.

of the $C_{12}EO_m$ ($m = 3, 7$)/water system as a function of EO chain length at 25 °C. Upon addition of decane, the lamellar phase (L_α) transformed into a lipophilic reverse hexagonal phase (H_2) in the $C_{12}EO_3$ system, whereas the transition from the hexagonal phase (H_1) to a hydrophilic discrete cubic liquid crystal phase (I_1) occurred in the more hydrophilic $C_{12}EO_7$ system. Thus, oil addition caused different changes in the liquid crystal phases depending on the surfactant character.

Two mechanisms have been used to explain the oil effects, as shown in Scheme 4. One is the "penetration effect"; that is, oil molecules penetrate into the surfactant palisade layer and expand the effective cross sectional area (a_s) of the individual molecules, which causes an $L_\alpha-H_2$ phase transition. For example, in the $C_{12}EO_3$/decane/water system above, the oil penetration effect makes the spontaneous curvature value less positive or negative. The other possible mechanism is the "swelling effect"; that is, oil molecules are solubilized in the core of aggregate and expand the volume of aggregates without changing a_s, leading to an H_1-I_1 transition in the $C_{12}EO_7$/decane/water system. The oil swelling effect produces an opposite result in curvature change. In addition, *m*-xylene had a strong penetration effect, resulting in an H_1-L_α phase transition in the $C_{12}EO_7$ system.

Another contrast experiment has been performed to observe the effects of the various oils on nonionic surfactant solutions. Kunieda et al.[281] studied the phase behavior of the long-chain poly(oxyethylene) oleyl ether ($C_{18:1}EO_{50.8}$)/water system in the absence or presence of *m*-xylene and *n*-decane. In this system, an aqueous micellar phase (W_m) and a discontinuous cubic phase (I_1) form; upon the addition of *m*-xylene, the I_1 phase changed to a lamellar phase via hexagonal (H_1) and bicontinuous cubic (V_1) phases in the concentrated surfactant region. By calculation of a_s from the SAXS data, it was determined that there was a strong penetration effect of *m*-xylene that caused the curvature to be less positive, but not negative, due to the steric hindrance of the extremely long EO headgroup. Consequently, the L_α phase was stable and solubilized a large amount of oil, in which a reverse vesicle formed. The phase diagram of

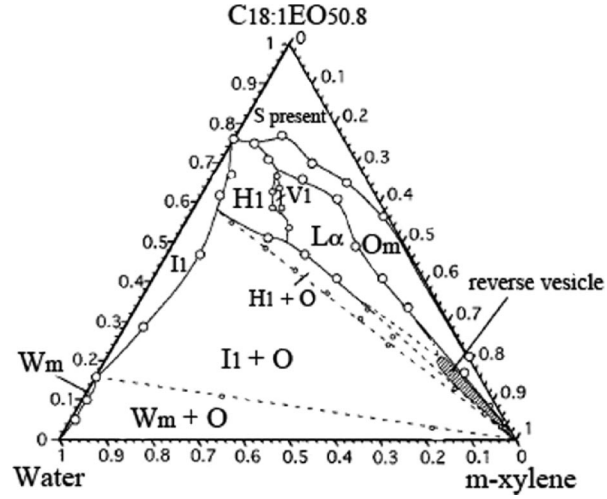

Figure 20. The phase diagram of the water/$C_{18:1}EO_{50.8}$/*m*-xylene system at 25 °C. Reverse vesicles are formed in the shaded region. Notations: S, solid present phase; O_m, surfactant liquid or reverse micellar solution phase; O, excess oil phase. Other notations are noted in text. The space group of the V_1 phase is considered to be *Ia3d* based on SAXS measurements. Reproduced with permission from ref 281. Copyright 1999 American Chemical Society.

$C_{18:1}EO_{50.8}$/*m*-xylene/water is shown in Figure 20. In contrast, the L_α phase or reverse vesicles were not observed upon the addition of n-decane to the $C_{18:1}EO_{50.8}$ aqueous solution, as a result of the weak penetration tendency of *n*-decane.

Wang et al.[282] investigated the effects of three oils on the mesh phases in the $C_{16}EO_6$/water system. These investigators showed that the penetration effect increased in the order of octadecane < decane < 1-hexene. The $C_{16}EO_6$/water system, in a concentration range of 48−62 wt % and upon cooling, shows the phase behavior in this sequence: an L_α phase; a random mesh phase, Mh_1 (0); a rhombohedral mesh phase, Mh_1 ($R\bar{3}m$); a bicontinuous cubic phase, V_1 (*Ia3d*); and a two-phase hexagonal region, $H_1 + L_\beta$. Upon heating, the phase behavior occurs in the sequence ($H_1 + L_\beta$) to V_1 to Mh_1 to L_α without exhibiting the rhombohedral mesh phase. The addition of oil does not greatly favor the formation of mesh phases as the oil content is increased. The phases disappeared in the order of V_1, Mh_1 ($R\bar{3}m$), and Mh_1 (0) when oil was added, and in the final oil-rich region, only the L_α phase was stable. In addition, the measurement of the surfactant molecule cross-sectional area verified the penetration effect sequence.

Recently, the solubilization of two triglycerides (1,2,3-trihexanoylglycerol, THG, and 1,2,3-tributanoylglycerol, TBG) in a $C_{12}EO_8$/water system has been studied by Alam et al.[283] They presented ternary phase diagrams of the two systems at 25 °C and observed the phase behavior of the $C_{12}EO_8$/water/THG system as a function of temperature. In this study of ternary systems, the addition of THG or TBG caused a transition from H_1 to L_α at high $C_{12}EO_8$ concentrations, whereas an H_1 to I_1 transition occurred at low surfactant content in the $C_{12}EO_8$/water/THG system. The anomalous transitions can be explained by two different oil effects. At high surfactant concentration, THG is distributed between the surfactant palisade layer and the core of the aggregates, while TBG penetrates into the palisade layer of the surfactant layer, causing an increase of a_s. At low surfactant concentration, THG is mainly solubilized in the cores of the aggregates and only results in the swelling of the aggregates.

As illustrated in this section, for the same amphiphiles at high surfactant concentration, different phases may be

obtained by the addition of different oils. In general, saturated hydrocarbons such as octadecane and *n*-decane have strong swelling tendencies, whereas the penetration effect is observed for aromatic or olefinic hydrocarbons, for example, *m*-xylene and 1-hexene. The triglycerides exhibited both swelling and penetration effects depending on surfactant concentration.

3.2.6. C_nEO_m/Water Systems in the Presence of Medium- and Long-Chain Alcohols

Unlike other common additives, such as inorganic salts or alkanes, alcohols (C_nOH) are usually regarded as cosurfactants, especially in the formation of microemulsions. Alcohols often have weak amphiphilic properties and can reduce surface tension because of their hydrophobic alkyl moieties and hydrophilic hydroxyl group. However, this property of alcohols depends on the alkyl chain length. Short-chain alcohols ($n < 4$), as well as glycerol, propylene glycol, and benzyl alcohol, are miscible with water, whereas medium- and long-chain alcohols ($n \geq 4$) are dissolved mainly into the oil phase. The effects of alcohols on aqueous surfactant systems have been reviewed by Zana.[284] Kahlweit et al.[285] found that phase diagrams of alkyl alcohol/water and C_nEO_m/water mixtures showed some striking similarities; namely, the alkyl alcohols behave like nonionic C_nEO_m surfactants. In investigations of the effect of alcohols on the phase behavior of microemulsions in C_nEO_m/water/oil systems,[286] it was found that alcohols adsorbed rather weakly at the water/oil interface. However, alcohols are strongly partitioned in interfacial films, when amphiphile layers appear in the microemulsions. Addition of alcohols effectively causes the oil phase to become less hydrophobic and the amphiphile phase less hydrophilic. Therefore, rather than cosurfactants, the alcohols should be regarded as cosolvents that distribute between the aqueous and oil-rich bulk phases and the interfacial film. Strey et al.[287] measured the amount of alcohol entering the monolayers of middle-phase microemulsions in C_8EO_5/C_nOH($n = 4$, 5, 6, 8, and 10)/octane/water systems by phase observations and SANS. They found that with increasing alcohol chain length, the efficiency of the amphiphile mixtures increased and the alcohols behaved more like surfactants. In the following section, oil-dissolved and water-soluble alcohols in nonionic surfactant systems are discussed.

Medium- and long-chain alcohols will affect C_nEO_m microemulsions, mainly influencing the hydrophilic−hydrophobic property of the amphiphile mixtures, which leads to changes in the curvature of the surfactant molecule layer. It is known that the addition of oil-soluble alcohols to nonionic surfactant solutions causes their cmc to decrease and favors aggregation.[284] According to additional work by Strey et al.,[288] the most prominent effect of oil-dissolved alcohols C_nOH ($n =$ 4, 6, 8, and 10) on the bilayers of the $C_{12}EO_5$/water system is to make the amphiphile mixtures more hydrophobic. The formation of L_α and L_3 phases in dilute $C_{12}EO_5$ aqueous solution can be shifted to lower temperatures and the stability of microstructures increased by adding longer-chain alcohols. Similar results were also observed in the phase investigation of the $C_{12}EO_4$/hexanol/water ternary system.[289] In addition, the extent of the alcohols dissolved in the bilayers was quantified by ^2H NMR experiments. The results showed that alcohols with longer alkyl chains exhibited a stronger partitioning into surfactant bilayers.[288] In a study of the phase behavior of C_8EO_5/C_8OH/water ternary mixtures,[24] the addition of alcohol induces the formation of L_α and L_3 phases, which do not appear in the simple C_8EO_5/water binary system. These results show that alcohols can increase the rigidity of the amphiphile mixture film and make it easier to form the various microstructures at lower temperatures. Furthermore, Freyssingeas et al.[290] have measured the membrane bending elasticity modulus (κ) of the L_α and L_3 phases in the $C_{12}EO_5$/hexanol/water system by DLS and high-resolution X-ray spectrometry and estimated the relative Gaussian curvature modulus ($\bar{\kappa}$). They found that the values of κ were nearly the same for both the L_α and L_3 phases; therefore, the alcohol addition does not significantly influence κ but causes $\bar{\kappa}$ to effect the phase transition.

Another $C_{12}EO_{23}$/alcohol/water system has been studied in detail.[291−293] Preu et al. studied the formation of micelles in $C_{12}EO_{23}$/C_nOH ($n = 4-7$)/water mixtures by SANS and modeled the sizes, shapes, aggregation numbers, internal structures, and distribution of micelles in these systems.[291] The pentanol partition coefficient was also inferred from NMR self-diffusion measurements. Tomisic et al.[292,293] investigated the structural properties of $C_{12}EO_{23}$/C_nOH ($n = 2-10$)/water ternary systems by SAXS and DLS measurements. Their data indicates that ethanol and propanol behave as cosolvents in these systems, breaking the micelles to form molecular solutions of the surfactants, whereas the medium- and long-chain alcohols behave more as cosurfactants due to their increased hydrophobicity, which assist the amphiphile mixtures to form more stable, self-organized structures.

Considering the surface properties of the ternary systems, an interesting phenomenon was observed in $C_{10}EO_8$/dodecanol/water and $C_{12}EO_8$/dodecanol/water systems.[294] In the surface tension−surfactant concentration curve of these surfactant solutions, the surface tension reaches a minimum and then increases up to a value very close to the surface tension of the pure surfactant solution with increasing surfactant content. This action is like that in C_nEO_m/*n*-hydrocarbons/water microemulsion systems and indicates that the highly surface-active, oil-soluble alcohols play a similar role to *n*-hydrocarbons in surfactant mixtures.

3.2.7. C_nEO_m/Water Systems in the Presence of Water-Soluble Alcohols

The effects of the water-soluble alcohols on C_nEO_m/water systems are different due to their different structures, such as the small *n*-alcohols (ethanol and propanol), or different functionality, that is, polyols (glycerol, sorbitol, ethylene glycol and propylene glycol). Some polyols behave like salts;[149] that is, glycerol and sorbitol show a "salting-out" effect, leading to a decrease of the cmc in C_nEO_m/water mixtures. In contrast, the water-soluble *n*-alcohols ($n < 4$), ethylene glycol (EG) and propylene glycol (PG), exhibit a "salting-in" effect. A surface tension experiment in $C_{12}EO_8$ aqueous solutions with the addition of EG or PG showed that the cmc increased markedly compared with the pure $C_{12}EO_8$/water solution at 25 °C.[152] Earlier work concerning the effect of ethylene glycol on C_nEO_m aqueous solutions indicated that the cmc increased remarkably with the alcohol content.[295] Penfold et al.[296] used SANS measurements to investigate the micelle structures in C_nEO_m/water solutions with added glycerol or ethylene glycol. As anticipated, glycerol added into $C_{12}EO_8$/water micelle solution decreased the hydration of the EO group, resulting in an increase in the micelle aggregation number and a decrease in the cloud point temperature. With the addition of ethylene glycol into

the $C_{12}EO_6$/water micelle system, similar results were obtained despite an increase in the cloud point temperature, which conflicted with the increase of the micelle aggregation number. The authors believed that the increase of cloud point was because of increased dehydration with temperature, leading to the suppression of the exchange rate of the solvent.

Subsequently, Aramaki et al.[172] presented a more complete picture of the effects of water-soluble alcohols (glycerol, 1-propanol, and propylene glycol) on the phase behavior of $C_{12}EO_8$ aqueous solution by SAXS and NMR self-diffusion measurements. In the $C_{12}EO_8$/glycerol/water system, a phase separation occurred at high glycerol content below 25 °C, which was not observed in other systems and due to the dehydration of glycerol. In all phase diagrams of mixtures including the three alcohol additives, a phase transition from the hexagonal crystal liquid phase (H_1) to an isotropic solution (W_m) took place. The SAXS data for the H_1 phases demonstrated that glycerol increased the interlayer spacing while 1-propanol and propylene glycol caused a decrease. In addition, 1-propanol and propylene glycol tended to penetrate into the palisade layer of the aggregates, causing the micelles to become smaller and finally dissipate to form molecular solutions as the alcohol content increased. These results indicate that polyol addition mainly caused the dehydration of C_nEO_m while the *n*-alcohols disrupted the nonionic micelles. Adding the water-soluble aromatic alcohol benzyl alcohol to $C_{12}EO_4$ aqueous solution led to a more stable lamellar phase compared with the $C_{12}EO_4$/water binary system.[297] The addition of benzyl alcohol also caused the appearance of a phase sequence, $L_{\alpha l}$ (lamellar phase made of vesicles) → $L_{\alpha h}$ (planar lamellar phase) → $L_{\alpha h}/L_3$ → L_3 → L_3/L, in the ternary-component bulk solution. Thus, benzyl alcohol behaves more like a cosurfactant rather than a cosolvent.

In summary, in addition to the temperature dependence, the phase behavior and microstructures of C_nEO_m/water systems can be easily reconstructed or controlled by oil or alcohol addition. Adjusting the type of additive (oil or alcohol) and the ratios of additive/surfactant, additive/water, or additive/additive provides a simple method to obtain desired aggregate structures.

3.3. Ternary Systems of C_nEO_m/Water/Nonionic Surfactants

Mixed surfactants in aqueous solution have attracted considerable attention in practical applications and theoretical studies. One reason is that the commercial surfactants are usually impure, that is, they may contain homologues of different alkyl chain lengths or different EO headgroups, such as with C_nEO_m surfactants. Another, more important, reason is that surfactants may be blended in synergistic mixtures that act to optimize the interfacial and bulk properties of the resulting solutions better than single-surfactant systems.[298−300] The "ideal solution approach"[301] and the "regular solution theory"[302,303] have been successively proposed to describe the micelle formation, surface adsorption, and other phase behaviors of multicomponent surfactant systems. The former approach is typically used in the investigation of surfactant homologue mixtures and focuses on the determination of the cmc, the composition of the mixed micelles, and the surface tension of the systems. The latter theory characterizes the departure of a solution from ideality with an interaction parameter, β, indicating the degree of synergism between surfactant molecules during monolayer or micelle formation.

3.3.1. Ideal Mixtures of Homologous C_nEO_m Surfactants

Binary mixtures of *n*-alkyl chain poly(oxyethylene) nonionic surfactant homologues in aqueous solutions may be regarded as ideal mixed systems. In this approach, since C_nEO_m homologues contain different hydrophilic EO groups or hydrophobic alkyl chains, it leads to the equilibrium area per surfactant molecule or the interactions of the molecules versus the composition of micelles straying away from a linear curve, actually producing a nonideal mixed system. However, since the departure from linear behavior is usually rather small, the cmc and surface activity in the mixed systems, as well as other physicochemical properties, may usually be predicted by an ideal solution approach; that is, the solution parameters in such systems usually lie between those of either single-surfactant system.

The interface adsorption of ideal mixed systems shows interesting phenomena regarding the surfactant structures and compositions at the interface. In early work, Rosen et al.[304] studied the adsorption of $C_{12}EO_3/C_{12}EO_8$ mixtures at the air−water interface by surface tension experiments and determined the surface composition of the binary mixtures by the regular solution treatment. Work on the same system was continued by Penfold et al.[305] who quantified the mole fraction of the interface adsorption monolayer from below the mixture cmc to ∼100 times the mixture cmc by neutron reflectivity technology and obtained similar results.[304] In this surfactant mixture, the surface excess of $C_{12}EO_3$ was higher than that of $C_{12}EO_8$ in the adsorption layer and increased with increasing concentration of $C_{12}EO_3$ up to the cmc of the mixture. An abrupt change occurred at the cmc, and beyond this the amount of the $C_{12}EO_3$ adsorbed decreased with further $C_{12}EO_3$ content. Using partial labeling of the alkyl chain and labeling of the EO groups in the mixed monolayer of $C_{12}EO_3/C_{12}EO_8$, a subsequent study has determined the changes of the surface components compared with single-surfactant systems.[306] Constraints imposed by the packing of EO_3 and EO_8 groups together caused a change of the surfactant structure compared with the pure monolayer; namely, the alkyl chains were more extended, the EO_3 groups were less hydrated, and the EO_8 groups were less extended and more hydrated. This work also verified that the abrupt change in mixture cmc was caused by changes in distribution of the two surfactant species between the bulk solution and the monolayer due to the onset of mixed micelle formation at the cmc, as proposed by Nikas et al.[307] These researchers generalized a two-dimensional gas approach to predict the surface tension and monolayer compositions of mixed $C_{12}EO_6/C_{12}EO_8$ and $C_{12}EO_6/C_{10}EO_4$ solutions. Furthermore, the results of surface tension measurements showed that the mixture cmc fell exactly between those of the pure surfactant solutions, suggesting essentially ideal mixing.[307] A similar conclusion was also obtained from surface tension experiments of a $C_{14}EO_8/C_{12}EO_4$ mixture in aqueous solution.[294]

In pure C_nEO_m aqueous solutions, micelles form beyond the cmc at a certain temperature and various microstructures such as lamella, vesicles, and liquid crystals may appear depending on temperature and surfactant concentration (section 2.1). However, few papers have focused on the formation and transitions of such microstructures in *mixed* C_nEO_m systems. The properties of the bulk solution, including micelle formation, have been the central concern and usually include the cmc, the interaction of mixed micelles, and the determination of micelle shape and size.[308,309] Kato et al.[308] calculated the cmc and the interaction parameters (β^M for

micellization and β^{σ} for monolayer formation) between surfactants in the $C_{12}EO_1/C_{14}EO_4$/water system. The cmcs of the mixed systems are very close to those obtained via experimental results from surface tension measurement, indicating an ideal mixing behavior of the two surfactants. In addition, both the β^{M} and β^{σ} values are small and negative, also indicating that the surfactant mixtures behave almost ideally during monolayer and micelle formation. Further, the β^{M} value was more negative than the β^{σ} value, indicating a stronger interaction between the surfactant molecules during monolayer formation. These properties depend on both of the surfactants having EO units as their head groups and long alkyl chains as their tails, which allow them to be closely packed during monolayer and micelle formation. Thomas et al.[309] studied the properties of mixed micelles in the $C_{12}EO_6/C_{12}EO_8$ aqueous solution by SLS and DLS measurements, determining factors such as their shape, size, molecular weight, and diffusion coefficients. The results indicated that the mixed micelles were rod-like and grew in one dimension with increasing temperature and surfactant concentration. In this work, a ladder model was used successfully to describe the mixed rod-like micelles.

Finally, the cloud point has been investigated for mixed C_nEO_m aqueous solutions according to the Flory−Huggins model.[310] Cloud point temperatures for mixtures with the same alkyl chain length but different EO groups increase with an increase in the EO chain length of either surfactant species. However, the cloud point temperatures decrease as a function of increasing alkyl chain length when the mixtures have the same number of EO units but different hydrocarbon chain lengths.

3.3.2. C_nEO_m Interact with Sugar-Based Nonionic Surfactants

Sugar-based nonionic surfactants are derived from hydrophilic sugar headgroups consisting of carbohydrate monomers, dimers, or polymers conjugated with hydrophobic alkyl chains and are classified as alkyl glycosides, alkyl polyglycosides, or glycolipids.[311−314] Since they are nontoxic, biodegradable, and biocompatible, sugar-based nonionic surfactants have been widely used in pharmaceutical, cosmetic, and food industries. Since these nonionic surfactants possess amphipathic properties, they can effectively reduce surface or interfacial tension and self-assemble in water into micelles (usually spherical with large aggregation numbers), lamellar phases, and lyotropic liquid crystal phases. In addition, they also generate thermotropic liquid crystals in their pure state upon melting.[314−316] Compared with the properties of poly(oxyethylene) nonionic surfactants (such as the cloud point), sugar-based nonionic surfactants have less dependence on the temperature in water due to the strength of the hydrogen bonding between the hydroxyl groups and water. These interactions lead to less dehydration over the relevant range of temperature.[314,317,318] For example, the cmc of a maltose-based nonionic surfactant, dodecyl-β-D-maltoside (DM), increases with temperature, which is obviously opposite to typical poly(oxyethylene) nonionic surfactants. In contrast, the cmc of the glucose-based surfactant, octyl glucoside, decreases with increasing temperature.[319]

At present, most reports have focused on the physicochemical properties of mixtures of C_nEO_m surfactants with sugar-based nonionic surfactants.[317,318,320−326] It is assumed that these mixtures will exhibit nearly ideal behavior because the strong bound hydration adhesion of the sugar headgroups prevents their interaction with the EO headgroups of C_nEO_m.[318,320,322,323] The surface tension measurements of pure C_8EO_4, pure octyl-β-D-maltopyranoside (OM), and C_8EO_4/OM in water exhibit the properties of an ideal mixture; namely, the mixed micelles are formed analogously to the micelles of each surfactant separately.[318] The calculated excess Gibbs energy of the mixed surfactant solution is nearly zero, which indicates that the hydrogen bonding between surfactant and water plays a larger role than interactions between C_8EO_4 and OM. For the $C_{12}EO_8$/DM/H_2O system,[315,320] the minimum areas per molecule, the maximum adsorption density, and the cmc values of their mixtures fall just between the values of the separate surfactants, which is in good agreement with ideal mixing. Similar results were also reported for the $C_{12}EO_5$/DM/H_2O,[322] $C_{12}EO_7$/DM/H_2O, and $C_{12}EO_7$/decyl-β-glucoside/H_2O systems.[323] Hence, glucoside- and maltoside-based nonionic surfactants show little significant interaction with C_nEO_m in solution.

Among the aggregates of C_nEO_m/sugar-based nonionic surfactant systems, the properties of mixed micellar solution have been studied in detail, such as shape, size, aggregation number, and viscoelasticity.[317,324−326] Spherical and elongated micelles are found to coexist in both the nonyl phenol ethoxylated ether/DM (1:1) aqueous solution and the nonyl phenol ethoxylated ether solution; in contrast, only small globular micelles form in the DM solutions.[324,326] Analogously, SANS and SLS data indicate that elongated micelles with high molar mass are present in the $C_{12}EO_6$/DM and the $C_{12}EO_6$ systems and grow with increasing $C_{12}EO_6$ fraction and surfactant concentration.[326] This suggests that the phase behavior may be dominated by C_nEO_m in C_nEO_m/sugar-based nonionic surfactant mixed systems. Moreover, wormlike micelles are induced from the spherical micelles in dilute aqueous solutions of sucrose hexadecanoate with the addition of $C_{12}EO_m$ ($m = 1-4$).[317,325] A sharp increase and a decrease in viscosity occur upon the addition of $C_{12}EO_n$ to dilute micelle solutions of sucrose hexadecanoate and finally lead to a phase separation. Nonetheless, the interesting processes of micelles changing from spheres to rods is inadequately studied in C_nEO_m homologues mixed systems.[308,309]

3.3.3. Nonideal Mixtures of Nonionic Surfactants

Some nonionic surfactants, such as poly(oxyethylene) cholesteryl ether ($ChEO_m$) and poly(oxyethylene) sorbitan monooleate (Tween 80), are nonhomologous to C_nEO_m surfactants mainly due to the different hydrophobic units that the former contain. When these compounds are mixed with C_nEO_m surfactants in aqueous solution, the mixed systems usually exhibit nonideal mixing behavior, that is, the properties of the complex fluids are deflected from ideal surfactant solution behavior. The nonideal behavior is caused by the significantly different molecular cross-sectional areas and volumes of the cholesterol- or oleate-derived surfactants, which together lead to a greater steric repulsion in surfactant microstructures. At present, studies of nonideal mixtures of nonionic surfactants in aqueous solution have been focused on the formation and the rheological behavior of viscoelastic solutions of wormlike micelles.[327−331]

Poly(oxyethylene) cholesteryl ether surfactants are unique nonionic surfactants, possessing a bulky and rigid hydrophobic unit compared with C_nEO_m surfactants. $ChEO_m$ surfactants can form liquid crystals with a lamellar structure in their pure state above their melting temperature[332] and

form a variety of self-organized aggregates in water, including micelles, lamella, and cubic and hexagonal structures.[333] When short EO chain, $C_{12}EO_m$ ($m = 1-4$), surfactants are added to dilute aqueous solutions of long EO chain $ChEO_m$ ($m = 10$ and 15), the resulting micelles are induced to grow in a unidimensional fashion leading to the formation of viscoelastic solutions.[327] The rheological behavior of the mixed systems over a wide range of shear frequency can be described by a Maxwell model and indicates that a transient network of wormlike micelles occurs after mixing. The sphere-to-long rod transition of the micelles is caused by the reduction of the mean interfacial curvature, which is due to the addition of $C_{12}EO_m$ with small headgroups. In addition, the effect of the EO headgroup of both $C_{12}EO_m$ and $ChEO_m$ on the rheological properties of the mixed micelle solutions has been studied. When the EO headgroup of $C_{12}EO_m$ ($m = 1-4$) is decreased in the $C_{12}EO_m/ChEO_m$ systems, the ability to induce the mixed micellar growth was increased at a fixed mixing fraction. On the other hand, upon increase of the EO units from 10 to 15 in $ChEO_m$, the $ChEO_m/C_{12}EO_3$ systems showed a sharp increase in the zero-shear viscosity and were shifted to a relatively higher concentration of $C_{12}EO_3$. Furthermore, the zero-shear viscosity of the micelle solution was increased at increased concentrations of $ChEO_m$. Similar observations were also shown in the above systems by SANS and DLS measurements,[328] as well as in a recent study of viscous wormlike solutions of $ChEO_m$ ($m = 13$ and 15)/$C_{12}EO_3$ surfactants.[330]

Another kind of nonideal mixture of nonionic surfactants, Tween 80 and C_nEO_3 ($n = 12$, 14, and 16), has been investigated in aqueous media by rheological and SAXS measurements.[331] As in the $ChEO_m/C_nEO_m$ systems, viscous wormlike micellar solutions are formed in the aqueous systems of Tween 80 in the presence of a small amount of C_nEO_3. When $C_{12}EO_3$ was replaced by $C_{14}EO_3$, micellar growth occurred more effectively. However, the use of $C_{16}EO_3$ in the system resulted in a phase separation before the formation of the viscoelastic solution. The effect of temperature was also studied in these systems; increased temperature caused one-dimensional micellar growth as in the $ChEO_m$ studies described above.

3.3.4. Mixed Fluorinated and Hydrogenated Poly(oxyethylene) Nonionic Surfactants in Aqueous Solution

In aqueous systems, fluorinated surfactants exhibit typical surfactant behavior when compared with hydrogenated analogues, that is, they may form various aggregates, micelles, vesicles, lamellae, or other liquid crystal structures.[334−336] However, the fluorinated surfactants do have some distinct properties in water: compared with corresponding hydrogenated analogues, they are more hydrophobic, possess a higher surface activity, and show a much lower cmc.[334,335] Also, because of the highly electronegative and relatively bulky fluorine atoms, a fluorocarbon chain is more rigid and bulky than hydrocarbon chains, and the fluorinated surfactants have higher chemical and thermal stability.

As mentioned in section 3.3.1, homologous C_nEO_m with different chain lengths are miscible in water, which is regarded as ideal mixture during surface adsorption and micellization. However, when a C_nEO_m and a fluorinated nonionic surfactant are mixed, the system deviates markedly from the behavior of ideal surfactant solutions.[337−340] Regular solution theory is employed most widely for explaining the interaction of molecules in mixtures of nonionic surfactant systems.[341] However, in the earliest studies of dilute micelle solutions of $C_{12}EO_6$ mixed with the fluorinated surfactant, $C_6F_{13}-C_2H_4-SC_2H_4-(OC_2H_4)_m$ (abbreviated R_FEO_m, where $m = 2$ and 7) in water,[337,338] it was thought that, in a very dilute micelle solution, ideal or nonideal mixing depended on the *hydrophilic EO* chains when the hydrocarbon chains of the two surfactant were fixed. Namely, in the $C_{12}EO_6/R_FEO_7$ system, the cmc value versus the mole fraction of fluorinated surfactant nearly follows that in pure surfactant micelles, which may show that the mixing is approximately ideal. In contrast, the $C_{12}EO_6/R_FEO_2$ system shows very different results, indicating nonideal behavior. Hence, the more symmetric the hydrophilic chains with constant hydrophobic tails in the fluorous and C_nEO_m surfactants, the more ideal mixing.

Nevertheless, recent research[339] on the mixing of $C_{12}EO_8$ and $C_8F_{17}C_2H_4(OC_2H_4)_9$ has suggested that this system exhibits a deviation from ideal mixing behavior through contrast variation SANS and ^{19}F NMR measurements; these data indicated a broader distribution of the micellar composition. Another investigation of the combination of $C_{10}EO_4$ and tetra(ethylene glycol) mono-1,1,7-trihydrododecafluoroheptyl ether (FC_7EO_4) arrives at the same conclusion that the mixing leads to markedly nonideal solutions; this was determined by calculating the excess Gibbs energy in the micelles, although the two surfactants have same hydrophilic headgroup.[340]

During the micellization of mixed fluorinated and hydrogenated nonionic surfactants in water, demixing of micelles will occur above the cmc.[339,341−346] In other words, since the fluorocarbons are both hydrophobic and lipophobic, two types of micelles will coexist in the micelle domain, fluorocarbon-rich micelles and hydrocarbon-rich micelles. This segregation phenomenon in fact reflects the mutual incompatibility between the fluorocarbon and hydrocarbon chains. Values of the calculated interaction parameter β are usually positive in these systems, which indirectly indicate demixing or antagonism between the surfactants.[338,343]

It appears to be difficult to get direct experimental proof of the coexisting micelles, and indirect evidence obtained by measuring the cmc requires very accurate experimental results. Hence, SANS and NMR techniques have been widely applied for more direct observation of fluorocarbon surfactant mixed micelles recently.[339,341,347,348] Neutron scattering values should be near zero for fully mixed micelles but change upon the demixing of micelles. Self-diffusing NMR measurements can provide a direct indication of the sizes of different micelles. For example, above 80 wt % water in the $C_{12}EO_8/C_8F_{17}C_2H_4(OC_2H_4)_9$ system (abbreviated $R^F{}_8EO_9$, and the following fluorinated surfactants follow the chemical structure $R^F{}_nEO_m$),[344] the two surfactants are fully miscible and mixed micelles form in all surfactant ratios. Between 60 and 80 wt % water, two micellar zones composed of fluorocarbon-rich and hydrocarbon-rich micelles are observed in the phase diagram. The mixed micelles are prolate ellipsoids with an axial ratio of 2.2 and an aggregation number larger than 100.[339] Analogous micellar segregation behavior can be found in the aqueous systems of $C_{18-1}EO_{10}$ mixed with $R^F{}_6EO_{11}$ or $R^F{}_7EO_8$.[345,346]

Finally, various self-assembled aggregates can form in the fluorinated and hydrogenated nonionic surfactant mixtures.[337,344−346] For instance, the $C_{12}EO_6/R_FEO_7$ system exhibits a remarkably symmetric phase diagram; with an

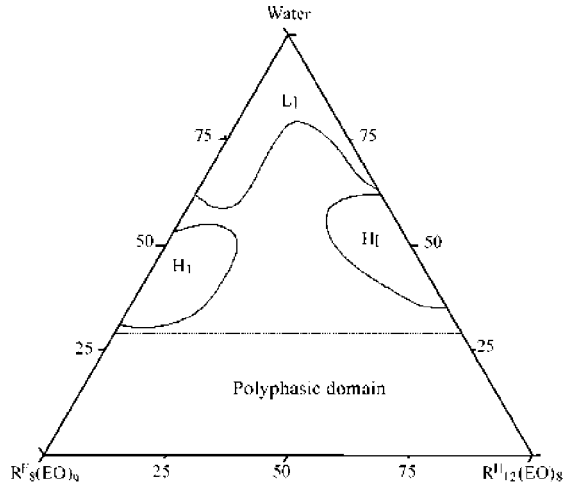

Figure 21. Phase diagram of $C_{12}EO_8/R^F_8EO_9$/water system at T = 20 °C. Reproduced with permission from ref 344. Copyright 2006 Elsevier Inc.

increase in surfactant concentration, a phase sequence of L_1, H_1, V_1, L_α, and L_2 is observed.[337] In the $C_{12}EO_8/R^F_8EO_9$ phase diagram,[344] as shown in Figure 21, one can see that below the two micellar zones, upon the decrease in surfactant concentration, two hexagonal phase occur, one containing mainly fluorinated surfactant and the other mainly hydrogenated.[344] Also, two lamellar phases of fluorinated and hydrogenated surfactants are observed in the $C_{18-1}EO_{10}/R^F_7EO_8$ system.[346] Some of the fluorous aggregate structures, especially hexagonal arrays, may be generally used as templates to prepare ordered, mesoporous silica-based materials.[344−346,349]

As mentioned above, studies of nonionic surfactant/C_nEO_m mixtures have generally focused on the nature of the poly(oxyethylene) nonionic surfactant. In both ideal and nonideal mixing, the properties of the bulk solutions and interfacial adsorption have attracted considerable attention. The driving forces between poly(oxyethylene) type nonionic surfactants cannot be explained solely by hydrophobic interactions but also include the steric interactions related to the size and the nature of the headgroups and tail groups and the van der Waals forces between molecules. Many features of ideal and nonideal mixed surfactant solutions still need to be investigated, such as richer mixing systems, aggregate transitions, and the rheology of these complex liquids.

3.4. Ternary Systems of C_nEO_m/Water/Water-Soluble Polymers

In addition to the variety of self-organized microstructures in aqueous solutions that are formed by C_nEO_m surfactants, nonionic amphiphilic polymers, including homopolymers and block copolymers, can also display rich phase behavior and peculiar adsorption properties in aqueous media. Ternary systems consisting of C_nEO_m, polymer, and water are fundamentally interesting to study in view of their diverse molecular structures and properties, as well as meeting the requirements for use in industrial processes. However, few papers reported on these types of nonionic mixtures before the mid-1990s,[350−353] compared with systems of ionic surfactants with polymers. Of interest here is the interaction of poly(oxyethylene) homopolymer (usually abbreviated as PEO or PEG) with nonionic C_nEO_m surfactants. While the molecular structures of PEG and PEO are identical, the molar mass of PEO is much higher than that of PEG, due to the difference in the approach to each polymer's synthesis. Previously, it had been considered that few special interactions or only rather weak interactions would exist between polymers and nonionic surfactants because of the absence of charges on either the polymer or amphiphile, as well as having similar structures (thus potentially similar properties) due to the presence of EO units.[350,351] According to the review of Saito,[352] there was no sign of interactions between PEO and nonionic C_nEO_m surfactants in mixtures containing both these components. However, a later review by Lindman[353] asserted that interactions do exist between various polymers and nonionic surfactants in their solutions. For instance, in the interesting study of foam formation in the PEO/$C_{12}EO_5$ aqueous solution,[354] the foam stabilization was considered to be related to amphiphile−polymer interaction. Thus, upon mixing water-soluble amphiphilic polymers and C_nEO_m in water, complexes and microstructural changes are expected to occur, which depend not only on the size and the structure of C_nEO_m but also on the molar mass and the type of polymer.

3.4.1. Ternary Systems of C_nEO_m/Water/Homopolymer

Poly(oxyethylene) (PEO) is a neutral, completely hydrophilic polymer, with unusual solubility properties. In interactions with ionic surfactants, anionic surfactants such as sodium dodecyl sulfate (SDS) and alkyltrimethylammonium surfactants have stronger affinity for PEO than do cationic surfactants.[355−358] The structures of the surfactant determine the strength of its interaction with polymers. The interactions may involve electrostatic, hydrophobic, or steric interactions and the influence of the configuration of the polymer; these factors may all have some influence on the final nature of the microstructures formed in solution.[359]

As mentioned, C_nEO_m nonionic surfactants had been thought to be unaffected by the presence of PEO.[350−352] The critical micelle concentration of C_8EO_3 was not affected by the presence of PEO,[350] and the aggregation number of $C_{12}EO_8$ micelles remained unchanged with the addition of 2% PEO over the entire temperature range investigated.[235] However, as noted by Feitosa and Brown and co-workers,[359−362] these results do not necessarily mean the absence of any interaction between the polymer and the nonionic surfactant. These authors studied a ternary aqueous solution of $C_{12}EO_8$ with a high molar mass of PEO using DLS measurements, time-resolved fluorescence quenching (TRFQ), and isothermal titration microcalorimetry.[361,362] The main difference in the newer study is the high molar mass of the PEO, namely, a higher molar mass of polymer led to greater interactions with the nonionic surfactant. The relaxation time distributions of PEO/$C_{12}EO_8$ aqueous solutions were bimodal at higher molar mass of PEO and concentrated surfactant solution, which suggested that free surfactant micelles coexisted with a more slowly relaxing component, representing the formation of a polymer coil/micellar cluster complex. Furthermore, the addition of PEO strongly decreased the cloud point temperature of the system, which indicates intermolecular interactions. Though the aggregation number of the micelles and the cmc did not change after the addition of PEO, these did not unambiguously reflect the strength of interaction between the components of the neutral polymer/surfactant system. A subsequent investigation of $C_{12}EO_8$ aqueous solution in the presence of poly(ethylene glycol) (PEG) also showed complex formation,[362] where the relaxation time distributions

were unimodal and bimodal at lower and higher concentrations, respectively. Upon an increase of either the PEG or the $C_{12}EO_8$ concentration, the aggregation number was nearly constant, owing to the increasing amount of surfactant micelles inside the complex. In addition, titration microcalorimetry results showed that the interaction between $C_{12}EO_8$ and PEG was exothermic by about 1.0 $kJ \cdot mol^{-1}$ at concentrations higher than the cmc of $C_{12}EO_8$.

In another ternary system of $C_{12}EO_5$, PEO, and water,[359,360] micelle clusters were also formed with large PEO coils; that is, the micelles may be loosely wrapped with PEO chains. The hydrodynamic radius of the complex increased with increasing temperature up to the cloud point as well as with the increase of the concentration of either component. The cloud point temperature of the system was decreased by the addition of PEO. Compared with the $C_{12}EO_8$ system, it was concluded that the longer the EO group in the nonionic surfactant, the weaker was the interaction between surfactant and polymer.[361] Moreover, in the $C_{12}EO_5$ system, at a given PEO concentration, the aggregation number (N) of the micelles was smaller in the presence of PEO than in its absence at low surfactant concentration; in contrast, N was larger at high surfactant concentration. The changes of the cloud point and the aggregation number, the formation of the polymer coil/micellar cluster complex, and the measurement of reaction enthalpy all indicate interactions between PEO and C_nEO_m. In particular, Makulska et al.[363] found that the addition of PEG will induce ordering in C_nEO_m ($n = 12$; $m = 5, 6, 8$) aqueous solutions when the PEG reaches a critical molecular mass.

Poly(acrylic acid) (PAA) is another polymer that has been investigated in solutions of nonionic C_nEO_m surfactants.[364−370] PAA is neutral at low pH (all carboxylate sites are protonated), but it becomes an anionic species at higher pH as the carboxylic acid functional groups are deprotonated. Saito et al.[364,365] were the first to investigate mixtures of C_nEO_m and PAA and showed that the interactions mainly included hydrophobic interactions and hydrogen bonding between the EO groups of the surfactant and the acid units of the polymer. Surfactants with longer EO head groups exhibited stronger interactions with the polymer (namely, more H-bonds arise between EO and acid units), and higher pH reduced intermolecular interactions. Subsequent experiments with the PAA/$C_{12}EO_8$/water system showed that no interaction occurred at pH > 8, presumably due to electrostatic repulsion between anionic carboxylate groups and the EO headgroups.[366] Above the cmc of the mixed system at pH = 3, the surface tension became higher, which indicates the surfactant film is modified by PAA. It was proposed that hydrogen bonding induced the polymer to collect at the interface of the surfactant film. The properties of the PAA/$C_{12}EO_8$ or $C_{12}EO_6$/water systems were also studied by additional methods, including surface tension, fluorescence, dye solubilization, viscosity, and pH methods.[367] Besides the cmc, the starting point of micellar aggregation on the PAA chain and the point at which free micelles appeared in the solution was determined. Studies by steady-state fluorescence and time-resolved fluorescence indicated a critical aggregation concentration (cac) lower than the cmc of the surfactant.[368] Upon addition of PAA, the fluorescence lifetime increased, suggesting that the polymer wraps around the micelle clusters, that is, a complex forms in the solution causing a decrease in the aggregation numbers. Despite this interaction, the presence of the polymer did not influence the temperature dependence of the aggregation number.

Using surface tension measurements and viscometry, Saito et al.[369] have also investigated the effect of surfactant hydrocarbon chain length on the interaction PAA and C_nEO_8 ($n = 10$, 12, and 14) in aqueous solutions. As expected, the cac decreased with increasing alkyl chain length. Further, a longer hydrocarbon chain led to a lower minimum point in the viscosity curve of the mixed systems. It was concluded that the surfactant could affect both the size and the shape of the polymer coil. In an alternative study, when PAA was covalently modified with hydrophobic units (producing a "homopolymer") and added to the lamellar phase of an $C_{12}EO_5$ aqueous solution,[370] the phase behavior was essentially independent of polymer molar mass and polydispersity, and membrane rigidity increased with increasing polymer concentration and hydrophobic substitution level.

At present, it is necessary to do further studies on the interactions between homopolymers and C_nEO_m to understand the details of the interactions present in such systems. Other homopolymers consisting of hydrophilic units, such as poly(acrylamide) (PAM) and poly(methyl acrylate) (PMMA), added to the nonionic surfactant systems have been rarely reported. The effects of the molecular weight, structure, and concentration of polymers on surfactant solutions and the significant changes of the system properties and phase behavior caused by the polymer−surfactant interactions remain open questions.

3.4.2. Ternary Systems of C_nEO_m/Water/Block Copolymer

Amphiphilic block copolymers can be synthesized in various structures, such as di-, tri-, or multiblock forms. The ABA-type copolymer PEO−PPO−PEO (PPO = poly(propylene oxide)) consists of two hydrophilic poly(oxyethylene) (PEO) blocks and a relatively hydrophobic poly(propylene oxide) block, and may be considered a typical polymer for studies with surfactant systems.[371] In water, these copolymers can self-assemble into a series of microstructures analogous to conventional C_nEO_m nonionic surfactants in aqueous solution. The microstructures formed depend mainly on the type of the monomers, the ratios of the block segments, the chain length, and the concentration.[372−375] When block copolymers and C_nEO_m surfactants are mixed in aqueous solution, the phase behavior and the self-organization may be dramatically different from those in pure amphiphile solutions. These systems are receiving more attention as a method for modifying solution properties, although mixed ternary systems including block polymers were ignored for some time. In this section, di- and triblock copolymer/surfactant systems will be discussed.

Some examples of amphiphilic AB, diblock copolymers are poly(propylene oxide)−poly(oxyethylene) (PPO−PEO),[372] poly(dimethylsiloxane)−poly(oxyethylene) (PDMS−PEO),[375−377] poly(butadiene)−poly(oxyethylene) (PB−PEO),[378] and poly(isoprene)−poly(oxyethylene) (PI−PEO).[379] In water, PDMS−PEO, with the molecule structure of $(CH_3)_3SiO-[(CH_3)_2SiO]_{n-2}-(CH_3)_2-SiCH_2CH_2CH_2-O-(CH_2CH_2O)_m-H$ ($Si_nC_3EO_m$), can form lamellar, hexagonal, and cubic liquid crystals, which are highly dependent on the ratio of EO to the total amphiphile.[375] Kunieda et al.[376] studied the phase behavior of a ternary system of $Si_{25}C_3EO_{51.6}$/$C_{12}EO_5$/water by SAXS. $Si_{25}C_3EO_{51.6}$ forms only lamellar liquid crystals (L_α) in water, while $C_{12}EO_5$ is known to form micellar, hexagonal (H_1), bicontinuous cubic (V_1), and lamellar (L_α)

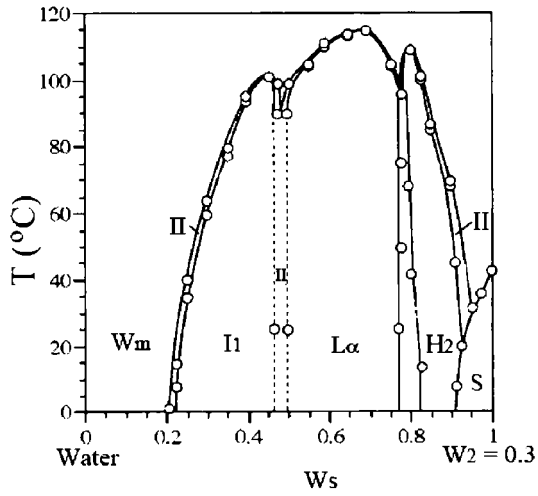

Figure 22. Phase diagram of the water/$Si_{25}C_3EO_{51.6}$/$C_{12}EO_5$ system as a function of temperature. The $C_{12}EO_5$/($C_{12}E_5$ + $Si_{25}C_3EO_{51.6}$) weight fraction is constant (W_2 = 0.3). II indicates a two-phase region. The other notations are described in the text. Reproduced with permission from ref 376. Copyright 2001 American Chemical Society.

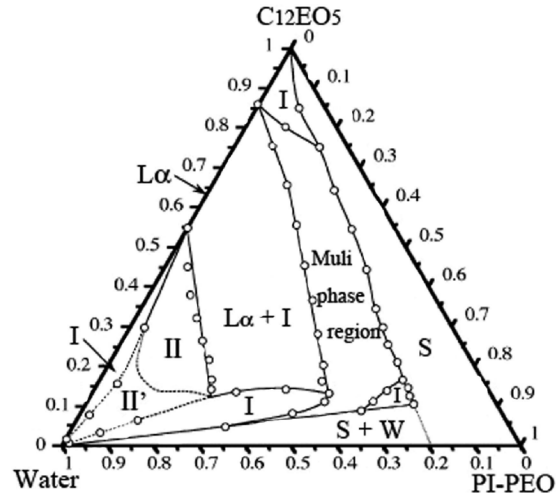

Figure 23. Ternary phase diagram of a water/$C_{12}EO_5$/PI−PEO system at 25 °C. The phase notations are as follows: I, isotropic liquid phase; II, two-liquid phase; S, solid phase; W, excess water phase. The other phase notations are described in the text. Reproduced with permission from ref 379. Copyright 2004 American Chemical Society.

phases in water with increasing concentration.[9] However, the mixture of $Si_{25}C_3EO_{51.6}$/$C_{12}EO_5$ at a 70/30 weight ratio forms various phases in aqueous solution over a wide range of temperature, including a discontinuous micelle cubic (I_1), L_α, reverse bicontinuous cubic (V_2), and reverse hexagonal (H_2) phases, as shown in Figure 22. It was found that the effective cross-sectional area per surfactant molecule surface was reduced upon addition of $C_{12}EO_5$. In addition, a small amount of $C_{12}EO_5$ may be dissolved in the copolymer L_α phase, whereas the copolymer is nearly insoluble in the $C_{12}EO_5$ L_α phase due to packing constraints. Hence, two L_α phases coexist in a surfactant-rich region. The spherical micelle of the I_1 phase was proposed to have a double-layer structure in which the surface was covered by surfactant and the core consisted only of poly(dimethylsiloxane) chains. Subsequently, Aramaki and Olsson[377] measured the self-diffusion constants of amphiphilic molecules in D_2O solutions of mixed $Si_nC_3EO_{51.6}$ (n = 25, 52) and $C_{12}EO_8$ by pulsed-field-gradient NMR. They observed that the miscibility of $Si_nC_3EO_{51.6}$ and $C_{12}EO_8$ in aqueous micelles decreased and coexisting L_α phases occurred when the PDMS chain was much longer than the alkyl chain of surfactant; the same phenomena was observed when the EO chain of surfactant was long. They also confirmed that the copolymer was insoluble in the small surfactant micelles.

Kunieda et al.[379] also studied the phase behavior of a mixture of PI−PEO diblock copolymer (approximately $C_{250}EO_{70}$) and a series of $C_{12}EO_m$ (m = 3, 5, 6, 7, and 9) surfactants in water by SAXS and DLS measurements. The PI−PEO systems behave similarly to the PDMS−PEO systems. Figure 23 is the ternary phase diagram of the water/$C_{12}EO_5$/PI−PEO system at 25 °C. It was found that the copolymer was insoluble in surfactant I_1, H_1, and L_α liquid crystals, whereas an isotropic copolymer fluid phase coexisted with these liquid crystals. However, the copolymer is soluble in long- and short-rod micelles of $C_{12}EO_5$ and $C_{12}EO_6$ because a rod−sphere transition may take place to accommodate the long PI chains inside the large spherical micelles. In the copolymer-rich region, a complex spherical micelle forms in which the surfactant molecules are located at the interface and the PI chains form an oil pool inside. The addition of PI−PEO increased the cloud point temperature of the surfactant aqueous solutions due to the formation of complex hydrophilic micelles.

Using cryo-TEM observations, Davis et al.[378] successfully observed the shapes and sizes of mixed block polymer/surfactant micelles and their concentration dependence in aqueous mixtures of $C_{12}EO_5$. The two neutral block copolymers investigated were diblock PB_{45}−PEO_{126} and the triblock PEO_{21}−PEE_{35} (poly(ethylethylene))−PEO_{21}. Cylindrical micelles of PEO_{21}−PEE_{35}−PEO_{21} are transformed into spherical micelles upon the addition of $C_{12}EO_5$, while large spherical micelles of PB_{45}−PEO_{126} are changed into smaller spheres upon mixing. These results provide the strongest evidence for a strong association between a copolymer and a nonionic surfactant. However, the diblock copolymer exhibits complete miscibility with the surfactant, while the triblock copolymer structure has only a limited miscibility. Hence, the triblock copolymer shows a different effect than the diblock polymers upon mixing with nonionic surfactants.

The water-soluble triblock copolymer primarily discussed here is PEO−PPO−PEO, a commercially available nonionic macromolecular surfactant (trade names, Poloxamer and Pluronic),[371] and is widely used in industrial applications and laboratory research. Since C_nEO_m nonionic surfactants are also widely used, it is important to study the interactions and phase behavior between these surfactants and PEO−PPO−PEO. Some excellent work has been reported recently by Ivanova et al.[380] who studied the phase behavior of PEO_{100}−PPO_{70}−PEO_{100} (F127) aqueous solution upon addition of C_8EO_4 by SAXS. A partial phase diagram was described, which included L_1, I_1, H_1, V_1, and L_α phases. It was suggested that C_8EO_4 as cosurfactant decreased the preferred curvature of molecular layer, leading to the increased variety of microstructures. Later, Wyn-Jones et al.[381] investigated the formation of mixed micelles in the F127/$C_{12}EO_6$/water system using isothermal titration calorimetry (ITC) and DSC and analyzed the results by regular solution theory (RST). In this instance, the researchers showed that the interaction between the two surfactants was synergistic. By comparison, the interaction between PEO_{13}−PPO_{30}−PEO_{13} (L64) and $C_{12}EO_6$ in water was also studied by ITC, DSC, and SANS,[382] which indicated there was strong association between the polymer and surfactant

and that mixed micelles were formed. From the data, the structure and composition of the mixed micelles and their aggregation number were determined. According to RST calculations, the interaction parameter of the mixed micelles was negative, showing a synergistic mixing. Therefore, with a given nonionic surfactant, the strength of the interaction between copolymer and surfactant is primarily determined by the structure of the copolymer.

Other PEO−PPO−PEO copolymer studies have been extended this line of thinking. For instance, PEO_{26}−PPO_{40}−PEO_{26} (P85) and PEO_{37}−PPO_{58}−PEO_{37} (P105) were studied by Kunieda et al.[383,384] The phase behavior and the parameters of liquid crystals were determined by SAXS for solutions of $C_{12}EO_5$ mixed with P85 or P105 with the same weight ratio of hydrophilic chain to total copolymer (f = 0.5). P85 forms a single lamellar liquid crystal (L_α) with $C_{12}EO_5$ in water at high concentration, whereas two L_α phases coexist in the P105/$C_{12}EO_5$/water system at high surfactant content, indicating that the thickness of the lipophilic part of the $C_{12}EO_5$ lamellar phase is too small to accommodate the large lipophilic chain of P105. It was also found that the partial molecular area of copolymer decreased and that of the surfactant increased with increased surfactant concentration in the mixed amphiphiles, indicating that the repulsion between neighboring copolymer EO groups decreased. Recently, a ternary system consisting of PEO_{20}−PPO_{68}−PEO_{20} (P123), $C_{12}EO_6$, and water has been investigated systematically by Löf et al.[385−387] In these studies, P123 was found to self-assemble in water into spherical micelles at ambient temperatures. Upon the addition of $C_{12}EO_6$, interactions between the polymer and surfactant led to the formation of mixed micelles with a cmc well below the cmc for pure $C_{12}EO_6$. ITC and DSC measurements showed a sphere-to-rod transition for the mixed micelles in the P123/$C_{12}EO_6$ system.[385] The transition temperature varied with the composition of the system and showed a minimum of about 40 °C for a $C_{12}EO_6$/P123 molar ratio between 2 and 3. In a subsequent rheological study, a large increase of the viscosity at the transition temperature and shear-thinning behavior was observed, also confirming that the mixed micelles grew and changed gradually in shape from sphere to rod with increasing temperature.[386] The kinetics of micelle growth in this system was also studied by time-resolved SLS and DLS measurements. The rate of growth was slow (>2000 s) but increased with the total concentration. In addition, two different molar ratios, 2.2 and 6.0, of $C_{12}EO_6$/P123 were investigated for comparison. The size of the mixed micelles in the latter system is smaller both before and after the transition, compared with those in the system with a smaller molar ratio. It is proposed that the addition of $C_{12}EO_6$ to P123 causes an increase of the curvature of the micelles, leading to the decrease in micellar size. Further investigations showed that between 25 and 45 °C, the composition induced structural changes in the mixed micelles.[387] At constant temperature, the mixed micelles formed at a low $C_{12}EO_6$/P123 molar ratio (<12) are spherical and do not grow with concentration, whereas at high molar ratio (≥48), the micelles are flexible and wormlike.

In only 20 years, this area has progressed from ignoring the interactions between polymers and nonionic surfactants to expanding this research area with great enthusiasm, that is, investigating homopolymers and di- or triblock copolymers mixed with various C_nEO_m surfactants. Mixtures of the two amphiphiles in water have displayed a rich variety of interactions and properties. The behavior of these systems is determined by many factors, such as the molar mass and structure of the polymer, the ratio of the polymer to surfactant, and the conventional factors of temperature and concentration. Hence, describing relationships among the most influential factors is needed for development of applications of these amphiphile polymer mixtures.

3.5. Ternary Systems of C_nEO_m/Water/Cationic Surfactants

It is known that the mixing of homologous C_nEO_m surfactants with the same headgroup but with different chain lengths displays approximately ideal behavior; that is, there is no net interaction between the surfactant species, or the excess entropy is approximately zero. Hence, the properties of mixed micelles (cmc, size, and shape) can be often predicted by the ideal solution approach. On the other hand, the properties of mixing C_nEO_m with polymers or with structurally different nonionic surfactants usually deviate from ideal behavior due to the existence of net interactions. The departure is not large when all of the amphiphile molecules contain EO groups. For the mixed systems of ionic surfactant and C_nEO_m nonionic surfactant, RST continues to be widely applied to deal with the properties of bulk solutions and at the interfaces.

In contrast, the interactions of *ionic* surfactants and C_nEO_m is usually stronger and more complex than that of C_nEO_m with nonionic surfactants or polymers.[298−300] Added C_nEO_m typically "inserts" into packed ionic surfactant molecules, shielding the repulsion between the head groups of these surfactants.[272] As a result of this shielding action, and in combination with hydrophobic interactions, the micelles in ionic surfactant/C_nEO_m systems form more easily and this leads to a decrease in the cmc. In addition, the interactions between anionic surfactants and C_nEO_m are stronger than that between cationic surfactants and C_nEO_m because the oxygen atoms in C_nEO_m are usually partially protonated by hydration leading to a partial positive charge on the nonionic surfactant.[300] Considering the structures of ionic surfactants and C_nEO_m, the interplay may depend on ion−dipole interactions between the head groups of the two types of surfactants. In comparisons of HCl, NaCl, and dodecylammonium chloride (DAC) mixed with C_8EO_4,[388,389] it was confirmed that Na^+ ions interacted with the EO groups of C_8EO_4, but Cl^- ions do not. Thus, the attractive interaction in the DAC and C_8EO_4 mixed system was proposed to be caused by ion−dipole interactions between the alkylammonium ion and the oxygen atoms of the C_8EO_4 molecule.

In the self-assembly of mixed ionic/nonionic surfactants, hydration, electrostatic, and steric interactions are important driving forces that cannot be ignored in models predicting their interaction. Further, these nonideal mixtures generally deviate extremely from ideal solutions. In many nonideally mixed systems, RST is applied to predict the details of the interactions in the micellization process. For example, predicting the mixed cmc requires knowledge of the cmc of both pure surfactants.[390] However, some experiments have shown that micelle properties are inadequately described by RST in mixed systems with a certain interaction strength,[390] for instance, sodium dodecyl sulfate (SDS)/$C_{12}EO_6$,[391,392] dodecyltrimethylammonium chloride (DTAC)/$C_{12}EO_6$,[391] and dodecyl-trimethylammonium bromide (DTAB)/$C_{12}EO_5$.[393] The micelle properties of these systems may be predicted by RST only by using an adjustable parameter.

To address the limitations described above, molecular thermodynamic theory (MT) has been developed to more accurately describe mixed micelles.[390,394−401] MT theory depends on calculating the free energy contributions of the mixed micelles, involving five parts: the transfer of surfactant tails from the aqueous solution to the core of the mixed micelles, the formation of the interface between the mixed micelles and aqueous solution, the packing of the micelles, the steric repulsive interactions among the surfactant head groups at the interface, and the electrostatic interactions among the surfactant head groups. By considering the free energy contributions of the micellization, MT can be used to predict the cmc, as well as the shape, size and compositions of the mixed micelles. Despite the development of this theoretical approach, the classical RST model is still widely applied in the description of mixed surfactant systems.

Most common cationic surfactants contain tetravalent nitrogen atoms to carry the cationic charge.[402] The presence of the positive charge allows cationic molecules to adsorb strongly to most surfaces, and these types of surfactants are often used in surface modification. In addition, cationic surfactants show higher aquatic toxicity than other typical surfactants. Quaternary ammonium-based surfactants mixed with C_nEO_m are the main focus of this section, to include alkyltrimethylammonium halide and dialkyldimethylammonium halide types.

3.5.1. Ternary Systems of C_nEO_m/Water/Alkyltrimethylammonium Surfactants

The phase behavior and the properties of C_nEO_m/water systems with the addition of cetyltrimethylammonium bromide (CTAB)[403−408] and dodecyltrimethylammonium bromide (DTAB)[409−413] have been intensely studied. In the aqueous system of CTAB and $C_{12}EO_6$, a mixed surfactant monolayer adsorbs at the air/solution interface. The molecular structures of the two surfactants in the mixed monolayer are similar to those in their pure monolayers.[403] However, $C_{12}EO_6$ surfactant molecules are preferentially immersed in the bulk solution rather than in the adsorbed monolayer. Additionally, it has been confirmed that a sphere-to-rod transition usually occurs for micelles of cationic surfactants with the addition of salt, leading to the formation of flexible micelles.[414] Analogously, as measured by static and dynamic light scattering, mixed micelles of CTAB/$C_{12}EO_6$ grow uniaxially to form entangled structures upon increasing the surfactant concentration in the presence of salt.[404] SANS data further shows that there is marked micellar growth with increasing concentration and mole fraction of CTAB.[405] It was noted that the addition of salt maintains the ionic strength of the solution, causing the actual measurement results to be closer to that of an ideal mixture.

Recently, the micellar structure transitions in aqueous systems of CTAB mixed with a series of $C_{12}EO_n$ ($n = 3-8$) surfactants have been studied by rheology, DLS, and SANS measurements.[406] It was found that $C_{12}EO_n$ affected the micellar structures of the cationic surfactants. The micelles grew progressively upon the addition of $C_{12}EO_n$ (particularly when $n \leq 5$), and $C_{12}EO_3$ was the most effective in promoting the micellar growth.

For such CTAB systems, different theoretical models have been applied to describe the properties of the mixed micelles. Zakharova et al.[407] studied the micelle behavior of CTAB and $C_{18}EO_{10}$ by surface tension measurements and kinetics. RST was used to analyze the experimental results and a negative value of the interaction parameter β was found, indicating an attractive interaction of the surfactants and reflecting a synergistic behavior in the mixture. Alternatively, molecular thermodynamic theory was also used to model the effect of counterion binding on micellar solution properties in the CTAB/$C_{12}EO_6$/water system.[408] In this study, the cmc, composition, shape, and size of the micelles, as well as the micellar aggregation number, were accurately predicted by the model, as the predictions were found to correspond well with experimental results.

In DTAB/C_nEO_m aqueous systems, mixed micelles have also been investigated. In an early report,[409] the volume changes, ΔV, of mixed micelles were used to study the interactions between DTAB and $C_{12}EO_7$ in water. It was found that the value of ΔV for the mixed DTAB/$C_{12}EO_7$ micelle solution is positive. In addition, the interaction parameter value is negative, suggesting synergetic mixing behavior. In the same study, SDS was mixed with $C_{12}EO_7$ and their intermolecular interaction was used as a comparison. The value of the interaction parameter for the SDS/$C_{12}EO_7$ system was more negative than that for the DTAB−$C_{12}EO_7$ system, indicating that the anionic surfactant has stronger interactions with the nonionic surfactant. Similar synergetic interactions were also observed in aqueous solutions of DTAB/$C_{12}EO_{23}$[410] or DTAB/$C_{13}EO_{23}$.[411] According to the experimental data, the compositions of the mixed micelles can be calculated by RST.

When DTAB is mixed with $C_{12}EO_m$ surfactants that have shorter EO chains, additional phase transitions occur. Kim et al.[412] studied the aqueous mixed micelle solution of DTAB and $C_{12}EO_5$ by viscosity measurements and SANS. The micellar length was unexpectedly found to shorten with an increase of ionic surfactant concentration. This observation suggests that strong, nonideal mixing of the two surfactants caused an end-cap energy decrease with increasing surfactant concentration, leading to a shortening of the micelles. In addition, Gradzielski et al.[413] found that a very small amount of added DTAB had a very pronounced effect on phase behavior, structure, and macroscopic properties of $C_{12}EO_4$ in aqueous solution. Pure $C_{12}EO_4$ has been noted for its ability to form bilayers and even vesicles in water at certain temperatures and concentrations.[94,108] The formation of these structures is enhanced by changing the bilayer through the incorporation of the ionic surfactants, leading to larger electrostatic repulsion between the vesicles. Rheology results indicated that the addition of DTAB leads to very viscous samples exhibiting birefringence and a large increase in the solution elastic properties. However, upon addition of excess amounts of DTAB, the elastic properties of the sample solution decrease again and the formed vesicles become structurally less defined.

Synergetic interactions are also observed in other mixed cationic/nonionic surfactant systems, for instance, decyltrimethylammonium bromide (DeTAB)/$C_{12}EO_4$/water[413] and tetradecyltrimethylammonium bromide (TTAB)/$C_{12}E_{23}$/water.[415]

3.5.2. Ternary Systems of C_nEO_m/Water/Dialkyldimethylammonium Surfactants

Dialkyl long-chain cationic surfactants, such as didodecyl- (DDAX),[416] dihexadecyl- (DHDAX),[417] and dioctadecyl- (DODAX)[418] trimethylammonium halide, display richer phase behavior in aqueous solution than single-chain cationic surfactants and spontaneously form micelles, bilayers, vesicles,

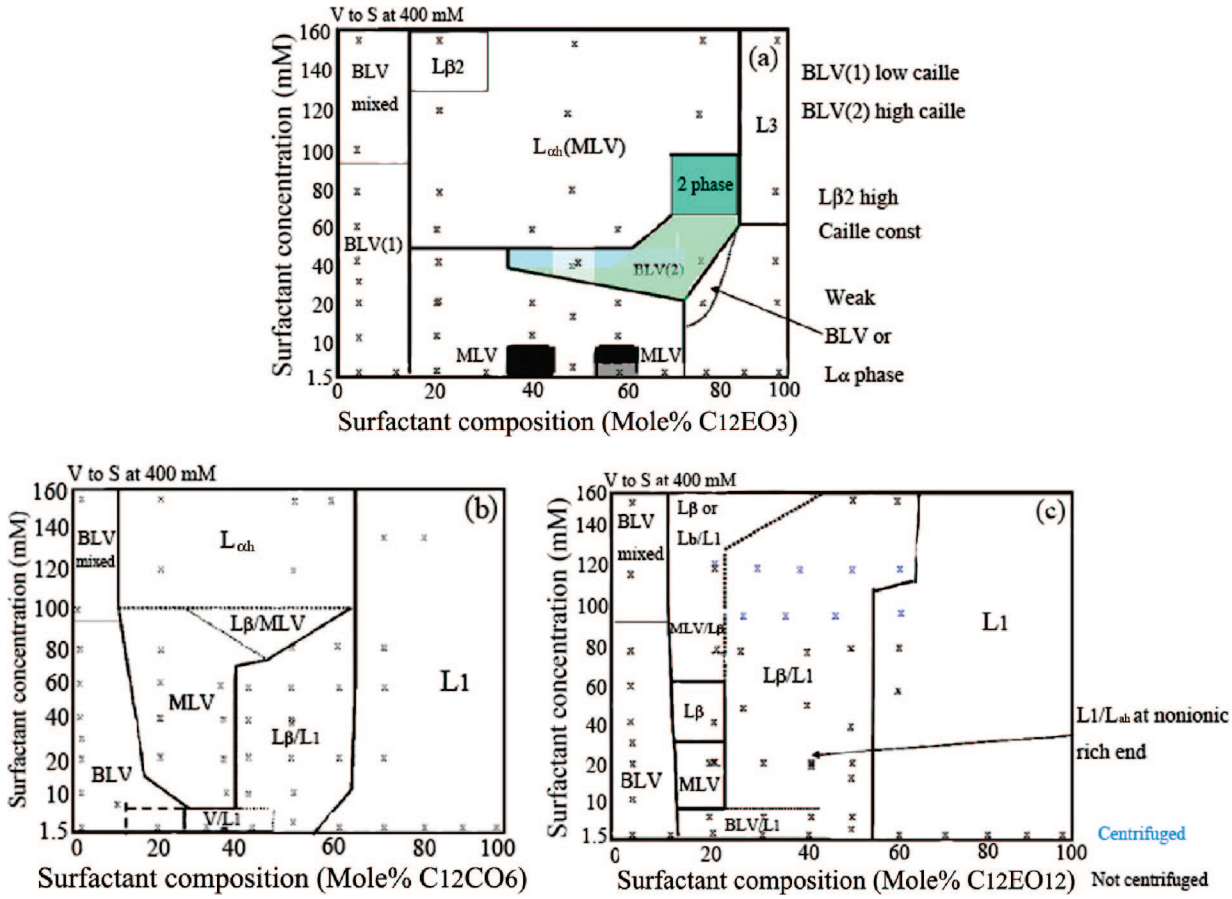

Figure 24. Phase diagrams for (a) DHDAB/$C_{12}EO_3$, (b) DHDAB/$C_{12}EO_6$, and (c) DHDAB/$C_{12}EO_{12}$. BLV and MLV refer to bilamellar and multilamellar vesicles, respectively. L_1 is micellar phase. $L_{\alpha l}$ is the coexisting phase of bilamellar and multilamellar vesicles. Caille const is inversely related to membrane rigidity. Reproduced with permission from ref 421. Copyright 2009 American Chemical Society.

and even sponge bodies at different surfactant concentrations. In particular, using scattering techniques and electron microscopy, giant bilayer structures are often observed in aqueous systems of these surfactants as a result of the low or zero spontaneous curvature of the surfactant molecular layer.[419−421] Considering the description of the packing parameter P,[13] giant bilayer structures are due to the presence of the dual hydrophobic chains causing an increase in P value. In practical application, as a major constituent of hair care products and laundry detergent, dialkyl cationic surfactants are usually used in combination with nonionic surfactants.[420,421] Mixing these cationic surfactants with C_nEO_m surfactants, which exhibit a range of spontaneous curvature from zero to high values, will produce complex systems with distinctive phase behavior and macroproperties. This is obviously important for the practical purpose of tailoring commercial and household surfactant products for their intended use.

The addition of C_nEO_m into a vesicle solution of dialkyl chain cationic surfactant can modify the permeability of the bilayer and the vesicle structure.[422,423] When $C_{12}EO_8$ was added to spontaneously formed vesicle dispersions of DODAX (X = Cl^- or Br^-), a vesicle-to-micelle transition was induced.[423] Experiments monitoring the turbidity, calorimetry, fluorescence quantum yield, anisotropy, and cryo-TEM of these solutions indicated the transition underwent three stages separated by two critical composition points. Up to the first critical point, the vesicles swell due to the solubilization of the cationic surfactants in the bilayers, and the bilayers become saturated. After the first critical point, the vesicles rupture and mixed micelles form, coexisting with vesicles or bilayer fragments. By the second critical point, the vesicle-to-micelle transition is complete. Later investigations into homologous $C_{12}EO_m$/DODAX (m = 5 and 7) aqueous systems also found that the vesicle-to-micelle transition followed a three-stage model.[424]

Recently, Tucker and Penfold et al.[425] have studied the surface properties and the structure of the aggregates formed in the ternary system of DDAB/$C_{12}EO_4$/D_2O via surface tension measurements and SANS. For DDAB and $C_{12}EO_4$ solutions with molar ratios, R_n, between 0.3 and 1, two break points were present in the curve of the surface tension as a function of the total concentration. Here, SANS results also strongly suggested a micelle-to-vesicle transition; in addition, when R_n = 0.3−0.8, nanoscale unilamellar vesicles were formed. Beyond a molar ratio as 0.8, a transition from small vesicles to relatively large bilamellar or multilamellar vesicles was observed in this mixed surfactant system.

In other recent studies,[419−421,426] the surface and solution behavior of the mixed DHDAB and $C_{12}EO_m$ (m = 3, 6, and 12) has been described in detail. In the ternary system of DHDAB/$C_{12}EO_3$/H_2O, different phase regions appear with a change in composition, as shown in Figure 24a.[420,421] At low total concentration, over $C_{12}EO_3$/DHDAB molar ratios 0:100 to 100:0, there are three discrete phase regions consisting of bilamellar vesicles (0:100 to 20:80), multilamellar vesicles (20:80 to 80:20), and a lamellar phase (80:20 to 100:0); this is similar to pure nonionic surfactant systems. At higher total concentrations, a wide continuous $L_{\alpha l}$ phase region (mixing of bilamellar and multilamellar

vesicles) is observed at molar ratios from 20:80 to 80:20. DLS measurements indicated that the vesicles have a diameter of 200−300 nm. For DHDAB/$C_{12}EO_6$ and DHDAB/$C_{12}EO_{12}$ mixtures, the cation-rich solutions are a vesicular ($L_{\alpha l}$) or a planar lamellar phase ($L_{\alpha h}$), and the nonionic surfactant-rich solutions are mainly a micellar phase (L_1).[419,421] At intermediate solution concentration, there is an extensive mixed L_α ($L_{\alpha l}$)/L_1 region. Increasing the EO headgroup of the nonionic surfactant from EO_6 to EO_{12} caused the phase behavior of the mixtures to shift toward micellar structures, as shown in Figure 24b,c. By a combination of neutron reflectivity and surface tension, strong interactions were found between the dialkyl chain cationic surfactant and nonionic surfactant, leading to a large departure from ideal mixing.[305] However, the extreme departure in the adsorption behavior is not consistent with existing theories for nonideal mixing,[421,426] suggesting that a new theoretical approach may be developed by these authors. In addition, in the series of experiments on mixing $C_{12}EO_m$ (m = 3, 6, and 12) with DHDAB, changing the ratios of the mixture or total concentration induced a variation in the membrane rigidity. This observation is related to undulations stabilizing the membrane and also reflects a change in the interaction between cationic and nonionic surfactants and the transitions of the microstructures.

3.5.3. Ternary Systems of C_nEO_m/Water/Other Cationic Surfactants

Croce et al.[427,428] studied the effects of adding $C_{18}EO_{18}$ or $C_{12}EO_{20}$ to aqueous solutions that included a longer chain cationic surfactant, erucyl bis(hydroxyethyl) methylammonium chloride (EHAC). In salt-free solutions, these surfactant mixtures were found to form spherical micelles. A core−shell model combined with a Hayter−Penfold potential[429] was used to describe the SANS data. On the other hand, in a KCl aqueous solution, mixed wormlike micelles were formed from the mixture of these surfactants, and further addition of nonionic surfactant promoted the breaking up of the mixed micelles. Sharma et al.[430] studied the interactions between the $C_{12}EO_6$ and a series of cationic gemini surfactants [$(C_{16}H_{33}N^+(CH_3)_2(CH_2)_mN^+(CH_3)_2C_{16}H_{33})_2Br^-$] ($m$ = 4 and 10), in an aqueous medium. The cmc and micelle aggregation numbers were measured by surface tension, DLS, and fluorescence spectroscopy. RST was used to predict the experimental results, which indicated an attractive interaction between the surfactants and reflected a synergistic behavior between the two surfactant types.

3.6. Ternary Systems of C_nEO_m/Water/Anionic Surfactants

It has been mentioned that the attractive interactions between *anionic* and nonionic surfactants are stronger than those between *cationic* and nonionic surfactants, due to the additional electrostatic interaction caused by the hydration of the EO groups in the nonionic surfactant.[298−300] At present, in the studies of anionic surfactants mixed with C_nEO_m, most reports have focused on evaluating the following compounds: sodium dodecyl sulfate (SDS),[391,392,431−443] sodium dodecyl benzene sulfonate (SDBS),[444−447] and sodium oleate (NaOL).[448,449] This focus is probably due to the solubility and the frequent practical applications of these anionic surfactants. In this section, the interactions and phase behavior of sodium-salt anionic surfactants/C_nEO_m/water systems will be discussed.

3.6.1. Ternary Systems of C_nEO_m/Water/Sodium Dodecyl Sulfate

The anionic surfactant SDS, mixed with a series of nonionic C_nEO_m surfactants, has been studied by various methods. In particular, SDS/$C_{12}EO_n$ mixtures have been investigated in detail, and the formation and properties of mixed micelles, the phase transition behaviors, and the intermolecular interactions have been significantly described, along with robust theoretical treatments. The interest in these systems is due to SDS and $C_{12}EO_n$ having the same hydrocarbon chain but different head groups, which decreases the complexity of model descriptions. Electron spin echo modulation (ESEM) has been used to investigate the micellar structures of an SDS/$C_{12}EO_6$ mixture[391] for comparison with the DTAB/$C_{12}EO_6$ system. The results indicated that the SDS head groups were less deeply located inside the EO head layer than DTAB head groups. The strong interaction of ions is the main driving force for the interactions, as has been mentioned, but it was also found that the cloud point of $C_{12}EO_6$ in water increased immediately after adding SDS.[431] Similar results on the cloud point increases were also obtained in the SDS/$C_{12}EO_5$ or $C_{12}EO_8$/water systems.[432] Finally, mixed systems of SDS and C_nEO_m surfactants have lower Krafft points than binary SDS aqueous solutions.

Lamellar structures and the bending energy of membranes in the $C_{12}EO_5$/water binary system are remarkably influenced by the addition of a small amount of SDS;[434] this is due to electrostatic interactions in the membranes as a result of weakly charging the swollen lamellar phases. The introduced electrostatic repulsion stiffens the membrane and suppresses layer undulations, leading to a reduction of the lamellar spacing. Freeze fracture electron transmission microscopy (FF-TEM) observations showed that the $C_{12}EO_3$/water system turned from a dilute lamellar phase into a vesicle solution upon addition of trace SDS.[434]

In another study of SDS/$C_{12}EO_4$/water systems,[108] the solvent self-diffusion coefficient was measured using PGSE NMR, which indicated the formation of vesicles at low nonionic surfactant compositions. The long-range orientation order of the vesicles increased, as expected, upon adding SDS, and rheology studies showed that the shear viscosity increased when SDS was added to the $C_{12}EO_4$ aqueous solution.[435] Rheo-SALS (small-angle light scattering) experiments revealed that the shear induced formation of multilamellar vesicles and the vesicle size decreased when the shear rate was increased. The SANS data further showed a decrease in layer spacing with increasing shear, indicating that water was squeezed out of the vesicles. In conclusion, the charges introduced by the addition of anionic SDS surfactant affect the behavior of the lamellar structures formed in C_nEO_m/water systems.

In contrast to the lamellar structures, mixed micelles in SDS/C_nEO_m systems have been more widely investigated. Specular neutron reflectivity has been used to determine the adsorption of SDS/$C_{12}EO_3$ mixtures at the air−solution interface; the composition of SDS in the adsorbed layer turns out to be in good agreement with RST predictions.[436] Surface tension and neutron scattering have been used to measure the adsorption and micellization in the SDS/$C_{12}EO_6$ system.[437] The cmc and composition of the mixed micelles in this mixture were also in close agreement with an RST model, and SANS data indicated the presence of spherical micelles. Both surface tension[433,437] and conductivity[438] measurements showed that the cmc of the SDS/C_nEO_m

system decreased with increasing SDS composition. The aggregation numbers of SDS/C_nEO_m mixed micelles have been determined by DLS, SLS,[392] fluorimetry[438,439] and SANS,[440] and compared with the predictions of both major theories (RST and MT). At low ionic surfactant concentration, the growth of mixed micelles is present; this is in part because the addition of SDS with its smaller headgroup reduces steric repulsion between the relatively larger C_nEO_m headgroups. At higher ionic surfactant composition, the micellar size *decreased* due to the increased electrostatic interaction between SDS headgroups. Hence, with ionic surfactant composition, there is usually a maximum value in the aggregation number of the SDS/C_nEO_m mixed micelles with the presence of NaCl.[392,440]

Separately, different models give rise to different predictions for the micelles formed in different mixed systems. The micellar structure (aggregation number, size, and composition) of SDS/$C_{12}EO_{23}$ is described adequately by RST;[439] in contrast, the properties of the micelles in the SDS/$C_{12}EO_6$ system are inadequately predicted by RST.[405,437] The departure from theory is accredited to subtle changes in the packing of the two different surfactant components. To elaborate, the MT model more accurately describes the SDS/$C_{12}EO_6$ system[392,440] because it considers the various energetic contributions of the mixed micelles.

Another anionic surfactant, sodium dodecyl hexa(ethyleneoxide) sulfate ($SDEO_6S$), has also been studied in solutions with $C_{12}EO_6$. The cmcs of both SDS and $SDEO_6S$ mixtures with $C_{12}EO_6$ are very similar, indicating that electrostatic interactions predominate over steric interactions in the formation of mixed micelles. However, the micelle aggregation number of the $SDEO_6S/C_{12}EO_6$ mixture decreases monotonically over the whole mixed ratio without a maximum point. This may indicate that there is no steric advantage to adding $SDEO_6S$ to the nonionic surfactant solution.

The studies described above on micelle solutions of SDS/C_nEO_m are generally performed in the presence of salt (mainly NaCl).[392,433,436−438,440] Addition of salting-out ions can lower the cloud point of nonionic surfactants in water (see section 3.1.3), and it is thought that the addition of salt decreases intermicellar interactions and the "nonideality" of SDS/C_nEO_m mixtures.[392] However, the addition of salt makes the system more complicated and may shift the balance of electrostatic and steric interactions between the polar groups in mixed micelles of SDS and C_nEO_m.[441] Different salts, NaCl, LiCl, and CsCl, have been added to SDS/$C_{12}EO_6$ solutions to study the influences of the counterions in the micellization process.[442] The strongest attractive interactions between the two different surfactants occurred when adding CsCl. The key for the stabilization of the mixed micelles was the reduction in the excess free energy of the hydration layer of the SDS/$C_{12}EO_6$ mixture, presumably caused by the coordination of Cs^+ to the EO head groups. In contrast, mixed micelles in salt-free systems of SDS/$C_{12}EO_6$/water have been studied.[441] Here, SANS experiments indicated that a maximum in the micelle aggregation number disappeared, and the micelle aggregation number decreased over the whole range of surfactant ratios.

Recently, Acharya et al.[443] have further studied the effect of adding short EO group, $C_{12}EO_n$ ($n = 2-4$), surfactants to dilute micellar solutions of SDS. Ternary phase diagrams of these mixed systems (Figure 25) were determined by POM, SAXS, and rheological measurements and are especially instructive for future developments in this area. After addition of SDS and mixing, the viscosity of the solutions increased sharply and a highly viscoelastic solution forms in these solutions. At high SDS concentration, a micellar → H_1 phase transition occurs upon adding $C_{12}EO_n$; this is due to the ability of the surfactants to penetrate into the palisade layer of the aggregates and reduce their interfacial curvature. At higher SDS concentration, successive addition of nonionic surfactant to the H_1 phase induced an $H_1 \rightarrow W_m \rightarrow L_\alpha$ transition. The viscoelastic micellar region is located near the apex of the H_1 region and extends toward the water-rich region. The oscillatory-shear rheological behavior of the viscoelastic solutions can be described by the Maxwell model at low frequency and the combined Maxwell−Rouse model at high shear frequency, which indicates that wormlike micelles entangle to form a transient network. SAXS data also showed that one-dimensional growth of micelles occurred in the SDS/$C_{12}EO_n$ ($n = 2-4$) aqueous solutions.

In addition to studies with monovalent cations, the effect of a divalent cation, Mg^{2+}, on $C_{12}EO_m$ ($m = 12$ and 15) surfactant solutions has been evaluated using magnesium dodecyl sulfate ($Mg(DS)_2$). These surfactant solutions have been studied by surface tension, viscometry, and DLS,[450] and RST adequately described the micellar properties of these solutions, showing a synergetic action in the mixed micelles. The counterion valency had a specific effect on the micelles, namely, $Mg(DS)_2$ had less interaction with the nonionic surfactants than SDS due to stronger condensation of the divalent cation.

3.6.2. Ternary Systems of C_nEO_m/Water/Sodium Alkyl or Alkyl Benzene Sulfonate

Sodium alkyl sulfonates (C_nSO_3Na) and sodium alkyl benzene sulfonates (C_nPhSO_3Na) have different molecular structures that affect their solution behaviors. The latter possesses a large volume hydrophobic group, the phenyl ring, causing larger steric interactions during its aggregation in aqueous solution. The difference in the structures should lead to differences in the interactions and properties of aqueous anionic/nonionic surfactant mixtures.

Analogous to SDS, the addition of a small amount of C_nSO_3Na ($n = 4$, 6, 8, or 10) can markedly change the phase behavior of $C_{12}EO_6$ aqueous solutions.[451] Longer chain sulfonate anionic surfactants move the cloud point curve up in temperature more effectively, leading to the formation of new high-temperature phases. A mixture of $C_6SO_3Na/C_6EO_5/H_2O$ showed a lowering of the cmc compared with the C_6EO_5/H_2O system due to the formation of mixed micelles.[452] The diffusion coefficients in these mixtures indicated a strong coupling between the diffusing species. Kaler[453] has studied the phase behavior in the $C_{10}SO_3Na/C_{12}EO_5/H_2O$ system for comparison with pure $C_{12}EO_5$ in water. Aqueous solutions of $C_{12}EO_5$ can form a highly swollen L_α phase in equilibrium with an L_3 phase, where the L_α phase is stabilized by steric interactions caused by bilayer undulations. The addition of anionic surfactant charged the bilayer, that is, enhanced the electrostatic interactions between components, which increased the bending constant of the surfactant bilayer and inhibited thermal undulations of the bilayer. Consequently, the repeat spacing of the L_α phase decreased, the swelling of the L_α phase ended at higher surfactant concentration, and the L_3 phase was replaced by a new bilayer phase.

Sodium alkyl benzene sulfonates are extremely important commercial anionic surfactants, which are used widely in

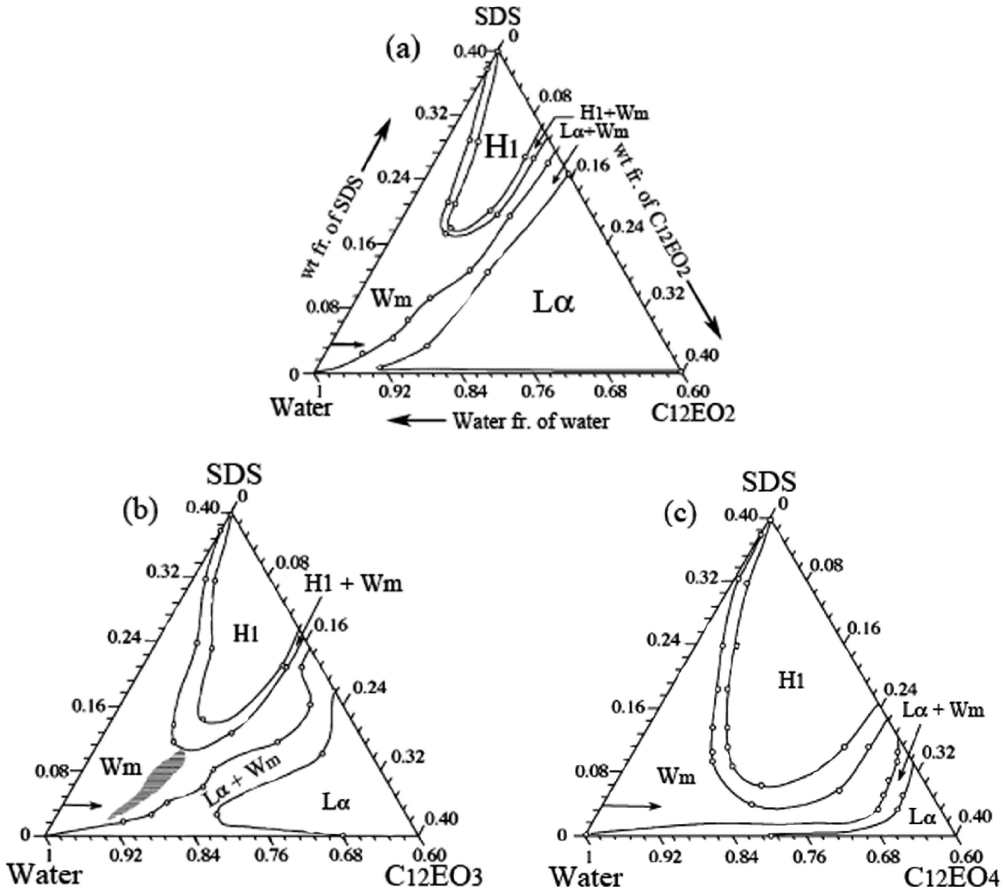

Figure 25. Phase diagrams of $C_{12}EO_n$/SDS/water ($n = 2-4$) systems at 25 °C. W_m is the micellar phase, and H_1 and L_α are the hexagonal and lamellar liquid crystalline phases, respectively. Reproduced with permission from ref 443. Copyright 2006 American Chemical Society.

detergent production. They are usually used in combination with an ethoxylated nonionic surfactant to optimize their properties. For instance, both $C_{12}EO_3$/sodium dodecyl-*p*-benzene sulfonate (SDBS) mixtures and $C_{12}EO_7$/SDBS mixtures exhibit lower oil−water interfacial tension than SDBS alone in water, which provides superior detergency.[444] In addition, the interfacial tension in these systems was found to decrease with time. Richards et al.[445] studied the liquid crystal and other phases of these mixtures by POM, SAXS, and DSC using a $C_{12}EO_6$/SDBS mixture (1:1 by weight) dispersed in water. Over the whole mixture concentration and temperature range, there were large micellar (0−50 wt %) and lamellar (50−95 wt %) regions in the phase diagram. Above 95 wt %, a liquid phase was formed that resembled molten electrolyte. During heating and cooling of the samples, transformations of the L_1 and L_α phases were also observed. Recently, a similar investigation of the phase behavior in an aqueous solution of the $C_{16}EO_8$/SDBS mixture (1:1 by weight) has been completed, and a partial phase diagram of the mixed system is given.[446] In this report, as the temperature and the mixture concentration were adjusted, a complex phase sequence occurred involving L_1, H_1, L_α, and other intermediate phases. In contrast to the pure $C_{16}EO_8$ aqueous solution, the I_1 and V_1 phases disappeared and other phase-region ranges changed markedly. In the $C_{16}EO_8$/SDBS mixture, it is particularly interesting that an L_1 phase lies between the H_1 and L_α phases upon increasing the mixture component over the temperature range of 25 to 35 °C. This may be caused by weak interactions between the micelles during the transition from rods to disks.

Another branched chain anionic surfactant, sodium 6-dodecyl benzene-4 sulfonate (b-SDBS), was added to $C_{12}EO_8$ and $C_{12}EO_{23}$ aqueous solutions[447] and studied by neutron reflectivity and SANS; it was found that small globular mixed micelles were formed in these systems. When Ca^{2+} ions were added into the $C_{12}EO_8$/b-SDBS system, a transition from micelle phase to vesicle phase occurred. However, the transition was not observed in the $C_{12}EO_{23}$/b-SDBS system. Upon the addition of NaCl to either of the above systems, the mixed micelles hardly changed, which was thought to be related to the changes of the counterions and the charges in the systems.

3.6.3. Ternary Systems of C_nEO_m/Water/Other Anionic Surfactants

The behavior of anionic sodium oleate (NaOL) and nonionic C_nEO_m ($n = 10, 12, 14$; $m = 6, 8$) in water has been modeled by RST.[448,449] The calculated interaction parameter indicated the presence of a rather strong attraction between the two surfactants and suggested nonideal mixing and synergetic interactions should be present upon micellization.

On the basis of the above discussion about the phase behavior and physicochemical properties in the mixed systems of ionic surfactant and C_nEO_m, it can be predicted that excess charges and the hydrophobic forces between alkyl chains can drive a mixed system to behave in a more complex fashion. In fact, the two effects also play a key role in many other mixed systems with excess counterions and have such effects as the promotion of phase transformations,

variable adsorption or desorption among aggregates and free ions, and changing the macroproperties of a solution. Hence, the additional charges and effective hydrophobic forces need to be adequately considered when coping with the complex mixing of surfactants and additives in theoretical models.

4. Theoretical Considerations for the Self-Assembled Structures of C_nEO_m

Nonionic surfactants, such as the C_nEO_m type described here, are neutral over a wide range of pH and may be either concentrated at an interface or self-assembled into aggregates. To select C_nEO_m molecules that yield desired structures (i.e., spherical, globular, or rod-like micelles, bilamellar or multilamellar vesicles, liquid crystals, etc.) in solution, it is necessary to know how the molecular structures of the surfactant or other physical factors control the shape and size of the resulting aggregates.

4.1. The Hydrophobic Effect: The Major Driving Force for the Aggregation of Amphiphiles in Aqueous Solutions

The hydrophobic effect is the major driving force for the formation of surfactant bilayers and micelles in aqueous solution. This phenomenon is commonly believed to play a similar role in the folding of globular proteins, although protein folding represents a much more complex system. However, because the hydrophobic effect is an entropic manifestation of solvation in remarkably complex liquids, construction of a valid molecular-scale description of hydrophobic interactions has proven to be very difficult.

An understanding of self-assembled structures of surfactants in solutions requires knowledge of the thermodynamics of self-assembly,[13] an adequate description of the interaction forces[454] between the amphiphilic molecules within aggregates, and an understanding of how these two factors are affected by the solution conditions. A general theoretical consideration from Tanford[455] and from Israelachivili, Mitchell, and Ninham[13] has significantly impacted most treatments of surfactant solutions for more than 30 years. The opposing forces of hydrophobic and hydrophilic interactions may be used to formulate a quantitative expression for the standard free energy change of surfactant aggregation. The formation and the growth of surfactant aggregates can be explained by considering the free energy expression and the geometrical relationships of the aggregates.

The hydrophobic effect results mainly from the entropic nature of the immiscibility of nonpolar compounds with water. The thermodynamic factors that give rise to the hydrophobic effect are complex and still incompletely understood. The free energy of transfer of a nonpolar compound from some reference state, such as water, into organic solution, ΔG, is made up of enthalpy, ΔH, and entropy, ΔS, terms:

$$\Delta G = \Delta H - T\Delta S \tag{2}$$

where T is the temperature. For surfactant self-assembly, much more detailed free energy models[395,456] have been formulated following the model of the standard free energy changes on aggregation pioneered by Tanford,[455] which was used to estimate the area per molecule, "a_s", of a thermodynamic equilibrium quantity. The standard free energy change for well-defined structures such as micelles has been described using three contributions, (i) a transfer free energy contribution arising from the transfer of a hydrocarbon chain from its unfavorable contact with water to the organic region of the aggregate core (a negative value), (ii) an interfacial free energy contribution made up of the entire surface area of the hydrocarbon having residual contact with water at the surface of the aggregate core (a positive value), and (iii) the repulsive interactions between the headgroups (a positive contribution).[455,457]

$$\left(\frac{\partial \Delta G^\circ_{\text{form}}}{kT}\right) = \left(\frac{\partial \Delta G^\circ_{\text{form}}}{kT}\right)_{\text{Transfer}} + \left(\frac{\partial \Delta G^\circ_{\text{form}}}{kT}\right)_{\text{Interface}} + \left(\frac{\partial \Delta G^\circ_{\text{form}}}{kT}\right)_{\text{headgroup}} \tag{3}$$

The absolute value of $\Delta G^\circ_{\text{form}}$ for nonionic C_nEO_m surfactants can be estimated. For example, the $\Delta G^\circ_{\text{form}}$ of $C_{12}EO_8$ is estimated to be $-12.36k_BT$, compared with an experimental value of $-13.22k_BT$.[456]

4.2. Optimal Headgroup Area and Molecular Packing Parameter: Predictions for Surfactant Self-Assembly

The major driving forces that govern the self-assembly of surfactants into well-defined structures arise from the competition of opposing forces of hydrophobic and hydrophilic interactions; these forces act mainly in the interfacial region of the structure and bulk solution. Hydrophobic attraction at the hydrocarbon−water interface induces the amphiphilic molecules to associate (a "hydrophobic collapse"). On the other hand, hydrophilic, ionic, or steric repulsion of the headgroups imposes the opposite requirement that these groups must remain in contact with water. Hydrophobic interactions tend to reduce and hydrophilic interactions tend to enlarge the interfacial area, "a_s", per molecule (i.e., the effective headgroup area) that is exposed to the aqueous phase. For nonionic C_nEO_m surfactants, the repulsive contributions include a hydration force contribution of headgroups and a steric contribution from the hydrocarbon chain.

As proposed by Israelachivili,[454] the total interfacial energy per molecule in an aggregate, denoted μ°_N, includes the contributions of the attractive interfacial free energy and the repulsive interfacial free energy. The attractive free energy is written as γa_s (γ is the interface tension with expected values lying between 20 and 50 $mJ \cdot m^{-2}$), and the repulsive interfacial free energy is written as K/a_s, which may include steric, hydration force, and electrostatic double-layer contributions (the electrostatic double-layer contribution may be neglected for nonionic C_nEO_m surfactants). However, the repulsive interfacial free energy does not have to be known explicitly but is inversely proportional to the surface area occupied per headgroup, a_s, that is, K/a_s. Now, the total free energy of formation may be written as

$$\Delta G^\circ_{\text{form}} = N\mu^\circ_N = N(\gamma a_s + K/a_s) \tag{4}$$

where N is the aggregation number and K is a constant. The minimum energy is therefore given as

$$\frac{\partial \Delta G^\circ_{\text{form}}}{\partial a_s} = \frac{\partial \mu^\circ_N}{\partial a_s} = 0$$

where

$$(\mu_N^\circ)_{min} = 2\gamma a_0$$

and

$$a_0 = \left(\frac{K}{\gamma}\right)^{1/2} \quad (5)$$

Here, a_0 is defined as the optimal surface area per molecule, located at the hydrocarbon−water interface. The standard free energy change for well-defined structures, such as micelles or bilayers, may now be expressed in the following convenient form:

$$\Delta G_{form}^\circ = N\mu_N^\circ = N\left[2\gamma a_0 + \frac{\gamma}{a_s}(a_s - a_0)^2\right] \quad (6)$$

in which the unknown constant K has been eliminated and ΔG_{form}° becomes a function of a_s, having two known or measurable parameters, γ and a_0. Thus from the total free energy change of the opposing interactions located at the hydrocarbon−water interface and at the hydrophilic headgroup−water interface of aggregates, one can conceptualize the idea of an optimal area per headgroup, at which the total interaction free energy change is a minimum, as shown in Figure 26.

On the basis of the concept of optimal area per molecule to balance the attractive hydrophobic interaction and repulsive headgroup interaction within an aggregate, Israelachvili et al.[13] developed the geometric packing parameter or surfactant shape factor, P, for surfactant molecules in various aggregates. P is defined as $v/(a_s l_c)$, in which a_s is the interfacial area occupied by a surfactant headgroup, l_c the critical chain length, and v the hydrocarbon volume. P values can be used to predict the aggregate shapes of surfactants in solutions. In general, the dimensionless factor P will predict the following phase structures: if $0 < P < {}^1/_3$, spherical micelles will form; if ${}^1/_3 \le P < {}^1/_2$, one expects elongated micelles; if ${}^1/_2 \le P < 1$, then disk-like micelles, lamellar structures, or vesicles are expected; if $P = 1$, mainly lamellar structures form; finally, if $P > 1$, the expected structures will be microemulsions or reversed micelles. From a quantitative point view P cannot predict the final structures for all the types of surfactants but may explain the aggregates of nonionic C_nEO_m surfactants qualitatively. The predictions for the aggregation behavior of nonionic surfactant systems have been confirmed by numerous experimental data as presented in sections 2 and 3 above. In general, the increase of nonionic surfactant concentration leads to aggregates in the same general sequence as ionic surfactant systems, namely, spheres, then rods, and finally disks or bilayers. While this rule of thumb is valid, it does not mean that all the structures will be observed for each nonionic surfactant. This is because factor P emphasizes the contribution of the surfactant headgroup in predicting the shapes and sizes of equilibrium aggregates, as opposed to considering the entire surfactant molecule and its interactions.

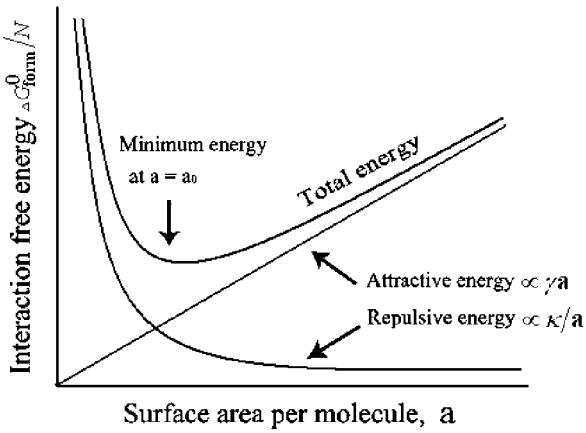

Figure 26. Optimal headgroup area, a_s, at which the opposing forces of the attractive hydrophobic interaction and repulsive headgroup interaction are balanced. Reproduced with permission from ref 454. Copyright 1992 Academic Press.

4.3. Curvature Free Energy: An Explanation for Different Bilayer Structures

It may be predicted that *bilayers* of nonionic C_nEO_m surfactants in solution will give various structures using the geometric packing parameter (P). However, numerous studies[105d,458] show that these bilayers can have different morphologies, such as disk-like micelles, connected and branched tubes (i.e., L_3 or sponge phases), flat bilayers (lamellar or stacked L_α phases), or disconnected and closed uni- or multilamellar vesicles. These different bilayer structures cannot be adequately explained on the basis of the geometric packing parameter (P). Theoretical consideration of curvature free energy in solution has been used to describe the different bilayers. The starting point for this model is

$$F = \oint g \, dA \quad (7)$$

where

$$g = \frac{1}{2}\kappa(c_1 + c_2 - c_0)^2 + \bar{\kappa}c_1c_2 \quad (8)$$

in which c_0 is spontaneous curvature; c_1 and c_2 are two principle curvature of bilayers, which determine the mean curvature, $c_1 + c_2$, and the Gaussian curvature, c_1c_2. κ and $\bar{\kappa}$ are the mean and Gaussian curvature elastic constants (i.e., the bending modulus and Gaussian curvature modulus, respectively) and A is the area of the bilayers. By considering the bending modulus and the Gaussian curvature, Helfrich presented a schematic phase diagram for bilayer phases, as shown in Figure 27.

Although various theoretical models have since been developed[460] and shown to accurately predict experimental observations, it should be noted that the model of the bilayer

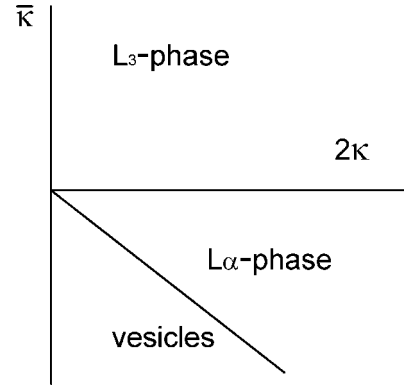

Figure 27. The predicted phase diagram of bilayer phases obeying the bending modulus, κ, and the Gaussian curvature modulus, $\bar{\kappa}$. Reproduced with permission from ref 459. Copyright 1994 IOP Institute of Physics.

bending energy proposed by Helfrich[461] for explaining different bilayers is the starting point of these subsequent descriptions. Additional terms within the entropy and interaction terms may be taken into account as follows. First, entropic factors will favor the splitting of a bilayer into many small vesicles because of increased disorder. This would stabilize vesicles despite the positive bending energy and the so-called edge energy at the boundary of flat bilayers of finite size where water is in contact with the hydrophobic interior of the membrane. Second, there are additional interaction forces between bilayers derived from van der Waals attraction between the hydrophobic groups or from electrostatic repulsion between charged headgroups; however, electrostatic repulsion may be neglected for C_nEO_m nonionic surfactants. The thermal undulation of bilayers is another factor, which lowers the bending rigidity of surfactant bilayers.[462] Finally, the composition fraction could be also an important factor, especially for the formation of bialyers in the multicomponent systems of C_nEO_m nonionic surfactants.

5. Conclusions and Outlook

In this review, the known binary and ternary systems of poly(oxyethylene) *n*-monoalkyl ether nonionic surfactants (C_nEO_m) with other types of surfactants or additives in bulk solutions have been discussed, including their phase behavior, the combined actions of surfactant mixtures (nonionic/nonionic and nonionic/ionic species), and the effects of various additives (salts, oils, alcohols, and polymers). The effect of adjusting experimental conditions (temperature, concentration, composition ratio, and shearing), and the relationship between the macroproperties of surfactant mixtures and their microstructures have been reviewed. Particularly, important phase diagrams of the mixed systems have been described in detail, which in combination with other diagrams in published reviews, may guide future work in this field. In the series of studies we have described, many basic experimental techniques have been applied to determine the microstructures and other physicochemical parameters, such as light scattering, neutron reflectivity, microscopy, NMR, ITC, fluoroscopy, and rheometry, etc.

Further, the regularities exhibited in multicomponent systems were also summarized in this review. In binary systems, self-assembly and phase structures depend on the C_nEO_m molecular structure (the mass fraction of the ethoxyl group), temperature, and surfactant concentration. Theoretically, the behavior of nonionic surfactants may be explained by the packing parameter or by the spontaneous curvature of a system. In ternary systems, the observed results are more complex. In addition to the above three factors that affect binary systems, ternary systems are affected by additional factors; these include salting-in and salting-out effects with added salts, surfactant swelling and penetration with oil additives, and the influence of water-soluble or oil-soluble alcohols if these are the additive. Additionally, the interactions between C_nEO_m and hydrosoluble polymers or ionic or nonionic surfactants, as well as composition ratios of all components need to be considered in accounting for the properties and structures formed in ternary surfactant mixtures. Various models have been used to predict the interplay of the components and the contribution of each constituent in the mixed systems to determine the microstructure and the physicochemical parameters of particular systems. In addition, driving forces in all the systems promoting the equilibrium state are related to the molecular structure and solvent polarity and are influenced by the experimental conditions.

At present, studies on the poly(oxyethylene) *n*-monoalkyl ethers continue to attract attention due to their significant practical applications. Future growth in this area is expected to continue; for instance, current published research has rarely focused on the influence of pressure on C_nEO_m surfactants.[463,464] For instance, it may be predicted that higher pressure will cause a maximum in the cmc value.[128,465] Despite significant work in RT-ILs, reports about the self-assembly of C_nEO_m surfactants in other nonaqueous solvents or cosolvents are few, mainly comprising $scCO_2$, formamide, glycols, hydrazine, or DMSO, even though these solutions may be particularly useful in industrial applications. Moreover, the rheological behavior of the mixed solutions has been rarely reported despite its effectiveness as a method to determine the microstructures and the macroproperties of surfactant systems. Finally, although the aggregates and structures formed in these C_nEO_m surfactant systems are easily regulated, they have been rarely used as templates or microreactors for materials preparation or local reactions;[466,467] hence there are still many fascinating issues to be investigated in this field.

6. Abbreviations and Terminology

AFM	atomic force microscopy
BLV	bilamellar vesicles
[bmim]BF_4	1-butyl-3-methylimidazolium tetrafluoroborate
[bmim]Cl	1-butyl-3-methylimidazolium chloride
[bmim]PF_6	1-butyl-3-methylimidazolium hexafluorophosphate
Brij35($C_{12}EO_{23}$)	poly(oxyethylene)-23-lauryl ether
Brij97	$C_{18}EO_{10}$ with a double bond at the C_9-C_{10} position
Brij700($C_{18}EO_{100}$)	poly(oxyethylene)-100-octadecyl ether
C_9PhEO_{50}	poly(oxyethylene)-50-nonylphenol ether
$C_{18:1}EO_{50.8}$	poly(oxyethylene)-50.8-oleyl ether
$C_{22}EO_6$	hexa(ethylene glycol) *cis*-13-docosenyl ether
$C_{30}EO_9$	nona(ethylene glycol) mono-(11-oxa-14,18,22,26-tetramethylheptacosyl) ether
cac	critical aggregation concentration
$ChEO_m$	poly(oxyethylene) cholesteryl ether
C_kMA	alkyl methacrylate
cmc	critical micelle concentration
C_nEO_m	poly(oxyethylene) monoalkyl ethers
CP	cloud point
cryo-TEM	cryo-transmission electron microscopy
CTAB	cetyltrimethylammonium bromide
DAC	dodecylammonium chloride
DDAX	didodecyl-trimethylammonium halide
DeTAB	decyltrimethylammonium bromide
DHDAX	dihexadecyl-trimethylammonium halide
DKE	sucrose monoalkanoate
DLS	dynamic light scattering
DM	dodecyl-β-D-maltoside
DODAX	dioctadecyltrimethylammonium halide
DSC	differential scanning calorimetry
DTAB	dodecyltrimethylamonium bromide
DTAC	dodecyltrimethylamonium chloride
EAN	ethylammonium nitrate
[emim]Tf_2N	1-ethyl-3-methylimidazolium bis(trifluoromethylsulfonyl)imide
EG	ethylene glycol
ESEM	electron spin echo modulation
F127	$PEO_{100}-PPO_{70}-PEO_{100}$
FF-TEM	freeze fracture transmission electron microscopy

*Fm*3*m*	a lattice of discontinuous cubic phase
FT-IR	Fourier-transform infrared spectroscopy
HLB	hydrophile−lipophile balance
H_0	spontaneous mean curvature
H_1	hexagonal phase
H_2	reversed hexagonal phase
I_1	cubic spherical micelle
*Ia*3*d*	a lattice of bicontinuous cubic phase
*Im*3*m*	a lattice of discontinuous cubic phase
Int.	intermediate phase
ITC	isothermal titration calorimetry
κ	bending elasticity modulus
$\bar{\kappa}$	Gaussian curvature modulus
L_1	normal micelles
L_2	reversed micelles
L_3	swelled sponges
L64	$PEO_{13}-PPO_{30}-PEO_{13}$
IGC	inverse gas chromatography
L_α	lamellar phase
L_α^H	disrupted lamellar phase
$L_{\alpha h}$	planar lamellar phase
$L_{\alpha l}$	lamellar phase made of vesicles
L_β	gel phase
$Mh_1(0)$	random mesh phase
$Mh_1(R\bar{3}m)$	rhombohedral mesh phase
MLVs	multilamellar vesicles
MT	molecular thermodynamic theory
NaOL	sodium oleate
NIR	near-infrared
NMR	nuclear magnetic resonance
OM	octyl-β-D-maltopyranoside
P85	$PEO_{26}-PPO_{40}-PEO_{26}$
P105	$PEO_{37}-PPO_{58}-PEO_{37}$
P123	$PEO_{20}-PPO_{68}-PEO_{20}$
P	geometric packing parameter
PAA	poly(acrylic acid)
PAM	poly(acrylamide)
PB	poly(butadiene)
PDMS	poly(dimethylsiloxane)
PEE	poly(ethylethylene)
PEO	poly(oxyethylene)
PMMA	poly(methyl acrylate)
PG	propylene glycol
PGSE	pulsed gradient spin−echo
PI	poly(isoprene)
PIT	phase transition temperature
*Pm*3*n*	a lattice of discontinuous cubic phase
*Pn*3*m*	a lattice of bicontinuous cubic phase
POM	polarized optical microscopy
PPO	poly(propylene oxide)
$R\bar{3}m$	a lattice of rhombohedral mesh structure
R_FEO_m	$C_6F_{13}-C_2H_4-SC_2H_4-(OC_2H_4)_m$
$R^F{}_nEO_m$	$C_nF_{2n+1}C_2H_4(OC_2H_4)_m$
RST	regular solution theory
RT-ILs	room-temperature ionic liquids
SANS	small-angle neutron scattering
SAXD	small-angle X-ray diffraction
SAXS	small-angle X-ray scattering
$scCO_2$	supercritical carbon dioxide
SDBS	sodium dodecyl benzene sulfonate
SDS	sodium dodecyl sulfate
SLS	static light scattering
TBG	1,2,3-tributanoylglycerol
THG	1,2,3-trihexanoylglycerol
TRFQ	time-resolved fluorescence quenching
TTAB	tetradecyltrimethylammonium bromide
Tween 80	poly(oxyethylene) sorbitan monooleate
V_1	normal "bicontinuous" cubic phase
V_2	reversed "bicontinuous" cubic phase
VEM	video enhanced microscope
VOCs	volatile organic compounds

7. Acknowledgments

The authors thank the NSFC (Grant No. 20625307) and National Basic Research Program of China (973 Program, 2009CB930103) for financial support. J.H. thanks Dr. J. David Van Horn (Visiting Professor, Shandong University) for editorial assistance.

8. References

(1) Schick, M. J., Ed. In *Nonionic Surfactants*; Surfactant Science Series, Vol. 1; Marcel Dekker: New York, 1967.
(2) Schick, M. J., Ed. In *Nonionic Surfactants: Physical Chemistry*; Surfactant Science Series, Vol. 23; Marcel Dekker: New York, 1987.
(3) (a) Manne, S.; Gaub, H. E. *Science* **1995**, *270*, 1480. (b) Liu, J. F.; Ducker, W. A. *J. Phys. Chem. B* **1999**, *103*, 8558.
(4) Velegol, S. B.; Fleming, B. D.; Biggs, S.; Wanless, E. J.; Tilton, R. D. *Langmuir* **2000**, *16*, 2548.
(5) Manne, S.; Warr, G. G. In *Supramolecular Structure in Confined Geometries*; Manne, S., Warr, G. G., Eds.; ACS symposium series 736; American Chemical Society: Washington, DC, 1999; pp 1−23.
(6) (a) Paria, S.; Khilar, K. C. *Adv. Colloid Interface Sci.* **2004**, *110*, 75. (b) Tiberg, F.; Brinck, J.; Grant, L. *Curr. Opin. Colloid Interface Sci.* **2000**, *4*, 411. (c) Zhang, R.; Somasundaran, P. *Adv. Colloid Interface Sci.* **2006**, *123−126*, 213. (d) Atkin, R.; Craig, V. S. J.; Wanless, E. J.; Biggs, S. *Adv. Colloid Interface Sci.* **2003**, *103*, 219. (e) Warr, G. G. *Curr. Opin. Colloid Interface Sci.* **2000**, *5*, 88–94.
(7) Fujii, M. In *Structure-Performance Relationships in Surfactants*, 2nd ed.; Esumi, K., Ueno, M., Eds.; Surfactant Science Series, Vol. 112; Marcel Dekker: New York, 2003; Ch 18.
(8) Chernik, G. G. *Curr. Opin. Colloid Interface Sci.* **2000**, *4*, 381.
(9) Mitchell, D. J.; Tiddy, G. J. T.; Waring, L.; Bostock, T.; McDonald, M. P. *J. Chem. Soc., Faraday Trans. 1* **1983**, *79*, 975.
(10) Karlstrom, G. *J. Phys. Chem.* **1985**, *89*, 4962.
(11) Ahlnas, T.; Karlstrom, G.; Lindman, B. *J. Phys. Chem.* **1987**, *91*, 4030.
(12) Leaver, M. S.; Olsson, U.; Wennerstrom, H.; Strey, R.; Wurz, U. *J. Chem. Soc., Faraday Trans.* **1995**, *91*, 4269.
(13) Israelachvili, J.; Mitchell, D. J.; Ninham, B. W. *J. Chem. Soc., Faraday Trans. 2* **1976**, *72*, 1525.
(14) Olsson, U.; Wennerstrom, H. *Adv. Colloid Interface Sci.* **1994**, *49*, 113.
(15) Anderson, D. M.; Wennerstrom, H.; Olsson, U. *J. Phys. Chem.* **1989**, *93*, 4243.
(16) Strey, R. *Colloid Polym. Sci.* **1994**, *272*, 1005.
(17) Hao, J.; Zemb, Th. *Curr. Opin. Colloid Interface Sci.* **2007**, *12*, 129.
(18) Greaves, T.; Drummond, C. J. *Chem. Soc. Rev.* **2008**, *37*, 1709.
(19) Araos, M. U.; Warr, G. G. *J. Phys. Chem. B* **2005**, *109*, 14275.
(20) Atkin, R.; Warr, G. G. *J. Phys. Chem. B* **2007**, *111*, 9309.
(21) Araos, M. U.; Warr, G. G. *Langmuir* **2008**, *24*, 9354.
(22) Rendall, K.; Tiddy, G. J. T. *J. Chem. Soc., Faraday Trans. 1* **1984**, *80*, 3339.
(23) Kato, M. In *Structure-Performance Relationships in Surfactants*, 2nd ed.; Esumi, K., Ueno, M., Eds.; Surfactant Science Series Vol. 112; Marcel Dekker: New York, 2003; Chapter 11.
(24) Penders, M. H. G. M.; Strey, R. *J. Phys. Chem.* **1995**, *99*, 6091.
(25) (a) Huibers, P. D. T.; Lobanov, V. S.; Katritzky, A. R.; Shah, D. O.; Karelson, M. *Langmuir* **1996**, *12*, 1462. (b) Katritzky, A. R.; Pacureanu, L. M.; Slavov, S. H.; Dobchev, D. A.; Karelson, M. *Ind. Eng. Chem. Res.* **2008**, *47*, 9687.
(26) Bulut, S.; Oskolkova, M. Z.; Schweins, R.; Wennerstrom, H.; Olsson, U. *Langmuir* **2010**, *26*, 5421.
(27) Nibu, Y.; Inoue, T. *J. Colloid Interface Sci.* **1998**, *205*, 231.
(28) Nibu, Y.; Inoue, T. *J. Colloid Interface Sci.* **1998**, *205*, 305.
(29) Portet, F.; Desbène, P. L.; Treiner, C. *J. Colloid Interface Sci.* **1997**, *194*, 379.
(30) Aveyard, R.; Binks, B. P.; Fletcher, P. D. I.; MacNab, J. R. *Langmuir* **1995**, *11*, 2515.
(31) Nibu, Y.; Suemori, T.; Inoue, T. *J. Colloid Interface Sci.* **1997**, *191*, 256.
(32) Huibers, P. D.; Shah, D. O.; Katritzky, A. R. *J. Colloid Interface Sci.* **1997**, *193*, 132.
(33) Funari, S. S.; Rapp, G. *J. Phys. Chem. B* **1997**, *101*, 732.
(34) Lynch, M. L.; Kochvar, K. A.; Burns, J. L.; Laughlin, R. G. *Langmuir* **2000**, *16*, 3537.
(35) Chen, Z.; Yan, Y.; Huang, X. *Colloids Surf. A* **2008**, *331*, 239.
(36) Laughlin, R. G.; Lynch, M. L.; Marcott, C.; Munyon, R. L.; Marrer, A. M.; Kochvar, K. A. *J. Phys. Chem. B* **2000**, *104*, 7354.
(37) Patrick, H. N.; Warr, G. G. *Colloids Surf. A* **2000**, *162*, 149.
(38) Levitz, P. *Langmuir* **1991**, *7*, 1595.

(39) Schick, M. J.; Atlas, S. M.; Eirich, F. R. *J. Phys. Chem.* **1962**, *66*, 1326.
(40) Santos, F. K. G.; Neto, E. L. B.; Moura, M. C. P. A.; Dantas, T. N. C.; Neto, A. A. D. *Colloids Surf. A* **2009**, *333*, 156.
(41) Ishii, S.; Ishikawa, S.; Mizuno, N.; Matsuoka, K.; Honda, C.; Endo, K. *J. Colloid Interface Sci.* **2008**, *317*, 115.
(42) Richtering, W. H.; Burchard, W.; Jahns, E.; Finkelmann, H. *J. Phys. Chem.* **1988**, *92*, 6032.
(43) Honda, C.; Katsumata, Y.; Yasutome, R.; Yamazaki, S.; Ishii, S.; Matsuoka, K.; Endo, K. *J. Photochem. Photobiol., A: Chem.* **2006**, *182*, 151.
(44) Funarit, S. S.; Holmes, M. C.; Tiddy, G. J. T. *J. Phys. Chem.* **1994**, *98*, 3015.
(45) Fairhurst, C. E.; Holmes, M. C.; Leaver, M. S. *Langmuir* **1997**, *13*, 4964.
(46) Minewaki, K.; Kato, T.; Yoshida, H.; Imai, M.; Ito, K. *Langmuir* **2001**, *17*, 1864.
(47) Mehta, S. K.; Chaudhary, S.; Kumar, B.; Bhasin, K. K. *J. Phys. Chem. B* **2009**, *113*, 7188.
(48) Griffin, W. C. *J. Soc. Cosmet. Chem.* **1954**, *5*, 259.
(49) Samii, A. A.; Karlstrom, G.; Lindman, B. *Langmuir* **1991**, *7*, 1067.
(50) Tasaki, K. *J. Am. Chem. Soc.* **1996**, *118*, 8459.
(51) Kjellander, R.; Florin, E. *J. Chem. Soc., Faraday Trans. 1* **1981**, *77*, 2053.
(52) Hirschfelder, J.; Stevenson, D.; Eyring, H. *J. Chem. Phys.* **1937**, *5*, 896.
(53) Goldstein, R. E. *J. Chem. Phys.* **1984**, *80*, 5340.
(54) Karlstrom, G. *J. Phys. Chem.* **1985**, *89*, 4962.
(55) Evans, H.; Tildesley, D. J.; Leng, C. A. *J. Chem. Soc., Faraday Trans. 1* **1987**, *83*, 1525.
(56) Warnheim, T.; Bokstrom, J.; Williams, Y. *Colloid Polym. Sci.* **1988**, *266*, 562.
(57) Samii, A. A.; Lindman, B.; Karlstrom, G. *Prog. Colloid Polym. Sci.* **1990**, *82*, 280.
(58) Nilsson, P. G.; Lindman, B. *J. Phys. Chem.* **1983**, *87*, 4756.
(59) Fujimatsu, H.; Ogasawara, S.; Kuroiwa, S. *Colloid Polym. Sci.* **1988**, *266*, 594.
(60) Laughlin, R. G. *The Aqueous Phase Behavior of Surfactants*; Academic Press: New York, 1994.
(61) Sakya, P.; Seddon, J. M.; Templer, R. H.; Mirkin, R. J.; Tiddy, G. J. T. *Langmuir* **1997**, *13*, 3706.
(62) Tschierske, C. *Curr. Opin. Colloid Interface Sci.* **2002**, *7*, 69.
(63) Conroy, J. P.; Hall, C.; Lang, C. A.; Rendall, K.; Tiddy, G. J. T.; Walsh, J.; Lindblom, G. P. *Colloid Polym. Sci.* **1990**, *82*, 253.
(64) Kunieda, H.; Shigeta, K.; Ozawa, K.; Suzuki, M. *J. Phys. Chem. B* **1997**, *101*, 7952.
(65) Holmes, M. C. *Curr. Opin. Colloid Interface Sci.* **1998**, *3*, 485.
(66) Tanford, C.; Nozekl, Y.; Rohde, F. *J. Phys. Chem.* **1977**, *81*, 1555.
(67) Kleshchanok, D.; Strunk, H.; Tuiniera, R.; Lang, P. R. *Phys. Chem. Chem. Phys.* **2006**, *8*, 869.
(68) Lee, Y.; Liu, H.; Wang, Y. *J. Chin. Inst. Chem. Eng.* **2002**, *33*, 439.
(69) Flory, P. J. *Principles of Polymer Chemistry*; Cornell University Press: New York, 1953.
(70) Ueno, M.; Takasawa, Y.; Miyashige, H.; Tabata, Y.; Meguro, K. *Colloid Polym. Sci.* **1981**, *259*, 761.
(71) Lindman, B.; Wennerstrom, H. *J. Phys. Chem.* **1991**, *95*, 6053.
(72) Kato, T.; Seimiya, T. *J. Phys. Chem.* **1986**, *90*, 3159.
(73) Nilsson, P. G.; Wennerstrom, H.; Lindman, B. *J. Phys. Chem.* **1983**, *87*, 1377.
(74) Brown, W.; Johnsen, R.; Stilbs, P.; Lindman, B. *J. Phys. Chem.* **1983**, *87*, 4548.
(75) Cummins, P. G.; Staples, E.; Penfold, J.; Heenan, R. K. *Langmuir* **1989**, *5*, 1195.
(76) Zulauf, M.; Weckstrom, K.; Havter, J. B.; Degiorgio, V.; Corti, M. *J. Phys. Chem.* **1985**, *89*, 3411.
(77) Cebula, D. J.; Ottewill, R. H. *Colloid Polym. Sci.* **1982**, *260*, 1118.
(78) Lum Wan, J. A.; Warr, G. G.; White, L. R.; Grieser, F. *Colloid Polym. Sci.* **1987**, *265*, 528.
(79) Yoshimura, S.; Shirai, S.; Einaga, Y. *J. Phys. Chem. B* **2004**, *108*, 15477.
(80) Attwood, D. *J. Phys. Chem.* **1968**, *72*, 339.
(81) (a) Corti, M.; Degiorgio, V. *Phys. Rev. Lett.* **1980**, *45*, 1045. (b) Corti, M.; Degiorgio, V. *J. Phys. Chem.* **1981**, *85*, 1442.
(82) Lin, Z.; Scriven, L. E.; Davis, H. T. *Langmuir* **1992**, *8*, 2200.
(83) Berheim-Groswasser, A.; Wachtel, E.; Talmon, Y. *Langmuir* **2000**, *16*, 4131.
(84) Berheim-Groswasser, A.; Tlusty, T.; Safran, S. A.; Talmon, Y. *Langmuir* **1999**, *15*, 5448.
(85) Tlusty, T.; Safran, S. A.; Menes, R.; Strey, R. *Phys. Rev. Lett.* **1997**, *78*, 2616.
(86) Raghavan, S. R.; Edlund, H.; Kaler, E. W. *Langmuir* **2002**, *18*, 1056.
(87) Zilman, A.; Safran, S. A.; Sottmann, T.; Strey, R. *Langmuir* **2004**, *20*, 2199.
(88) Blom, A.; Warr, G. G. *Langmuir* **2005**, *21*, 11850.
(89) Heerklotz, H.; Tsamaloukas, A.; Kita-Tokarczyk, K.; Strunz, P.; Gutberlet, T. *J. Am. Chem. Soc.* **2004**, *126*, 16544.
(90) Corti, M.; Minero, C.; Degiorgio, V. *J. Phys. Chem.* **1984**, *88*, 309.
(91) Kato, T.; Anzai, S.; Seimiya, T. *J. Phys. Chem.* **1987**, *91*, 4655.
(92) Kato, T.; Anzai, S.; Seimiya, T. *J. Phys. Chem.* **1990**, *94*, 7255.
(93) Kato, T.; Terao, T.; Tsukada, M.; Seimiya, T. *J. Phys. Chem.* **1993**, *97*, 3910.
(94) Bryskhe, K.; Bulut, S.; Olsson, U. *J. Phys. Chem. B* **2005**, *109*, 9265.
(95) Borbely, S. *Langmuir* **2000**, *16*, 5540.
(96) Phillies, G. D. J.; Hunt, R. H.; Strang, K.; Sushkin, N. *Langmuir* **1995**, *11*, 3408.
(97) Hakansson, B.; Hansson, P.; Regev, O.; Soderman, O. *Langmuir* **1998**, *14*, 5730.
(98) Kato, T.; Terao, T.; Seimiya, T. *Langmuir* **1994**, *10*, 4688.
(99) Kato, T.; Terao, T.; Tsukada, M.; Seimiya, T. *J. Phys. Chem.* **1993**, *97*, 3910.
(100) Kato, T.; Taguchi, N.; Terao, T.; Seimiya, T. *Langmuir* **1995**, *11*, 4661.
(101) Hayter, J. B.; Zulauf, M. *Colloid Polym. Sci.* **1982**, *260*, 1023.
(102) Zulauf, M.; Rosenbusch, J. P. *J. Phys. Chem.* **1983**, *87*, 856.
(103) Glatter, O.; Fritz, G.; Lindner, H.; Brunner-Popela, J.; Mittelbach, R.; Strey, R.; Egelhaaf, S. U. *Langmuir* **2000**, *16*, 8692.
(104) Kaler, E. W.; Herrington, K. L.; Murthy, A. K.; Zasadzinski, J. A. N. *Science* **1989**, *245*, 1371.
(105) (a) Hao, J.; Hoffmann, H.; Horbaschek, K. *J. Phys. Chem. B* **2000**, *104*, 10144. (b) Hao, J.; Hoffmann, H.; Horbaschek, K. *Langmuir* **2001**, *17*, 4151. (c) Hao, J.; Liu, W.; Xu, G.; Zheng, L. *Langmuir* **2003**, *19*, 10635. (d) Hao, J.; Yuan, Z.; Liu, W.; Hoffmann, H. *J. Phys. Chem. B* **2004**, *108*, 19163. (e) Hao, J.; Hoffmann, H. *Curr. Opin. Colloid Interface Sci.* **2004**, *9*, 279. (f) Song, A.; Dong, S.; Jia, X.; Hao, J.; Liu, W.; Liu, T. *Angew. Chem., Int. Ed.* **2005**, *44*, 4018. (g) Li, H.; Jia, X.; Li, Y.; Shi, X.; Hao, J. *J. Phys. Chem. B* **2006**, *110*, 68. (h) Li, H.; Hao, J. *J. Phys. Chem. B* **2007**, *111*, 7719. (i) Li, X.; Dong, S.; Jia, X.; Song, A.; Hao, J. *Chem.—Eur. J.* **2007**, *13*, 9495. (j) Shen, Y.; Hao, J.; Hoffmann, H. *Soft Matter* **2007**, *3*, 1407.
(106) (a) Hao, J.; Wang, J.; Liu, W.; Abdel-Rahem, R.; Hoffmann, H. *J. Phys. Chem. B* **2004**, *108*, 1168. (b) Wang, J.; Song, A.; Jia, X.; Hao, J.; Liu, W.; Hoffmann, H. *J. Phys. Chem. B* **2005**, *109*, 11126. (c) Song, A.; Jia, X.; Teng, M.; Hao, J. *Chem.—Eur. J.* **2007**, *13*, 496. (d) Teng, M.; Song, A.; Liu, L.; Hao, J. *J. Phys. Chem. B* **2008**, *112*, 1671.
(107) Medronho, B.; Shafaei, S.; Szopko, R.; Miguel, M. G.; Olsson, U.; Schmidt, C. *Langmuir* **2008**, *24*, 6480.
(108) Olsson, U.; Nakamura, K.; Kunieda, H.; Strey, R. *Langmuir* **1996**, *12*, 3045.
(109) Le, T. D.; Olsson, U.; Mortensen, K.; Zipfel, J.; Lindner, P.; Richtering, W. *Langmuir* **2001**, *17*, 999.
(110) Nettesheim, F.; Zipfel, J.; Olsson, U.; Renth, F.; Lindner, P.; Richtering, W. *Langmuir* **2003**, *19*, 3603.
(111) Leaver, M.; Fogden, A.; Holmes, M. C.; Fairhurst, C. *Langmuir* **2001**, *17*, 35.
(112) Fairhurst, C. E.; Holmes, M. C.; Leaver, M. S. *Langmuir* **1996**, *12*, 6336.
(113) Funarit, S. S.; Holmes, M. C.; Tiddy, G. J. T. *J. Phys. Chem.* **1992**, *96*, 11029.
(114) Rancon, Y.; Charvolin, J. *J. Phys. Chem.* **1988**, *92*, 2646.
(115) Rancon, Y.; Charvolin, J. *J. Phys. Chem.* **1988**, *92*, 6339.
(116) Briganti, G.; Segre, A. L.; Capitani, D.; Casieri, C.; La Mesa, C. *J. Phys. Chem. B* **1999**, *103*, 825.
(117) Henriksson, U.; Klason, T. *J. Phys. Chem.* **1983**, *87*, 3802.
(118) Burgoyne, J.; Holmes, M. C.; Tiddy, G. J. T. *J. Phys. Chem.* **1995**, *99*, 6054.
(119) Funari, S. S.; Rapp, G. *Proc. Natl. Acad. Sci. U.S.A.* **1999**, *96*, 7756.
(120) Butler, P. *Curr. Opin. Colloid Interface Sci.* **1999**, *4*, 214.
(121) Baciu, M.; Olsson, U.; Leaver, M. S.; Holmes, M. C. *J. Phys. Chem. B* **2006**, *110*, 8184.
(122) Dimitrova, G. T.; Tadros, Th. F.; Luckham, P. F.; Kipps, M. R. *Langmuir* **1996**, *12*, 315.
(123) Lindman, B.; Soderman, O.; Wennerstrom, H. In *Surfactant Solutions: New Methods of Investigation*; Zana, R., Ed.; Surfactant Science Series, Vol. 22; Marcel Dekker: New York, 1987; Chapter 6.
(124) (a) Hoffmann, H.; Rehage, H. In *Surfactant Solutions: New Methods of Investigation*, Zana, R., Ed.; Surfactant Science Series, Vol. 22; Marcel Dekker: New York, 1987; Chapter 4. (b) Hoffmann, H.; Ulbricht, W. In *Structure-Performance Relationships in Surfactants*, 2nd ed.; Esumi, K., Ueno, M., Eds.; Surfactant Science Series, Vol. 112; Marcel Dekker: New York, 2003; Chapter 10.
(125) Richtering, W. *Curr. Opin. Colloid Interface Sci.* **2001**, *6*, 446.
(126) Oliviero, C.; Coppola, L.; Gianferri, R.; Nicotera, I.; Olsson, U. *Colloids Surf. A* **2003**, *228*, 85.
(127) Bulut, S.; Gonzalez-Perez, A.; Olsson, U. *Langmuir* **2008**, *24*, 22.

(128) Bossev, D. P.; Kline, S. R.; Israelachvili, J. N.; Paulaitis, M. E. *Langmuir* **2001**, *17*, 7728.
(129) Cates, M. E.; Milner, S. T. *Phys. Rev. Lett.* **1989**, *62*, 1856.
(130) Panizza, P.; Roux, D.; Vuillaume, V.; Lu, C -Y. D.; Cates, M. E. *Langmuir* **1996**, *12*, 248.
(131) Rehage, H.; Hoffmann, H. *Mol. Phys.* **1991**, *74*, 933.
(132) Hoffmann, H.; Thunig, C.; Schmiedel, P.; Munkert, U. *Langmuir* **1994**, *10*, 3972.
(133) Németh, Zs.; Halász, L.; Pálinkás, J.; Bóta, A.; Horányi, T. *Colloids Surf. A* **1998**, *145*, 107.
(134) Evans, D. F.; Yamauchi, A.; Roman, R.; Casassa, E. Z. *J. Colloid Interface Sci.* **1982**, *88*, 89.
(135) Evans, D. F.; Yamauchi, A.; Wei, G. J.; Bloomfield, V. A. *J. Phys. Chem.* **1983**, *87*, 3537.
(136) Anderson, J. L.; Pino, V.; Hagberg, E. C.; Sheares, V. V.; Armstrong, D. W. *Chem. Commun.* **2003**, 2444.
(137) Nakashima, T.; Kimizuka, N. *Chem. Lett.* **2002**, 1018.
(138) Hao, J.; Song, A.; Wang, J.; Chen, X.; Zhuang, W.; Shi, F.; Zhou, F.; Liu, W. *Chem.—Eur. J.* **2005**, *11*, 3936.
(139) Gao, H.; Li, J.; Han, B.; Chen, W.; Zhang, J.; Zhang, R.; Yan, D. *Phys. Chem. Chem. Phys.* **2004**, *6*, 2914.
(140) Eastoe, J.; Gold, S.; Rogers, S. E.; Paul, A.; Welton, T.; Heenan, R. K.; Grillo, I. *J. Am. Chem. Soc.* **2005**, *127*, 7302.
(141) Evans, D. F.; Kaler, E. W.; Benton, W. J. *J. Phys. Chem.* **1983**, *87*, 533.
(142) Tamura-Lis, W.; Lis, L. J.; Quinn, P. J. *J. Phys. Chem.* **1987**, *91*, 4625.
(143) Tamura-Lis, W.; Lis, L. J.; Quinn, P. J. *Biophys. J.* **1988**, *53*, 489.
(144) Abraham, M. H. *Chem. Soc. Rev.* **1993**, *22*, 73.
(145) Fletcher, K. A.; Pandey, S. *Langmuir* **2004**, *20*, 33.
(146) Tran, C. D.; Yu, S. *J. Colloid Interface Sci.* **2005**, *283*, 613.
(147) Patrascu, C.; Gauffre, F.; Nallet, F.; Bordes, R.; Oberdisse, J.; Viguerie, N. L.; Mingotaud, C. *ChemPhysChem* **2006**, *7*, 99.
(148) Inoue, T.; Misono, T. *J. Colloid Interface Sci.* **2008**, *326*, 483.
(149) Friberg, S. E.; Yin, Q.; Pavel, F.; Mackay, R. A.; Holbrey, J. D.; Seddon, K. R.; Aikens, P. A. *J. Dispersion Sci. Technol.* **2000**, *21*, 185.
(150) Wang, Z.; Liu, F.; Gao, Y.; Zhuang, W.; Xu, L.; Han, B.; Li, G.; Zhang, G. *Langmuir* **2005**, *21*, 4931.
(151) Evans, D. F.; Chen, S. H.; Schriver, G. W.; Arnett, E. M. *J. Am. Chem. Soc.* **1981**, *103*, 481.
(152) Seguin, C.; Eastoe, J.; Clapperton, R.; Heenan, R. K.; Grillo, I. *Colloids Surf. A* **2006**, *282—283*, 134.
(153) Jonstromer, M.; Sjoberg, M.; Warnheim, T. *J. Phys. Chem.* **1990**, *94*, 7549.
(154) Desimone, J. M. *Science* **2002**, *297*, 799.
(155) Desimone, J. M.; Keiper, J. S. *Curr. Opin. Colloid Interface Sci.* **2001**, *5*, 333.
(156) Eastoe, J.; Gold, S. *Phys. Chem. Chem. Phys.* **2005**, *7*, 1352.
(157) Eastoe, J.; Gold, S.; Steytler, D. C. *Langmuir* **2006**, *22*, 9832.
(158) McClain, J. B.; Betts, D. E.; Canelas, D. A.; Samulski, E. T.; Desimone, J. M.; Londono, J. D.; Cochran, H. D.; Wignall, G. D.; Chillura-Martino, D.; Triolo, R. *Science* **1996**, *274*, 2049.
(159) Hoefling, T. A.; Enick, R. M.; Beckman, E. J. *J. Phys. Chem.* **1991**, *95*, 7127.
(160) Consani, K. A.; Smith, R. D. *J. Supercrit. Fluids* **1990**, *3*, 51.
(161) Eastoe, J.; Dupont, A.; Steytler, D. C. *Curr. Opin. Colloid Interface Sci.* **2003**, *8*, 267.
(162) Kirby, C. F.; McHugh, M. A. *Chem. Rev.* **1999**, *99*, 565.
(163) Liu, J.; Han, B.; Li, G.; Liu, Z.; He, J.; Yang, G. *Fluid Phase Equilib.* **2001**, *187—188*, 247.
(164) Yee, G. G.; Fulton, J. L.; Smith, R. D. *Langmuir* **1992**, *8*, 377.
(165) Hollamby, M. J.; Trickett, K.; Mohamed, A.; Eastoe, J. *Langmuir* **2009**, *25*, 12909.
(166) Ritter, J. M.; Paulaitis, M. E. *Langmuir* **1990**, *6*, 934.
(167) Chennamsetty, N.; Bock, H.; Scanu, L. F.; Siperstein, F. R.; Gubbins, K. E. *J. Chem. Phys.* **2005**, *122*, 094710.
(168) Sjoberg, M.; Henriksson, U.; Warnheim, T. *Langmuir* **1990**, *6*, 1205.
(169) Beesley, A. H.; Evans, D. F.; Laughlin, R. G. *J. Phys. Chem.* **1988**, *92*, 791.
(170) Ray, A. *J. Am. Chem. Soc.* **1969**, *91*, 6511.
(171) Warnheim, T.; Jonsson, A. *J. Colloid Interface Sci.* **1988**, *125*, 627.
(172) Aramaki, K.; Olsson, U.; Yamaguchi, Y.; Kunieda, H. *Langmuir* **1999**, *15*, 6226.
(173) Seguin, C.; Eastoe, J.; Heenan, R. K.; Grillo, I. *J. Colloid Interface Sci.* **2007**, *315*, 714.
(174) Seguin, C.; Eastoe, J.; Heenan, R. K.; Grillo, I. *Langmuir* **2007**, *23*, 4199.
(175) Rico, I.; Lattes, A. *J. Phys. Chem.* **1986**, *90*, 5870.
(176) Gopal, R.; Singh, J. R. *J. Phys. Chem.* **1973**, *77*, 554.
(177) Belmajdoub, A.; El Bayed, K.; Brondeau, J.; Canet, D.; Rico, I.; Lattes, A. *J. Phys. Chem.* **1988**, *92*, 3569.
(178) Auvray, X.; Petipas, C.; Anthore, R.; Rico, I.; Lattes, A.; Samii, A. A. Z.; de Savignac, A. *Colloid Polym. Sci.* **1987**, *265*, 925.
(179) Alexandridis, P. *Macromolecules* **1998**, *31*, 6935.
(180) Warnheim, T.; Sjoberg, M. *J. Colloid Interface Sci.* **1989**, *131*, 402.
(181) Couper, A.; Gladden, D.; Ingram, B. *Discuss. Faraday Soc.* **1975**, *59*, 63.
(182) Friberg, S. E.; Liang, Y. C. *Colloids Surf.* **1987**, *24*, 325.
(183) Ramadan, M.; Evans, D. F.; Lumry, R.; Philion, S. *J. Phys. Chem.* **1985**, *89*, 3405.
(184) Long, F. A.; McDevit, W. F. *Chem. Rev.* **1952**, *51*, 119.
(185) McDevit, W. F.; Long, F. A. *J. Am. Chem. Soc.* **1952**, *74*, 1773.
(186) Bostrom, M.; Williams, D. R. M.; Ninham, B. W. *Langmuir* **2001**, *17*, 4475.
(187) Corrin, M. L.; Harkins, W. D. *J. Am. Chem. Soc.* **1947**, *69*, 679.
(188) Anacker, E. W.; Ghose, H. M. *J. Phys. Chem.* **1963**, *67*, 1713.
(189) Klevens, H. B. *J. Phys. Chem.* **1948**, *52*, 130.
(190) Hobbs, M. E. *J. Phys. Chem.* **1951**, *55*, 675.
(191) Mukerjee, P. *J. Phys. Chem.* **1965**, *69*, 4038.
(192) Mukerjee, P. *J. Phys. Chem.* **1970**, *74*, 3824.
(193) Ray, A.; Nemethy, G. *J. Am. Chem. Soc.* **1971**, *93*, 6787.
(194) Carale, T. R.; Pham, Q. T.; Blankschtein, D. *Langmuir* **1994**, *10*, 109.
(195) Hsiao, L.; Dunning, H. N.; Lorenz, P. B. *J. Phys. Chem.* **1956**, *60*, 657.
(196) Hofmeister, F. *Arch. Exp. Pathol. Pharmakol.* **1888**, *24*, 247.
(197) Collins, K. D.; Washabaugh, M. W. *Q. Rev. Biophys.* **1985**, *18*, 323.
(198) Cacace, M. G.; Landau, E. M.; Ramsden, J. J. *Q. Rev. Biophys.* **1997**, *30*, 241.
(199) Kunz, W.; Lo Nostro, P.; Ninham, B. W. *Curr. Opin. Colloid Interface Sci.* **2004**, *9*, 1.
(200) Kunz, W.; Henle, J.; Ninham, B. W. *Curr. Opin. Colloid Interface Sci.* **2004**, *9*, 19.
(201) Leontidis, E. *Curr. Opin. Colloid Interface Sci.* **2002**, *7*, 81.
(202) Bostrom, M.; Williams, D. R. M.; Ninham, B. W. *Curr. Opin. Colloid Interface Sci.* **2004**, *9*, 48.
(203) Balasubramanian, D.; Mitra, P. *J. Phys. Chem.* **1979**, *83*, 2724.
(204) Kabalnov, A.; Olsson, U.; Wennerstroem, H. *J. Phys. Chem.* **1995**, *99*, 6220.
(205) Alexandridis, P.; Holzwarth, J. F. *Langmuir* **1997**, *13*, 6074.
(206) Von Hippel, P. H.; Wong, K. Y. *Science* **1964**, *145*, 577.
(207) Hribar, B.; Southall, N. T.; Vlachy, V.; Dill, K. A. *J. Am. Chem. Soc.* **2002**, *124*, 12302.
(208) Bostrom, M.; Williams, D. R. M.; Ninham, B. W. *Langmuir* **2001**, *17*, 4475.
(209) Bostrom, M.; Williams, D. R. M.; Ninham, B. W. *Langmuir* **2002**, *18*, 6010.
(210) Edwards, S. A.; Williams, D. R. M. *Curr. Opin. Colloid Interface Sci.* **2004**, *9*, 139.
(211) Gurau, M. C.; Lim, S.-M.; Castellana, E. T.; Albertorio, F.; Kataoka, S.; Cremer, P. S. *J. Am. Chem. Soc.* **2004**, *126*, 10522.
(212) Schott, H.; Han, S. K. *J. Pharm. Sci.* **1975**, *64*, 658.
(213) Schott, H.; Han, S. K. *J. Pharm. Sci.* **1976**, *65*, 975.
(214) Bahadur, P.; Li, P.; Almgren, M.; Brown, W. *Langmuir* **1992**, *8*, 1903.
(215) Jain, N. J.; Aswal, V. K.; Goyal, P. S.; Bahadur, P. *Colloids Surf. A* **2000**, *173*, 85.
(216) Desai, P. R.; Jain, N. J. *Colloids Surf. A* **2001**, *178*, 57.
(217) Alexandridis, P.; Holzwarth, J. F. *Langmuir* **1997**, *13*, 6074.
(218) Pandit, N.; Trygstad, T.; Croy, S.; Bohorquez, M.; Koch, C. *J. Colloid Interface Sci.* **2000**, *222*, 213.
(219) Binana-Limbele, W.; Van Os, N. M.; Rupert, L. A. M.; Zana, R. *J. Colloid Interface Sci.* **1991**, *144*, 458.
(220) Weckström, K. *Chem. Phys. Lett.* **1985**, *119*, 503.
(221) Imae, T. *J. Phys. Chem.* **1988**, *92*, 5721.
(222) Imae, T. *Langmuir* **1989**, *5*, 205.
(223) Deguchi, K.; Meguro, K. *J. Colloid Interface Sci.* **1975**, *50*, 223.
(224) Gordon, J. E. *J. Phys. Chem.* **1970**, *74*, 3823.
(225) Mukerjee, P. *Adv. Colloid Interface Sci.* **1967**, *1*, 241.
(226) Puwada, S.; Blankschtein, D. *J. Chem. Phys.* **1990**, *92*, 3710.
(227) Blankschtein, D.; Thurston, G. M.; Benedek, G. B. *J. Chem. Phys.* **1986**, *85*, 7268.
(228) Weckström, K.; Zulauf, M. *J. Chem. Soc., Faraday Trans. 1.* **1985**, *81*, 2947.
(229) Weckström, K.; Papageorgiou, A. C. *J. Colloid Interface Sci.* **2007**, *310*, 151.
(230) Sharma, K. S.; Patil, S. R.; Rakshit, A. K. *Colloids Surf. A* **2003**, *219*, 67.
(231) Rodriguez, C.; Kunieda, H. *Langmuir* **2000**, *16*, 8263.
(232) Iwanaga, T.; Suzuki, M.; Kunieda, H. *Langmuir* **1998**, *14*, 5775.
(233) Zheng, L.; Minamikawa, H.; Harada, K.; Inoue, T.; Chernik, G. G. *Langmuir* **2003**, *19*, 10487.
(234) Inoue, T.; Yokoyama, Y.; Zheng, L. *J. Colloid Interface Sci.* **2004**, *274*, 349.

(235) Pelik, O.; Dag, O. *Angew. Chem., Int. Ed.* **2001**, *40*, 3799.
(236) Dag, O.; Samarskaya, O.; Tura, C.; Gunay, A.; Cuelik, O. *Langmuir* **2003**, *19*, 3671.
(237) Dag, O.; Alayoglu, S.; Tura, C.; Celik, O. *Chem. Mater.* **2003**, *15*, 2711.
(238) Dag, O.; Alayoglu, S.; Uysal, I. *J. Phys. Chem. B* **2004**, *108*, 8439.
(239) Attard, G. S.; Bartlett, P. N.; Coleman, N. R. B.; Elliott, J. M.; Owen, J. R. *Langmuir* **1998**, *14*, 7340.
(240) Hoar, T. P.; Schulman, J. H. *Nature* **1943**, *7*, 9.
(241) Schulman, J. H.; Stoeckenius, W.; Prince, L. *J. Phys. Chem.* **1959**, *63*, 1677.
(242) Shinoda, K. *J. Colloid Interface Sci.* **1967**, *24*, 4.
(243) Kahlweit, M.; Strey, R. *Angew. Chem., Int. Ed.* **1985**, *24*, 654.
(244) Strey, R. *Curr. Opin. Colloid Interface Sci.* **1996**, *1*, 402.
(245) Hellweg, T. *Curr. Opin. Colloid Interface Sci.* **2002**, *7*, 50.
(246) Li, X.; Kunieda, H. *Curr. Opin. Colloid Interface Sci.* **2003**, *8*, 327.
(247) Winsor, P. A. In *Solvent Properties of Amphiphilic Compounds*; Butterworth: London, 1954.
(248) Winsor, P. A. *Chem. Rev.* **1968**, *68*, 1.
(249) Friberg, S.; Lapczynska, I.; Gillberg, G. *J. Colloid Interface Sci.* **1976**, *56*, 19.
(250) Scriven, L. E. *Nature* **1976**, *263*, 123.
(251) Talmon, Y.; Prager, S. *J. Chem. Phys.* **1982**, *76*, 1535.
(252) Olsson, U.; Schurtenberger, P. *Langmuir* **1993**, *9*, 3389.
(253) Leaver, M.; Furo, I.; Olsson, U. *Langmuir* **1995**, *11*, 1524.
(254) Vasilescu, M.; Caragheorgheopol, A.; Almgren, M.; Brown, W.; Alsins, J.; Johannsson, R. *Langmuir* **1995**, *11*, 2893.
(255) Olsson, U.; Wennerström, H. *Adv. Colloid Interface Sci.* **1994**, *49*, 113.
(256) Olsson, U.; Wuerz, U.; Strey, R. *J. Phys. Chem.* **1993**, *97*, 4535.
(257) Lichterfeld, F.; Schmeling, T.; Strey, R. *J. Phys. Chem.* **1986**, *90*, 5762.
(258) Kunieda, H.; Shinoda, K. *J. Colloid Interface Sci.* **1980**, *75*, 601.
(259) Kunieda, H.; Shinoda, K. *J. Colloid Interface Sci.* **1985**, *107*, 107.
(260) Kunieda, H.; Ishikawa, N. *J. Colloid Interface Sci.* **1985**, *107*, 122.
(261) Kahlweit, M.; Strey, R.; Firman, P.; Haase, D.; Jen, J.; Schomacker, R. *Langmuir* **1988**, *4*, 499.
(262) Kahlweit, M.; Strey, R.; Schomaecker, R.; Haase, D. *Langmuir* **1989**, *5*, 305.
(263) Kahlweit, M.; Strey, R.; Busse, G. *J. Phys. Chem.* **1990**, *94*, 3881.
(264) Kahlweit, M.; Strey, R.; Firman, P.; Haase, D. *Langmuir* **1985**, *1*, 281.
(265) Kahlweit, M.; Strey, R.; Firman, P. *J. Phys. Chem.* **1986**, *90*, 671.
(266) Kahlweit, M.; Strey, R.; Haase, D.; Firman, P. *Langmuir* **1988**, *4*, 785.
(267) Choy, D.; Chen, S.-H. *Phys. Rev. E* **2000**, *61*, 4148.
(268) Choy, D.; Chen, S.-H. *Phys. Rev. E* **2001**, *63*, 021401.
(269) Kunieda, H.; Shinoda, K. *J. Colloid Interface Sci.* **1985**, *107*, 107.
(270) Kahlweit, M.; Lessner, E.; Strey, R. *J. Phys. Chem.* **1983**, *87*, 5032.
(271) Lade, O.; Beizai, K.; Sottmann, T.; Strey, R. *Langmuir* **2000**, *16*, 4122.
(272) Rosen, M. J.; Murphy, D. S. *Langmuir* **1991**, *7*, 2630.
(273) Aveyard, R.; Binks, B. P.; Fletcher, P. D. I. *Langmuir* **1989**, *5*, 1210.
(274) Leitao, H.; Somoza, A. M.; Telo da Gama, M. M.; Sottmann, T.; Strey, R. *J. Chem. Phys.* **1996**, *105*, 2875.
(275) Sottmann, T.; Strey, R. *J. Chem. Phys.* **1997**, *106*, 8606.
(276) Wennerstrom, H.; Balogh, J.; Olsson, U. *Colloids Surf. A* **2006**, *291*, 69.
(277) Kunieda, H.; Nakamura, K.; Evans, D. F. *J. Am. Chem. Soc.* **1991**, *113*, 1051.
(278) Kunieda, H.; Nakamura, K.; Davis, H. T.; Evans, D. F. *Langmuir* **1991**, *7*, 915.
(279) (a) Kunieda, H.; Nakamura, K.; Olsson, U.; Lindman, B. *J. Phys. Chem.* **1993**, *97*, 9525. (b) Kunieda, H.; Rajagopalan, V. In *Vesicles*; Rosoff, M., Ed.; Surfactant Science Series, Vol. 62; Marcel Dekker: New York, 1996; Chapter 3.
(280) Kunieda, H.; Ozawa, K.; Huang, K.-L. *J. Phys. Chem. B* **1998**, *102*, 831.
(281) Kunieda, H.; Shigeta, K.; Suzuki, M. *Langmuir* **1999**, *15*, 3118.
(282) Wang, Y.; Holmes, M. C.; Leaver, M. S.; Fogden, A. *Langmuir* **2006**, *22*, 10951.
(283) Alam, M. M.; Varade, D.; Aramaki, K. *J. Colloid Interface Sci.* **2008**, *325*, 243.
(284) Zana, R. *Adv. Colloid Interface Sci.* **1995**, *57*, 1.
(285) Kahlweit, M.; Busse, G.; Jen, J. *J. Phys. Chem.* **1991**, *95*, 5580.
(286) Kahlweit, M.; Strey, R.; Busse, G. *J. Phys. Chem.* **1991**, *95*, 5344.
(287) Strey, R.; Jonstroemer, M. *J. Phys. Chem.* **1992**, *96*, 4537.
(288) Jonstriimer, M.; Strey, R. *J. Phys. Chem.* **1992**, *96*, 5993.
(289) Valiente, M. *Colloids Surf. A* **1995**, *105*, 265.
(290) Freyssingeas, E.; Nallet, F.; Roux, D. *Langmuir* **1996**, *12*, 6028.
(291) Preu, H.; Zradba, A.; Rast, S.; Kunz, W.; Hardy, E. H.; Zeidler, M. D. *Phys. Chem. Chem. Phys.* **1999**, *1*, 3321.
(292) Tomsic, M.; Rogac, M. B.; Jamnik, A.; Kunz, W.; Touraud, D.; Bergmann, A.; Glatter, O. *J. Phys. Chem. B* **2004**, *108*, 7021.
(293) Tomsic, M.; Rogac, M. B.; Jamnik, A.; Kunz, W.; Touraud, D.; Bergmann, A.; Glatter, O. *J. Colloid Interface Sci.* **2006**, *294*, 194.
(294) Lin, S. Y.; Lin, Y. Y.; Chen, E. M.; Hsu, C. T.; Kwan, C. C. *Langmuir* **1999**, *15*, 4370.
(295) Nemethy, G.; Ray, A. *J. Phys. Chem.* **1971**, *75*, 809.
(296) Penfold, J.; Staples, E.; Tucker, I.; Cummins, P. *J. Colloid Interface Sci.* **1997**, *185*, 424.
(297) Montalvo, G.; Rodenas, E.; Valiente, M. *J. Colloid Interface Sci.* **1998**, *202*, 232.
(298) Scamehorn, J. F., Ed. In *Phenomena in Mixed Surfactant Systems*; ACS Symposium Series 311, American Chemical Society: Washington, DC, 1986.
(299) Rosen, M. J. In *Surfactants and Interfacial Phenomena*, 2nd ed.; Wiley-Interscience: New York, 1989.
(300) Rosen, M. J. *Langmuir* **1991**, *7*, 885.
(301) Clint, J. H. *J. Chem. Soc., Faraday Trans. 1* **1975**, *71*, 1327.
(302) Rubingh, D. N. In *Solution Chemistry of Surfactants*; Mittal, K. L., Ed.; Plenum: New York, 1979; Vol. 1.
(303) Holland, P. M.; Rubingh, D. N. *J. Phys. Chem.* **1983**, *87*, 1984.
(304) Rosen, M. J.; Hua, X. Y. *J. Colloid Interface Sci.* **1982**, *86*, 164.
(305) Penfold, J.; Staples, E.; Thompson, L.; Tucker, I. *Colloids Surf. A* **1995**, *102*, 127.
(306) Penfold, J.; Staples, E.; Tucker, I.; Thomas, R. K. *Colloids Surf. A* **1998**, *201*, 223.
(307) Nikas, Y. J.; Puwada, S.; Blankschtein, D. *Langmuir* **1992**, *8*, 2680.
(308) Islam, M. N.; Kato, T. *J. Colloid Interface Sci.* **2005**, *289*, 581.
(309) Thomas, H. G.; Lomakin, A.; Blankschtein, D.; Benedek, G. B. *Langmuir* **1997**, *13*, 209.
(310) Inoue, T.; Ohmura, H.; Murata, D. *J. Colloid Interface Sci.* **2003**, *258*, 374.
(311) Soderman, O.; Johansson, I. *Curr. Opin. Colloid Interface Sci.* **2000**, *4*, 391.
(312) Hoffmann, B.; Platz, G. *Curr. Opin. Colloid Interface Sci.* **2001**, *6*, 171.
(313) Hato, M. *Curr. Opin. Colloid Interface Sci.* **2001**, *6*, 268.
(314) Stubenrauch, C. *Curr. Opin. Colloid Interface Sci.* **2001**, *6*, 160.
(315) Warr, G. G.; Drummond, C. J.; Grieser, F.; Ninham, B. W.; Evans, D. F. *J. Phys. Chem.* **1986**, *90*, 4581.
(316) Coppola, L.; Gordano, A.; Procopio, A.; Sindona, G. *Colloids Surf. A* **2002**, *196*, 175.
(317) Maestro, A.; Acharya, D. P.; Furukawa, H.; Gutierrez, J. M.; Quintela, M. A. L.; Ishitobi, M.; Kunieda, H. *J. Phys. Chem. B* **2004**, *108*, 14009.
(318) Matsubara, H.; Takumi, H.; Takamatsu, T.; Takiue, T.; Aratono, M. *Colloid Polym. Sci.* **2009**, *287*, 1077.
(319) Aoudia, M.; Zana, R. *J. Colloid Interface Sci.* **1998**, *206*, 158.
(320) Drummond, C. J.; Warr, G. G.; Grieser, F.; Ninham, B. W.; Evans, D. F. *J. Phys. Chem.* **1985**, *89*, 2103.
(321) Liljekvist, P.; Kjellin, M.; Eriksson, J. C. *Adv. Colloid Interface Sci.* **2001**, *89*−*90*, 293.
(322) Zhang, R.; Zhang, L.; Somasundaran, P. *J. Colloid Interface Sci.* **2004**, *278*, 453.
(323) Rosen, M. J.; Sulthana, S. B. *J. Colloid Interface Sci.* **2001**, *239*, 528.
(324) Zhang, R.; Somasundaran, P. *Langmuir* **2004**, *20*, 8552.
(325) Engelskirchen, S.; Acharya, D. P.; Roman, M. G.; Kunieda, H. *Colloids Surf. A* **2006**, *279*, 113.
(326) Baverback, P.; Oliveira, C. L. P.; Garamus, V. M.; Varga, I.; Claesson, P. M.; Pedersen, J. S. *Langmuir* **2009**, *25*, 7296.
(327) Acharya, D. P.; Kunieda, H. *J. Phys. Chem. B* **2003**, *107*, 10168.
(328) Moitzi, C.; Freiberger, N.; Glatter, O. *J. Phys. Chem. B* **2005**, *109*, 16161.
(329) Varade, D.; Abreu, C. R.; Shrestha, L. K.; Aramaki, K. *J. Phys. Chem. B* **2007**, *111*, 10438.
(330) Ahmed, T.; Aramaki, K. *J. Colloid Interface Sci.* **2008**, *327*, 180.
(331) Varade, D.; Ushiyama, K.; Shrestha, L. K.; Aramaki, K. *J. Colloid Interface Sci.* **2007**, *312*, 489.
(332) Quintela, M. A. L.; Akahane, A.; Rodriguez, C.; Kunieda, H. *J. Colloid Interface Sci.* **2002**, *247*, 186.
(333) Sato, T.; Hossain, Md. K.; Acharya, D. P.; Glatter, O.; Chiba, A.; Kunieda, H. *J. Phys. Chem. B* **2004**, *108*, 12927.
(334) Kunieda, H.; Shinoda, K. *J. Phys. Chem.* **1976**, *80*, 2468.
(335) Shrestha, R. G.; Shrestha, L. K.; Sharma, S. C.; Aramaki, K. *J. Phys. Chem. B* **2008**, *112*, 10520.
(336) Rossi, S.; Karlsson, G.; Ristori, S.; Martini, G.; Edwards, K. *Langmuir* **2001**, *17*, 2340.
(337) Ravey, J. C.; Gherbi, A.; Stebe, M. J. *Prog. Colloid Polym. Sci.* **1989**, *79*, 272.
(338) Ravey, J. C.; Gherbi, A.; Stebe, M. J. *Prog. Colloid Polym. Sci.* **1991**, *84*, 95.

(339) Almgren, M.; Garamus, V. M.; Nordstierna, L.; Blin, J. L.; Stebe, M. J. *Langmuir* **2010**, *26*, 5355.
(340) Villeneuve, M.; Normura, T.; Matsuki, H.; Kaneshina, S.; Aratono, M. *J. Colloid Interface Sci.* **2001**, *234*, 127.
(341) Peyre, V. *Curr. Opin. Colloid Interface Sci.* **2009**, *14*, 30.
(342) Matsuoka, K.; Moroi, Y. *Curr. Opin. Colloid Interface Sci.* **2003**, *8*, 227.
(343) Funasaki, N.; Hada, S. *J. Phys. Chem.* **1983**, *87*, 342.
(344) Blin, J. L.; Henzel, N.; Stebe, M. J. *J. Colloid Interface Sci.* **2006**, *302*, 643.
(345) Michaux, F.; Blin, J. L.; Stebe, M. J. *Langmuir* **2007**, *23*, 2138.
(346) Michaux, F.; Blin, J. L.; Stebe, M. J. *J. Phys. Chem. B* **2008**, *112*, 11950.
(347) Dong, S. L.; Li, X.; Xu, G. Y.; Hoffmann, H. *J. Phys. Chem. B* **2007**, *111*, 5903.
(348) Dong, S. L.; Xu, G. Y.; Hoffmann, H. *J. Phys. Chem. B* **2008**, *112*, 9371.
(349) Xiao, F. S. *Curr. Opin. Colloid Interface Sci.* **2005**, *10*, 94.
(350) Brackman, J. C.; Van Os, N. M.; Engberts, J. B. F. N. *Langmuir* **1988**, *4*, 1266.
(351) Anthony, O.; Zana, R. *Langmuir* **1994**, *10*, 4048.
(352) Saito, S. In *Polymer-Surfactant Interactions: Non-ionic Surfactants*; Schick, M. J., Ed.; Marcel Dekker: New York, 1987.
(353) Lindman, B.; Thalberg, K. In *Interactions of Surfactants with Polymers and Proteins*; Goddard, E. D., Ananthapadmanabhan, K. P., Eds.; CRC Press: Boca Raton, FL, 1993.
(354) Cohen-Addad, S.; di Meglio, J. M. *Langmuir* **1994**, *10*, 773.
(355) Cabane, B. *J. Phys. Chem.* **1977**, *81*, 1639.
(356) Ruckenstein, E.; Huber, G.; Hoffmann, H. *Langmuir* **1987**, *3*, 382.
(357) Brown, W.; Fundin, J.; da Graca Miguel, M. *Macromolecules* **1992**, *25*, 7192.
(358) Almgren, M.; Hansson, P.; Mukhtar, E.; Stam, J. V. *Langmuir* **1992**, *8*, 2405.
(359) Feitosa, E.; Brown, W.; Hansson, P. *Macromolecules* **1996**, *29*, 2169.
(360) Feitosa, E.; Brown, W.; Vasilescu, M.; Vethamuthu, M. S. *Macromolecules* **1996**, *29*, 6837.
(361) Feitosa, E.; Brown, W.; Vethamuthu, M. S. *Langmuir* **1996**, *12*, 5985.
(362) Feitosa, E.; Brown, W.; Wang, K.; Barreleiro, P. C. A. *Macromolecules* **2002**, *35*, 201.
(363) Makulska, S.; Chudy, E.; Urbaniak, K.; Wieczorek, S. A.; Zywocinski, A.; Holyst, R. *J. Phys. Chem. B* **2007**, *111*, 7948.
(364) Saito, S.; Taniguchi, T. *J. Colloid Interface Sci.* **1973**, *44*, 114.
(365) Saito, S. *Colloid Polym. Sci.* **1979**, *257*, 266.
(366) Maloney, C.; Huber, K. *J. Colloid Interface Sci.* **1994**, *164*, 463.
(367) Anghel, D. F.; Saito, S.; Iovescu, A.; Baran, A. *Colloids Surf. A* **1994**, *90*, 89.
(368) Vasilescu, M.; Anghel, D. F.; Almgren, M.; Hansson, P.; Saito, S. *Langmuir* **1997**, *13*, 6951.
(369) Anghel, D. F.; Saito, S.; Bran, A.; Iovescu, A. *Langmuir* **1998**, *14*, 5342.
(370) Yang, B. S.; Lal, J.; Richetti, P.; Marques, C. M.; Russel, W. B.; Prud'homme, R. K. *Langmuir* **2001**, *17*, 5834.
(371) Alexandridis, P.; Holzwarth, T. A. *Colloids Surf. A* **1995**, *96*, 1.
(372) Hajduk, D. A.; Kossuth, M. B.; Hillmyer, M. A.; Bates, F. S. *J. Phys. Chem. B* **1998**, *102*, 4269.
(373) Battaglia, G.; Ryan, A. J. *Macromolecules* **2006**, *39*, 798.
(374) Blanazs, A.; Armes, S. P.; Ryan, A. J. *Macromol. Rapid Commun.* **2009**, *30*, 267.
(375) Kunieda, H.; Uddin, Md. H.; Horii, M.; Furukawa, H.; Harashima, A. *J. Phys. Chem. B* **2001**, *105*, 5419.
(376) Kunieda, H.; Uddin, Md. H.; Furukawa, H.; Harashima, A. *Macromolecules* **2001**, *34*, 9093.
(377) Aramaki, K.; Olsson, U. *J. Colloid Interface Sci.* **2007**, *312*, 52.
(378) Zheng, Y.; Davis, H. T. *Langmuir* **2000**, *16*, 6453.
(379) Kunieda, H.; Kaneko, M.; Lpez-Quintela, M. A.; Tsukahara, M. *Langmuir* **2004**, *20*, 2164.
(380) Ivanova, R.; Alexandridis, P.; Lindman, B. *Colloids Surf. A* **2001**, *183−185*, 41.
(381) Couderc, S.; Li, Y.; Bloor, D. M.; Holzwarth, J. F.; Wyn-Jones, E. *Langmuir* **2001**, *17*, 4818.
(382) Couderc-Azouani, S.; Sidhu, J.; Thurn, T.; Xu, R.; Bloor, D. M.; Penfold, J.; Holzwarth, J. F.; Wyn-Jones, E. *Langmuir* **2005**, *21*, 10197.
(383) Hossain, Md. K.; Hinata, S.; Lopez-Quintela, A.; Kunieda, H. *J. Dispersion Sci. Technol.* **2003**, *24*, 411.
(384) Aramaki, K.; Hossain, Md. K.; Rodriguez, C.; Uddin, Md. H.; Kunieda, H. *Macromolecules* **2003**, *36*, 9443.
(385) Löf, D.; Niemiec, A.; Schillén, K.; Loh, W.; Olofsson, G. *J. Phys. Chem. B* **2007**, *111*, 5911.
(386) Löf, D.; Schillén, K.; Torres, M. F.; Müller, A. J. *Langmuir* **2007**, *23*, 11000.
(387) Schillén, K.; Jansson, J.; Löf, D.; Costa, T. *J. Phys. Chem. B* **2008**, *112*, 5551.
(388) Matsubara, H.; Ohta, A.; Kameda, M.; Villeneuve, M.; Ikeda, N.; Aratono, M. *Langmuir* **1999**, *15*, 5496.
(389) Matsubara, H.; Ohta, A.; Kameda, M.; Ikeda, N.; Aratono, M. *Langmuir* **2000**, *16*, 7589.
(390) Hines, J. D. *Curr. Opin. Colloid Interface Sci.* **2001**, *6*, 350.
(391) Baglioni, P.; Dei, L.; Rivara-Minten, E.; Kevan, L. *J. Am. Chem. Soc.* **1993**, *115*, 4286.
(392) Shiloach, A.; Blankschtein, D. *Langmuir* **1998**, *14*, 7166.
(393) Kwon, S. Y. *Langmuir* **2008**, *24*, 10674.
(394) Nagarajan, R. *Langmuir* **1985**, *1*, 331.
(395) Nagarajan, R.; Ruckenstein, E. *Langmuir* **1991**, *7*, 2934.
(396) Shiloach, A.; Blankschtein, D. *Langmuir* **1998**, *14*, 1618.
(397) Sarmoria, C.; Puvvada, S.; Blankschtein, D. *Langmuir* **1992**, *8*, 2690.
(398) Puvvada, S.; Blankschtein, D. *J. Phys. Chem.* **1992**, *96*, 5567.
(399) Naor, A.; Puvvada, S.; Blankschtein, D. *J. Phys. Chem.* **1992**, *96*, 7830.
(400) Blankschtein, D.; Shiloach, A.; Zoeller, N. *Curr. Opin. Colloid Interface Sci.* **1997**, *2*, 294.
(401) Khana, A.; Marquesa, E. F. *Curr. Opin. Colloid Interface Sci.* **2000**, *4*, 402.
(402) Holmberg, K.; Jönsson, B.; Kronberg, B.; Lindman, B. In *Surfactants and Polymers in Aqueous Solution*, 2nd ed; Wiley: New York, 2002.
(403) Penfold, J.; Staples, E.; Cummins, P.; Tucker, I.; Thomas, R. K.; Simister, E. A.; Lu, J. R. *J. Chem. Soc., Faraday Trans.* **1996**, *92*, 1549.
(404) McDonald, J. A.; Rennie, A. R. *Langmuir* **1995**, *11*, 1493.
(405) Penfold, J.; Staples, E.; Thompson, L.; Tucker, I.; Hines, J.; Thomas, R. K.; Lu, J. R.; Warren, N. *J. Phys. Chem. B* **1999**, *103*, 5204.
(406) Patel, T.; Ghoshb, G.; Aswal, V.; Bahadur, P. *Colloids Surf. A* **2009**, *333*, 145.
(407) Zakharova, L.; Valeeva, F.; Zakharov, A.; Ibragimova, A.; Kudryavtseva, L.; Harlampidi, H. *J. Colloid Interface Sci.* **2003**, *263*, 597.
(408) Goldsipe, A.; Blankschtein, D. *Langmuir* **2005**, *21*, 9850.
(409) Funasaki, N.; Hada, S.; Neya, S. *J. Phys. Chem.* **1986**, *90*, 5469.
(410) Palous, J. L.; Turmine, M.; Letellier, P. *J. Phys. Chem. B* **1998**, *102*, 5886.
(411) Suradkar, Y. R.; Bhagwat, S. S. *J. Chem. Eng. Data* **2006**, *51*, 2026.
(412) Kim, S.; Kwon, S. Y.; hyuk Moon, J.; Kim, M. W. *Chem. Phys. Lett.* **2008**, *464*, 82.
(413) Kinzel, S.; Gradzielski, M. *Langmuir* **2008**, *24*, 10123.
(414) Imae, T.; Ikeda, S. *J. Phys. Chem.* **1986**, *90*, 5216.
(415) Sharma, K. S.; Patil, S. R.; Rakshit, A. K.; Glenn, K.; Doiron, M.; Palepu, R. M.; Hassan, P. A. *J. Phys. Chem. B* **2004**, *108*, 12804.
(416) Dubois, M.; Zemb, T. *Langmuir* **1991**, *7*, 1352.
(417) Tucker, I.; Penfold, J.; Thomas, R. K.; Grillo, I.; Barker, J. G.; Mildner, D. F. R. *Langmuir* **2008**, *24*, 6509.
(418) Feitosa, E.; Brown, W. *Langmuir* **1997**, *13*, 4810.
(419) Tucker, I.; Penfold, J.; Thomas, R. K.; Grillo, I.; Barker, J. G.; Mildner, D. F. R. *Langmuir* **2008**, *24*, 7674.
(420) Tucker, I.; Penfold, J.; Thomas, R. K.; Grillo, I.; Mildner, D. F. R.; Barker, J. G. *Langmuir* **2008**, *24*, 10089.
(421) Tucker, I.; Penfold, J.; Thomas, R. K.; Tildesley, D. J. *Langmuir* **2009**, *25*, 3932.
(422) Inoue, T. In *Vesicles*; Rosoff, M., Ed.; Surfactant Science Series Vol. 62; Marcel Dekker: New York, 1996; p 151.
(423) Barreleiro, P. C. A.; Olofsson, G.; Brown, W.; Edwards, K.; Bonassi, N. M.; Feitosa, E. *Langmuir* **2002**, *18*, 1024.
(424) Feitosa, E.; Bonassi, N. M.; Loh, W. *Langmuir* **2006**, *22*, 4512.
(425) Grillo, I.; Penfold, J.; Tucker, I.; Cousin, F. *Langmuir* **2009**, *25*, 3932.
(426) Penfold, J.; Staples, E.; Tucker, I.; Thomas, R. K. *Langmuir* **2004**, *20*, 1269.
(427) Croce, V.; Cosgrove, T.; Dreiss, C. A.; Maitland, G.; Hughes, T.; Karlsson, G. *Langmuir* **2004**, *20*, 7984.
(428) Croce, V.; Cosgrove, T.; Dreiss, C. A.; Maitland, G.; Hughes, T. *Langmuir* **2004**, *20*, 9978.
(429) Hayter, J.; Penfold, J. *Mol. Phys.* **1981**, *42*, 109.
(430) (a) Sharma, K. S.; Rodgers, C.; Palepu, R. M.; Rakshit, A. K. *J. Colloid Interface Sci.* **2003**, *268*, 482. (b) Sharma, K. S.; Hassan, P. A.; Rakshit, A. K. *Colloids Surf. A* **2006**, *289*, 17.
(431) De Salvo Souza, L.; Corti, M.; Cantu, L.; Degiorgio, V. *Chem. Phys. Lett.* **1986**, *131*, 160.
(432) Karlstroem, G.; Carlsson, A.; Lindman, B. *J. Phys. Chem.* **1990**, *94*, 5005.
(433) Feitosa, E.; Brown, W. *Langmuir* **1998**, *14*, 4460.
(434) Schomaecker, R.; Strey, R. *J. Phys. Chem.* **1994**, *98*, 3908.
(435) Nettesheim, F.; Zipfel, J.; Lindner, P.; Richtering, W. *Colloids Surf. A* **2001**, *183−185*, 563.
(436) Staples, E.; Thompson, L.; Tucker, I.; Penfold, J.; Thomas, R. K.; Lu, J. R. *Langmuir* **1993**, *9*, 1651.
(437) Penfold, J.; Staples, E.; Thompson, L.; Tucker, I.; Hines, J.; Thomas, R. K.; Lu, J. R. *Langmuir* **1995**, *11*, 2496.
(438) Iglesias, E.; Montenegro, L. *Phys. Chem. Chem. Phys.* **1999**, *1*, 4865.
(439) Ghosh, S.; Moulik, S. P. *J. Colloid Interface Sci.* **1998**, *208*, 357.

(440) Penfold, J.; Staples, E.; Tucker, I. *J. Phys. Chem. B* **2002**, *106*, 8891.
(441) Garamus, V. M. *Langmuir* **2003**, *19*, 7214.
(442) Goloub, T. P.; Pugh, R. J.; Zhmud, B. V. *J. Colloid Interface Sci.* **2000**, *229*, 72.
(443) Acharya, D. P.; Sato, T.; Kaneko, M.; Singh, Y.; Kunieda, H. *J. Phys. Chem. B* **2006**, *110*, 754.
(444) Verma, S.; Kumar, V. V. *J. Colloid Interface Sci.* **1998**, *207*, 1.
(445) Richards, C.; Tiddy, G. J. T.; Casey, S. *Colloids Surf. A* **2006**, *288*, 103.
(446) Richards, C.; Tiddy, G. J. T.; Casey, S. *Colloid Polym. Sci.* **2008**, *286*, 31.
(447) Penfold, J.; Thomas, R. K.; Dong, C. C.; Tucker, I.; Metcalfe, K.; Golding, S.; Grillo, I. *Langmuir* **2007**, *23*, 10140.
(448) Haque, Md. E.; Das, A. R.; Rakshit, A. K.; Moulik, S. P. *Langmuir* **1996**, *12*, 4084.
(449) Theander, K.; Pugh, R. J. *J. Colloid Interface Sci.* **2003**, *267*, 9.
(450) Joshi, T.; Mata, J.; Bahadur, P. *Colloids Surf. A* **2005**, *260*, 209.
(451) Douglas, C. B.; Kaler, E. W. *Langmuir* **1991**, *7*, 1097.
(452) Castaldi, M.; Costantino, L.; Ortona, O.; Paduano, L.; Vitagliano, V. *Langmuir* **1998**, *14*, 5994.
(453) Douglas, C. B.; Kaler, E. W. *J. Chem. Soc., Faraday Trans.* **1994**, *90*, 471.
(454) Israelachivili, J. N. Intermolecular and surface forces, 2nd Ed. Academic Press Inc.: San Diego, CA, 1992.
(455) Tanford, C. *The Hydrophobic Effect: Formation of Micelles and Biological Membranes*, New York: Wiley-Interscience, 1973.
(456) Stephenson, B. C.; Goldsope, A.; Beers, K. J.; Blankschtein, D. *J. Phys. Chem. B* **2007**, *111*, 1045.
(457) Nagarajan, R. *Langmuir* **2002**, *18*, 31.
(458) Jung, H. T.; Lee, S. Y.; Kaler, E. W.; Coldren, B.; Zaadzinski, J. A. *Proc. Natl. Acad. Sci. U.S.A.* **2002**, *99*, 15318.
(459) Helfrich, W. *J. Phys.: Condens. Matter* **1994**, *6*, A79.
(460) Hoffmann, H.; Ulbricht, W. *Recent Res. Dev. Phys. Chem.* **1998**, *2*, 113.
(461) Helfrich, W. *Z. Naturforsch.* **1973**, *28c*, 693.
(462) (a) Helfrich, W. *J. Phys. (Paris)* **1985**, *46*, 1263; **1986**, *47*, 321; **1987**, *48*, 285. (b) Peliti, L.; Leibler, S. *Phys. Rev. Lett.* **1985**, *54*, 1960.
(463) (a) Tanaka, M.; Kaneshina, S.; Tomida, T.; Noda, K.; Aoki, K. *J. Colloid Interface Sci.* **1973**, *3*, 525. (b) Macdonald, A. G. *Philos. Trans. R. Soc. London, Ser. B* **1984**, *304*, 47. (c) Kato, M.; Hayashi, R. *Biosci., Biotechnol., Biochem.* **1999**, *63*, 1321. (d) Ferdinand, S.; Lesemann, M.; Paulaitis, M. E. *Langmuir* **2000**, *16*, 10106. (e) Baden, N.; Kajimoto, O.; Hara, K. *J. Phys. Chem. B* **2002**, *106*, 8621. (f) Nishikido, N. *J. Colloid Interface Sci.* **1990**, *2*, 401.
(464) (a) Winter, R.; Czeslik, C. *Z. Kristallogr.* **2000**, *215*, 454. (b) Winter, R. *Curr. Opin. Colloid Interface Sci.* **2001**, *6*, 303.
(465) (a) Lesemann, M.; Thirumoorthy, K.; Kim, Y. J.; Jonas, J.; Paulaitis, M. E. *Langumir* **1998**, *14*, 5339. (b) Lesemann, M.; Nathan, H.; Dinoia, T. P.; Kirby, C. F.; Mchugh, M. A.; Van Zanten, J. H.; Paulaitis, M. E. *Ind. Eng. Chem. Res.* **2003**, *42*, 6425.
(466) (a) Zhao, D.; Huo, Q.; Feng, J.; Chmelka, B. F.; Stucky, G. D. *J. Am. Chem. Soc.* **1998**, *120*, 6024. (b) Zhu, H. Y.; Riches, J. D.; Barry, J. C. *Chem. Mater.* **2002**, *14*, 2086. (c) Santra, S.; Tapec, R.; Theodoropoulou, N.; Dobson, J.; Hebard, A.; Tan, W. *Langmuir* **2001**, *17*, 2900. (d) Moore, V. C.; Strano, M. S.; Haroz, E. H.; Hauge, R. H.; Smalley, R. E. *Nano Lett.* **2003**, *10*, 1379.
(467) (a) Raman, N. K.; Anderson, M. T.; Brinker, C. J. *Chem. Mater.* **1996**, *8*, 1682. (b) Mann, S.; Ozin, G. A. *Nature* **1996**, *382*, 313. (c) Antonietti, M. *Curr. Opin. Colloid Interface Sci.* **2001**, *6*, 244. (d) Cushing, B. L.; Kolesnichenko, V. L.; OConnor, C. J. *Chem. Rev.* **2004**, *104*, 3893. (e) Vriezema, D. M.; Aragonès, M. C.; Elemans, J. A. A.; Cornelissen, J. J. L. M.; Rowan, A. E.; Nolte, R. J. M. *Chem. Rev.* **2005**, *105*, 1445. (f) Eastoe, J.; Hollamby, M. J.; Hudson, L. *Adv. Colloid Interface Sci.* **2006**, *128−130*, 5. (g) Meldrum, F. C.; Colfen, H. *Chem. Rev.* **2008**, *108*, 4332.

CR9003743